

GAS PHASE ION-MOLECULE CHEMISTRY. I. ION CYCLOTRON  
RESONANCE INVESTIGATIONS OF ORGANOPHOSPHORUS  
COMPOUNDS. II. REACTIONS OF ALUMINUM  
IONS WITH ALKYL HALIDES

Thesis by  
Ronald Vernon Hodges

In Partial Fulfillment of the Requirements  
for the Degree of  
Doctor of Philosophy

California Institute of Technology  
Pasadena, California

1978

(Submitted November 14, 1977)

## ACKNOWLEDGMENTS

The largest share of credit for my scientific growth over the past four years must go to my adviser, Jack Beauchamp. I have appreciated his example, guidance and encouragement. I have also benefited from the assistance, examples, helpful discussions and commiseration provided by other members of the Beauchamp group. I have especially enjoyed working with Peter Armentrout on the metal ion beam instrument. I will take with me many pleasant memories of good times with Jack and the group. Wayne Berman, in particular, has been a good friend and competitor in innumerable ping pong games.

I want to thank two friends outside the Beauchamp group, Bill Croasmun and Marv Goodgame, for their fellowship. It has been good that Mike Ingle has been a part of my graduate as well as undergraduate career. I wish the best for him and Jean and I hope that our paths cross again often. I am thankful for the fellowship and support of many friends at Pasadena First Nazarene Church.

I thank the National Science Foundation and the California Institute of Technology for providing the financial support for my graduate studies.

Technical assistance from a number of people has been indispensable. William W. Schuelke and Anton W. Stark of the Chemistry Shops are responsible for much work on the ion beam apparatus. The expert typing of Joyce L. Lundstedt and Betty Reister is gratefully acknowledged.



## ABSTRACT

The properties and reactions of a series of phosphate and phosphite esters have been studied using the techniques of ion cyclotron resonance spectroscopy. The positive and negative ion chemistry of these species has been examined and their gas phase base strengths (proton affinities) and adiabatic ionization potentials measured. Effects of constrained geometry on the base strengths of phosphites are explored by comparing a series of cyclic phosphites with acyclic analogs. Axial and equatorial phosphorus lone pairs in six membered phosphite rings differing only by inversion of configuration at phosphorus are shown to have significantly different base strengths. A linear correlation exists between the proton affinities and first adiabatic ionization potentials of all trivalent phosphorus compounds for which data are available. This has implications for the electronic structure of these species, strongly suggesting that the highest occupied molecular orbital is the phosphorus lone pair. The results of these experiments are useful in the design of schemes for chemical ionization mass spectrometric analysis of phosphorus esters, which include widely used pesticides.

An ion beam apparatus is used to study the gas phase reactions of aluminum ions with a series of alkyl halides. The variation of product distributions with collision energy is reported. The observed reactivity of aluminum ions is discussed in terms of the electronic structure of aluminum, the reaction thermodynamics and proposed reaction mechanisms.

## TABLE OF CONTENTS

	Page
INTRODUCTION	1
CHAPTER I    Properties and Reactions of Trimethyl Phosphite, Trimethyl Phosphate, Triethyl Phosphate, and Trimethyl Phosphorothionate by Ion Cyclotron Resonance Spectroscopy	6
CHAPTER II    Nucleophilic Reactions of Anions with Trimethyl Phosphate in the Gas Phase by Ion Cyclotron Resonance Spectroscopy	51
CHAPTER III    Effects of Molecular Structure on Basicity. The Gas Phase Proton Affinities of Cyclic Phosphites	71
CHAPTER IV    The Proton Affinities of Pyridine, Phospha- benzene, and Arsabenzene	90
CHAPTER V    Gas Phase Organometallic Chemistry. Reactions of $\text{Al}^+$ with Alkyl Halides	110

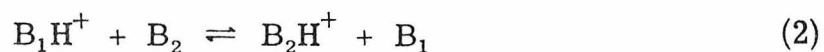
## INTRODUCTION

In 1952 observation<sup>1</sup> of the gas phase ion-molecule reaction 1, in which the chemically intriguing ion  $\text{CH}_5^+$  is produced, triggered a rapid expansion of the field of gas phase ion-molecule chemistry. The ion-molecule chemistry of a large number of organic and simple



inorganic molecules has been investigated by a variety of mass spectrometric techniques.<sup>2, 3</sup> The study of ion-molecule chemistry has benefited two areas of chemistry which are particularly relevant to the material presented in this thesis: the acid-base properties of molecules and analytical mass spectrometry.

The development of techniques for measuring the equilibrium constants for gas phase proton transfer between bases ( $\text{B}_1$  and  $\text{B}_2$ ) (reaction 2) has permitted quantitative determinations of the base



strengths (proton affinities) of molecules in the absence of complicating solvation effects.<sup>4-6</sup> These data make possible the assessment of effects of molecular and electronic structure on the intrinsic basicity of molecules.

Chemical ionization (CI) mass spectrometry is an analytical tool in which reactions between reagent ions and sample molecules are employed to generate ions which comprise the CI mass spectrum of the sample.<sup>7</sup> Mass spectra obtained in this way are often more useful than

electron impact mass spectra in the identification of sample molecules because ions whose masses are directly related to the molecular weight of the sample are usually formed. Electron impact often fails to produce a molecular ion.

Chapters I-IV of this thesis report the results of ion cyclotron resonance<sup>3, 8</sup> investigations of the ion-molecule chemistry and gas phase base strengths (proton affinities) of several organophosphorus compounds. Phosphorus esters were chosen as the focus of the investigation, because of the important role that these compounds play in the chemistry of living organisms.<sup>9-11</sup> A number of phosphorus esters are widely used pesticides.<sup>12</sup> Particular emphasis in Chapters I and II has been placed on the implications which the ion-molecule chemistry of phosphorus esters has for the development of CI mass spectrometric schemes for the detection of these compounds.

Molecular properties related to the proton affinity of organophosphorus compounds are discussed in Chapters I, III and IV. Chapter III is devoted to an exploration of the relationships of proton affinity to molecular conformation in a series of constrained phosphites. This chapter also reports the observation of a linear correlation between proton affinity and ionization potential of trivalent phosphorus compounds. The implications of this correlation for the electronic structure of these molecules is discussed.

The final chapter, Chapter V, is concerned with an entirely different area of ion-molecule chemistry, that of metal ions. An ion beam apparatus is employed to study the reactions of aluminum ions with

a series of alkyl halides. The use of a beam apparatus makes available an additional experimental variable, the collision energy. The observed reactivity of aluminum ions is discussed in terms of the electronic structure of aluminum, the reaction thermodynamics and proposed mechanisms.

## References

- (1) V. L. Tal'roze and A. K. Lyubimova, Dokl. Akad. Nauk. SSSR, 86, 909 (1952).
- (2) For reviews of ion-molecule chemistry and experimental methods see: P. Ausloos, Ed., 'Interactions Between Ions and Molecules,' Plenum Press, New York, N.Y., 1974; J. L. Franklin, Ed., 'Ion-Molecule Reactions,' Vols. I and II, Plenum Press, New York, N.Y., 1972; E. W. McDaniel, V. Čermák, A. Dalgarno, E. E. Ferguson, and L. Friedman, 'Ion-Molecule Reactions,' Wiley, New York, N.Y., 1970; J. H. Futrell and T. O. Tiernan in 'Fundamental Processes in Radiation Chemistry,' P. Ausloos, Ed., Wiley-Interscience, New York, N.Y., 1968, Chapter 4; R. F. Gould, Ed., 'Ion-Molecule Reactions in the Gas Phase,' American Chemical Society Publications, Washington, D.C., 1966.
- (3) T. A. Lehman and M. M. Bursey, 'Ion Cyclotron Resonance Spectrometry,' Wiley, New York, N.Y., 1976.
- (4) R. W. Taft in 'Proton Transfer Reactions,' E. Caldin and V. Gold, Eds., Wiley, New York, N.Y., 1975, p. 31.
- (5) J. F. Wolf, R. H. Staley, I. Koppel, M. Taagepera, R. T. McIver, Jr., J. L. Beauchamp, and R. W. Taft, J. Am. Chem. Soc., 99, 5417 (1977).
- (6) R. Yamdagni and P. Kebarle, J. Am. Chem. Soc., 98, 1320 (1976).
- (7) G. W. A. Milne and M. J. Lacey, CRC Crit. Rev. Anal. Chem., 4, 45 (1974).

- (8) J. L. Beauchamp, Ann. Rev. Phys. Chem., 22, 527 (1971).
- (9) D. W. Hutchinson, Organophosphorus Chem., 6, 124 (1974).
- (10) J. Matheja and E. T. Degens, "Structural Biology of Phosphates," Gustav Fischer Verlag, Stuttgart, Germany, 1971.
- (11) H. G. Khorana, "Some Recent Developments in the Chemistry of Phosphate Esters of Biological Interest," Wiley, New York, N. Y., 1961.
- (12) R. D. O'Brien, "Toxic Phosphorus Esters, Chemistry, Metabolism and Biological Effects," Academic Press, New York, N. Y., 1960.

## CHAPTER I

Properties and Reactions of Trimethyl Phosphite, Trimethyl  
Phosphate, Triethyl Phosphate, and Trimethyl  
Phosphorothionate by Ion Cyclotron Resonance Spectroscopy

by

Ronald V. Hodges, Thomas J. McDonnell, and J. L. Beauchamp\*

Contribution No. 5699 from the Arthur Amos Noyes  
Laboratory of Chemical Physics, California Institute of  
Technology, Pasadena, California 91125

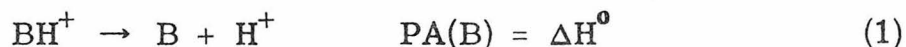


## ABSTRACT

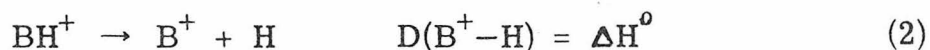
The gas phase ion-molecule reactions occurring in trimethyl phosphite, trimethyl phosphate, triethyl phosphate and trimethyl phosphorothionate have been investigated by ion cyclotron resonance spectroscopy. Protonated parent ions, tetracoordinated phosphonium ions, and cluster ions are the reaction products observed. The proton affinities of these compounds have been determined to be 218.2, 209.5, 214 and 211.9 kcal/mol, respectively (relative to  $\text{PA}(\text{NH}_3) = 202.3$  kcal/mol). Homolytic bond dissociation energies of the protonated species are calculated using adiabatic ionization potentials determined by photoelectron spectroscopy. The trends in these quantities are discussed. A reasonable value for the correlated homolytic bond dissociation energy of trimethyl phosphite indicates that the first ionization potential of this molecule should be assigned to the phosphorus lone pair. The application of chemical ionization mass spectrometry to the analysis of phosphorus esters is briefly discussed.

The solution chemistry of organophosphorus compounds is a large and well studied branch of organic chemistry.<sup>1</sup> However, relatively few studies of the gas phase ion chemistry of phosphorus compounds have been reported. The ion-molecule reactions in phosphine and the methyl phosphines have been investigated.<sup>2-6</sup> Proton transfer reactions and condensation reactions with loss of simple molecules and radicals are the processes which occur at pressures below 0.05 Torr. Above this pressure the formation of cluster ions is also observed.<sup>5</sup> Ion-molecule reactions of  $\text{PF}_3$ ,<sup>7,8</sup>  $\text{OPF}_3$ ,<sup>8-10</sup> and  $\text{SPF}_3$ <sup>10</sup> have also been reported.

The gas phase proton affinities of several phosphorus compounds have been determined by icr techniques and are listed in Table I.<sup>6,7,9,11</sup> The proton affinity of a base, B, is defined as the standard enthalpy change for reaction 1. The homolytic bond dissociation energy,



$\text{D(B}^+-\text{H)}$ , is defined as the standard enthalpy change for reaction 2. It is related to the proton affinity of B by the adiabatic ionization potentials of B and H (eq 3). Strictly defined, the homolytic bond dissociation



$$\text{D(B}^+-\text{H)} = \text{PA(B)} + \text{IP(B)} - \text{IP(H)} \quad (3)$$

energy is calculated using the first adiabatic ionization potential of B in eq 3. However, for the purpose of comparisons among homologous compounds, the correlated homolytic bond dissociation energy must be considered.<sup>12</sup> This quantity is calculated from eq 3, using the adiabatic

ionization potential of the orbital of B which corresponds to the bonding orbital in  $B-H^+$ . For the phosphorus compounds studied to date the first ionization potential corresponds to ionization from this orbital. Adiabatic ionization potentials and homolytic bond dissociation energies for these compounds are given in Table I.

The esters of phosphoric acid play important roles in biological processes.<sup>13-15</sup> The phosphate moiety,  $PO_4$ , is a structural component of DNA, RNA, and phospholipid membranes. It is also involved in biochemical reactions, such as those of ATP. Some phosphorus esters interfere with nerve impulse transmission by inhibition of acetylcholine esterase.<sup>16</sup> These compounds are used as selective pesticides.

An understanding of the relationships between the chemical properties of phosphorus esters and their biological activity is essential in order to predict their behavior in living organisms. For example, effective pesticides must be able to penetrate the ion barrier of insect nervous systems.<sup>17</sup> Therefore, the basicity of potential pesticides must be low enough such that they are un-ionized under physiological conditions.<sup>18</sup>

A knowledge of phosphorus chemistry is important for the development of analytical techniques for phosphorus esters. In particular, the design of chemical ionization mass spectrometric techniques<sup>19</sup> for these compounds requires a knowledge of their gas phase ion chemistry. This paper presents the results of an ion cyclotron resonance (icr) investigation of the gas phase ion-molecule reactions and proton affinities of four simple phosphorus esters: trimethyl phosphite,

Table I. Proton Affinities, Adiabatic Ionization Potentials, and Homolytic Bond Dissociation Energies of Phosphorus Esters and Related Phosphorus Compounds

Molecule	PA <sup>a, b</sup>	IP <sup>a</sup>	D(B <sup>+</sup> -H) <sup>a</sup>
P(OCH <sub>3</sub> ) <sub>3</sub>	218.2 ± 0.3	196 (8.50) <sup>c</sup>	101
SP(OCH <sub>3</sub> ) <sub>3</sub>	211.9 ± 0.3	199 (8.65) <sup>d</sup>	97
OP(OCH <sub>3</sub> ) <sub>3</sub>	209.5 ± 0.3	230 (9.99) <sup>e</sup>	126
OP(OC <sub>2</sub> H <sub>5</sub> ) <sub>3</sub>	214 ± 2	226 (9.79) <sup>e</sup>	126
PH <sub>3</sub>	187.4 <sup>f</sup>	230 (9.96) <sup>f</sup>	103
CH <sub>3</sub> PH <sub>2</sub>	201.8 <sup>f</sup>	210 (9.12) <sup>e</sup>	98
(CH <sub>3</sub> ) <sub>2</sub> PH	214.0 <sup>f</sup>	195 (8.47) <sup>e</sup>	96
P(CH <sub>3</sub> ) <sub>3</sub>	223.5 <sup>f</sup>	187 (8.11) <sup>e</sup>	97
PF <sub>3</sub>	160 ± 5 <sup>g</sup>	269 (11.66) <sup>h</sup>	116
OPF <sub>3</sub>	174 <sup>i</sup>	294 (12.77) <sup>h</sup>	154

<sup>a</sup>kcal/mol. Values in parentheses in eV. <sup>b</sup>Proton affinities relative to PA(NH<sub>3</sub>) = 202.3 kcal/mol (see Reference 11). <sup>c</sup>Estimated from the photoelectron spectrum published in Reference 42. <sup>d</sup>Private communication from A. H. Cowley. <sup>e</sup>Estimated from the photoelectron spectrum obtained in this laboratory. <sup>f</sup>Reference 11. <sup>g</sup>Reference 7. <sup>h</sup>P. J. Bassett and D. R. Lloyd, J. Chem. Soc. Dalton, 248 (1972). <sup>i</sup>Reference 9.

trimethyl phosphate, triethyl phosphate, and trimethyl phosphorothionate.

### Experimental Section

The general features of icr instrumentation and its operation in trapped ion experiments have been previously described.<sup>20, 21</sup> All experiments were performed at room temperature.

Reaction paths were identified by double resonance experiments.<sup>20</sup> Spectral intensities in the figures have been corrected to ion abundance by dividing the measured intensity by ion mass.<sup>20, 21</sup>

Pressure measurements were made using a Schulz-Phelps gauge located adjacent to the icr cell. This gauge is calibrated for each gas for a given emission current (5  $\mu$ A) and magnetic field (6 kG) against an MKS Instruments Baratron Model 90H1-E capacitance manometer in the region  $10^{-5}$ - $10^{-3}$  Torr. Pressures in the trapped ion experiments were in the range  $10^{-7}$ - $10^{-5}$  Torr. The esters adhered to the walls of the apparatus and pumped out very slowly. For this reason the pressure tended to drift during an experiment and accurate calibration of the Schulz-Phelps gauge was difficult. The accuracy of the pressures reported here is estimated to be  $\pm 50\%$ . The principal errors in the rate constants and equilibrium constants are due to this uncertainty.

Photoelectron spectra were obtained using a photoelectron spectrometer of standard design built in the Caltech shops. The instrument comprises a helium discharge lamp,  $127^\circ$  electrostatic analyzer and Channeltron electron multiplier. Spectra were accumulated in a Tracor-Northern NS-570A multichannel scaler with 4 K memory. Argon

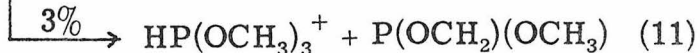
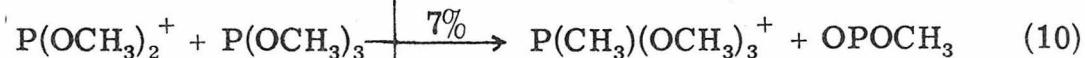
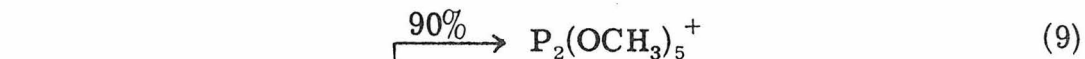
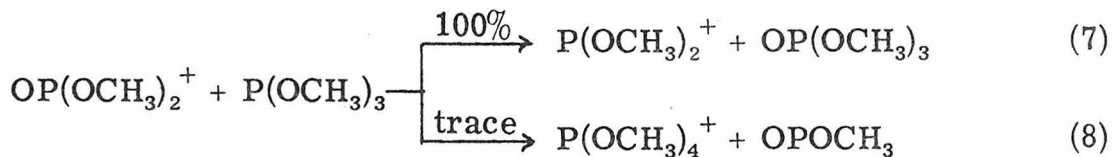
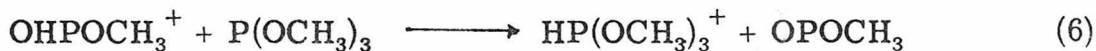
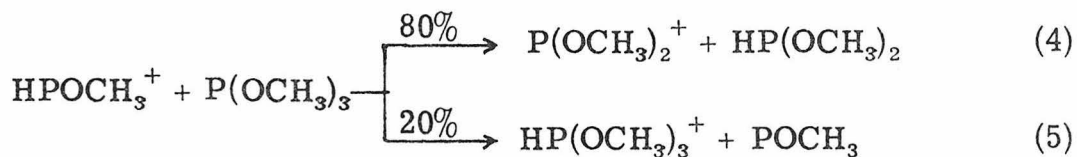
was used to calibrate all spectra. The ionization potentials reported here have error limits of  $\pm 0.02$  eV as determined from the width of the argon peaks.

All chemicals were reagent grade materials from commercial sources and were used as supplied.

## Results

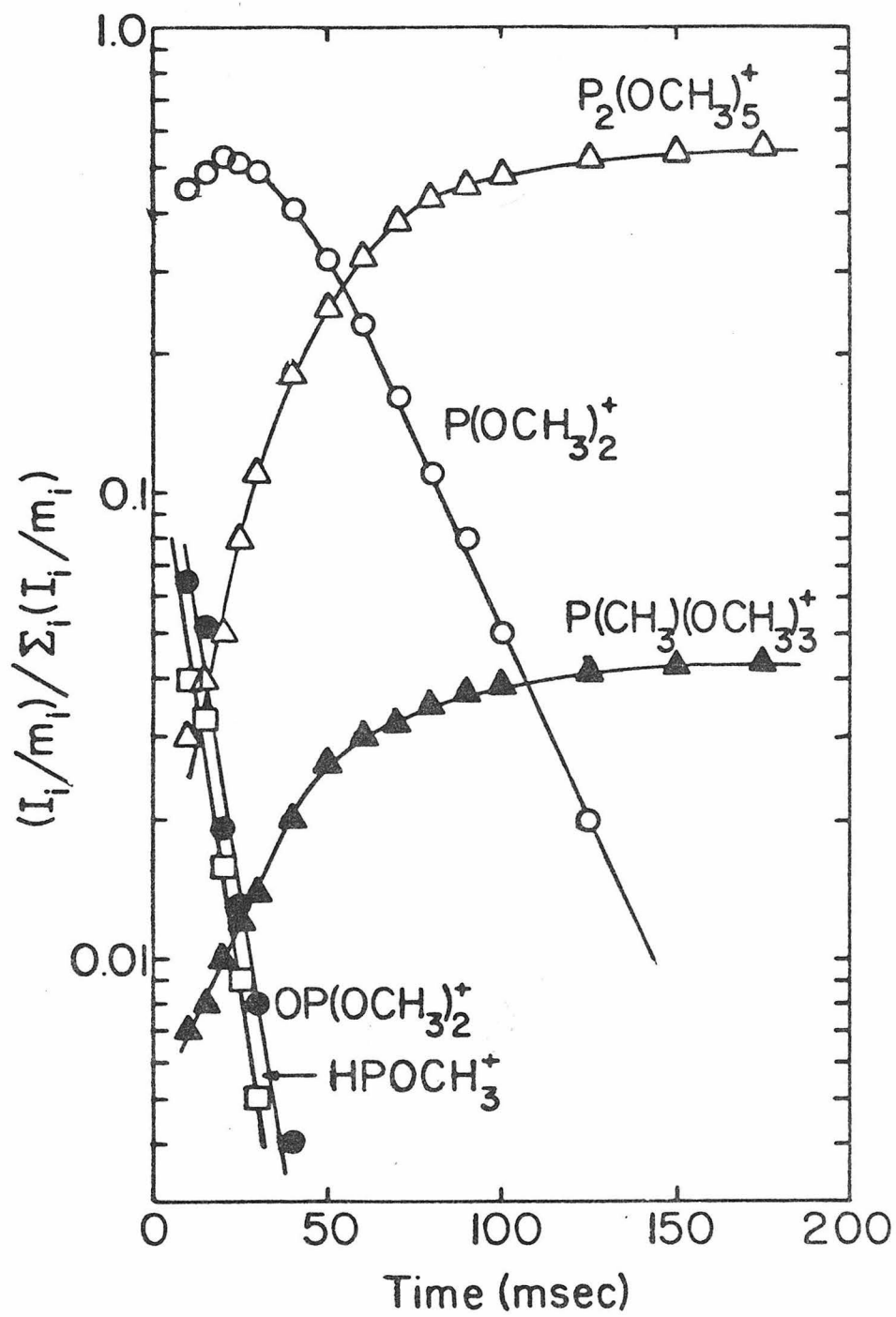
Trimethyl Phosphite. Mass Spectrum. The icr mass spectrum of trimethyl phosphite agrees with the reported spectrum.<sup>22</sup> The ions present in the mass spectrum at 20 eV are  $\text{P}(\text{OCH}_3)_2^+$  (m/e 93, 26%),  $\text{P}(\text{OCH}_3)_3^+$  (m/e 124, 21%),  $\text{OP}(\text{OCH}_3)_2^+$  (m/e 109, 20%),  $\text{HP}(\text{OCH}_3)_2^+$  (m/e 94, 15%),  $\text{HPOCH}_3^+$  (m/e 63, 10%), and  $\text{OHPOCH}_3^+$  (m/e 79, 8%).

Ion Chemistry. The variation of the relative ion abundances with time is given in Figures 1 and 2. The ion  $\text{P}(\text{OCH}_3)_2^+$  (m/e 93), which is formed by electron impact, also results from reactions of  $\text{HPOCH}_3^+$  (m/e 63) and  $\text{OP}(\text{OCH}_3)_2^+$  (m/e 109) with the neutral (reactions 4 and 7).<sup>23</sup>



## FIGURE 1

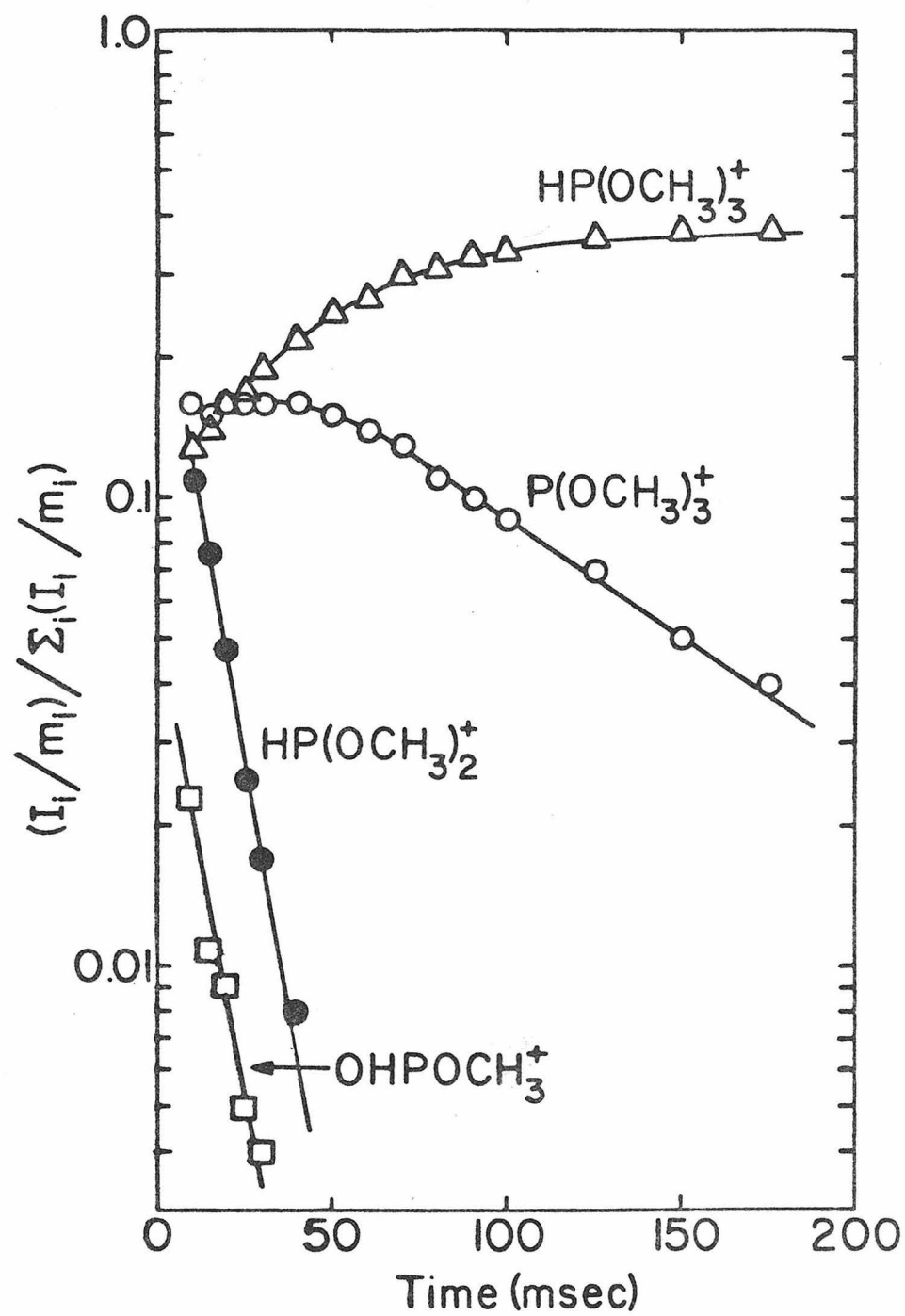
Temporal variation of ion concentration in trimethyl phosphite at  $5.6 \times 10^{-6}$  Torr pressure and 20 eV electron energy (see Figure 2).

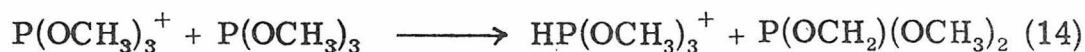
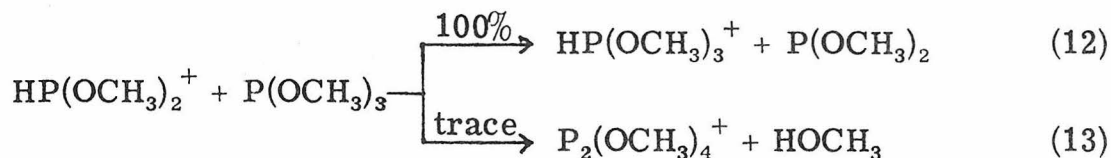




## FIGURE 2

Temporal variation of ion concentrations in trimethyl phosphite at  $5.6 \times 10^{-6}$  Torr pressure and 20 eV electron energy (see Figure 1).





The principal reaction of  $\text{P}(\text{OCH}_3)_2^+$  is the clustering reaction 9 to form  $\text{P}_2(\text{OCH}_3)_5^+$  (m/e 217), which is the most abundant ion at long times.  $\text{P}(\text{OCH}_3)_2^+$  also undergoes methyl cation transfer, yielding  $\text{P}(\text{CH}_3)(\text{OCH}_3)_3^+$  (m/e 139) (reaction 10), and proton transfer to give  $\text{HP}(\text{OCH}_3)_3^+$  (m/e 125) (reaction 11). The protonated parent ion,  $\text{HP}(\text{OCH}_3)_3^+$  is also formed by proton transfer from  $\text{HPOCH}_3^+$  (m/e 63),  $\text{OHPOCH}_3^+$  (m/e 79),  $\text{HP}(\text{OCH}_3)_2^+$  (m/e 109), and  $\text{P}(\text{OCH}_3)_3^+$  (m/e 124) (reactions 5, 6, 12, and 14). Proton transfer from the parent ion,  $\text{P}(\text{OCH}_3)_3^+$ , initially does not take place. It may be formed in a relatively unreactive excited state which then is collisionally deactivated. This phenomenon has been observed previously for the parent ions of  $(\text{CH}_3)_3\text{As}^{24}$  and  $(\text{CH}_3)_3\text{N}^{25}$ . Small quantities of the ions  $\text{P}(\text{OCH}_3)_4^+$  (m/e 155) and  $\text{P}_2(\text{OCH}_3)_4^+$  (m/e 186) are produced in minor reactions of  $\text{OP}(\text{OCH}_3)_2^+$  and  $\text{HP}(\text{OCH}_3)_2^+$ , respectively (reactions 8 and 13).

Rate constants for the reactions of the primary ions are listed in Table II. These values were calculated from the limiting slopes of semilog plots of ion abundance vs. time. Pseudo first order kinetics are assumed.

Proton Affinity. In mixtures of  $\text{P}(\text{OCH}_3)_3$  with pyridine and with cyclohexylamine the ratio of the protonated parent ions reached a constant value. Double resonance experiments confirmed that proton transfer between the bases was occurring. Equilibrium constants

Table II. Rate Constants for the Ion-Molecule Reactions in Trimethyl Phosphite<sup>a</sup>

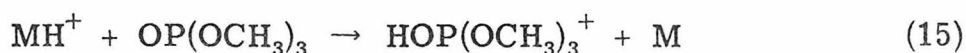
Reaction	$k_1^b$	$\Sigma k_1^b$
$\text{HPOCH}_3^+ + \text{P}(\text{OCH}_3)_3 \begin{cases} \rightarrow \text{P}(\text{OCH}_3)_2^+ + \text{HP}(\text{OCH}_3)_2 \\ \rightarrow \text{HP}(\text{OCH}_3)_3^+ + \text{POCH}_3 \end{cases}$	3.8 1.0	4.8
$\text{OHPOCH}_3^+ + \text{P}(\text{OCH}_3)_3 \rightarrow \text{HP}(\text{OCH}_3)_3^+ + \text{OPOCH}_3$	6.5	
$\text{OP}(\text{OCH}_3)_2^+ + \text{P}(\text{OCH}_3)_3 \begin{cases} \rightarrow \text{P}(\text{OCH}_3)_2^+ + \text{OP}(\text{OCH}_3)_3 \\ \rightarrow \text{P}(\text{OCH}_3)_4^+ + \text{OPOCH}_3 \end{cases}$	5.8 < 0.1	5.8
$\text{P}(\text{OCH}_3)_2^+ + \text{P}(\text{OCH}_3)_3 \begin{cases} \rightarrow \text{P}_2(\text{OCH}_3)_5^+ \\ \rightarrow \text{P}(\text{CH}_3)(\text{OCH}_3)_3 + \text{OPOCH}_3 \\ \rightarrow \text{HP}(\text{OCH}_3)_3^+ + \text{P}(\text{OCH}_2)(\text{OCH}_3) \end{cases}$	1.4 0.1 0.05	1.6
$\text{HP}(\text{OCH}_3)_2^+ + \text{P}(\text{OCH}_3)_3 \begin{cases} \rightarrow \text{HP}(\text{OCH}_3)_3^+ + \text{P}(\text{OCH}_3)_2 \\ \rightarrow \text{P}_2(\text{OCH}_3)_4^+ + \text{HOCH}_3 \end{cases}$	4.8 < 0.1	4.8
$\text{P}(\text{OCH}_3)_3^+ + \text{P}(\text{OCH}_3)_3 \rightarrow \text{HP}(\text{OCH}_3)_3^+ + \text{P}(\text{OCH}_2)(\text{OCH}_3)_2$	0.5	

<sup>a</sup>All data from trapped-ion studies at 20 eV. <sup>b</sup>In units of  $10^{-10} \text{ cm}^3 \text{ molecule}^{-1} \text{ sec}^{-1}$ . Each constant is an average of three determinations. Accuracy in rate constants estimated to be  $\pm 50\%$  due to uncertainties in pressure measurement.

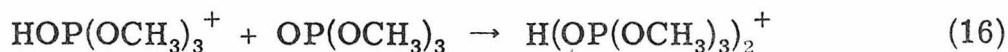
measured in these experiments are summarized in Table III, along with free energies and enthalpies of proton transfer. Entropy effects were assumed to be small and limited to symmetry number corrections.<sup>11, 26</sup> These data yield  $PA(P(OCH_3)_3) = 218.2 \pm 0.3$  kcal/mol. All proton affinities are relative to  $PA(NH_3) = 202.3$  kcal/mol.

Trimethyl Phosphate. Mass Spectrum. The icr mass spectrum of trimethyl phosphate at 70 eV agrees with the reported spectrum.<sup>27</sup> The principal ions in the 70 eV mass spectrum are  $HPO(OCH_3)_2^+$  (m/e 110, 46%),  $HPO(OCH_3)^+$  (m/e 79, 14%),  $H_2PO(OCH_3)^+$  (m/e 80, 14%),  $OP(OCH_3)_2^+$  (m/e 109, 11%),  $HOPO(OCH_3)^+$  (m/e 95, 10%), and  $OP(OCH_3)_3^+$  (m/e 140, 6%).

Ion Chemistry. The time evolution of the ion abundances in trimethyl phosphate is shown in Figures 3 and 4. The protonated parent is the dominant secondary ion. Double resonance experiments demonstrated that this ion is formed in reaction 15, where  $MH^+$  equals  $OP(OCH_3)_3^+$  (m/e 140),  $HPO(OCH_3)_2^+$  (m/e 110),  $HOPO(OCH_3)^+$  (m/e 95),  $H_2PO(OCH_3)^+$  (m/e 80) and  $HPO(OCH_3)^+$  (m/e 79). The protonated parent



clusters to form a proton bound dimer (reaction 16). The remaining



primary ion,  $OP(OCH_3)_2^+$  (m/e 109), transfers a methyl cation to the neutral to form  $(CH_3O)_4P^+$  (m/e 155) and clusters (reactions 17 and 18).

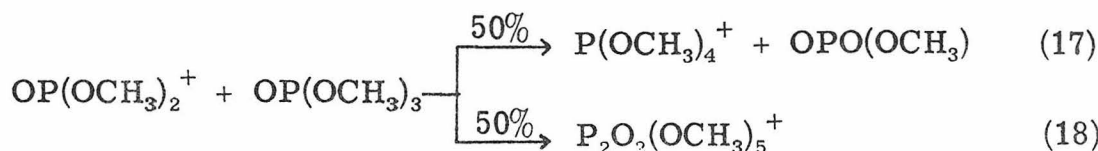


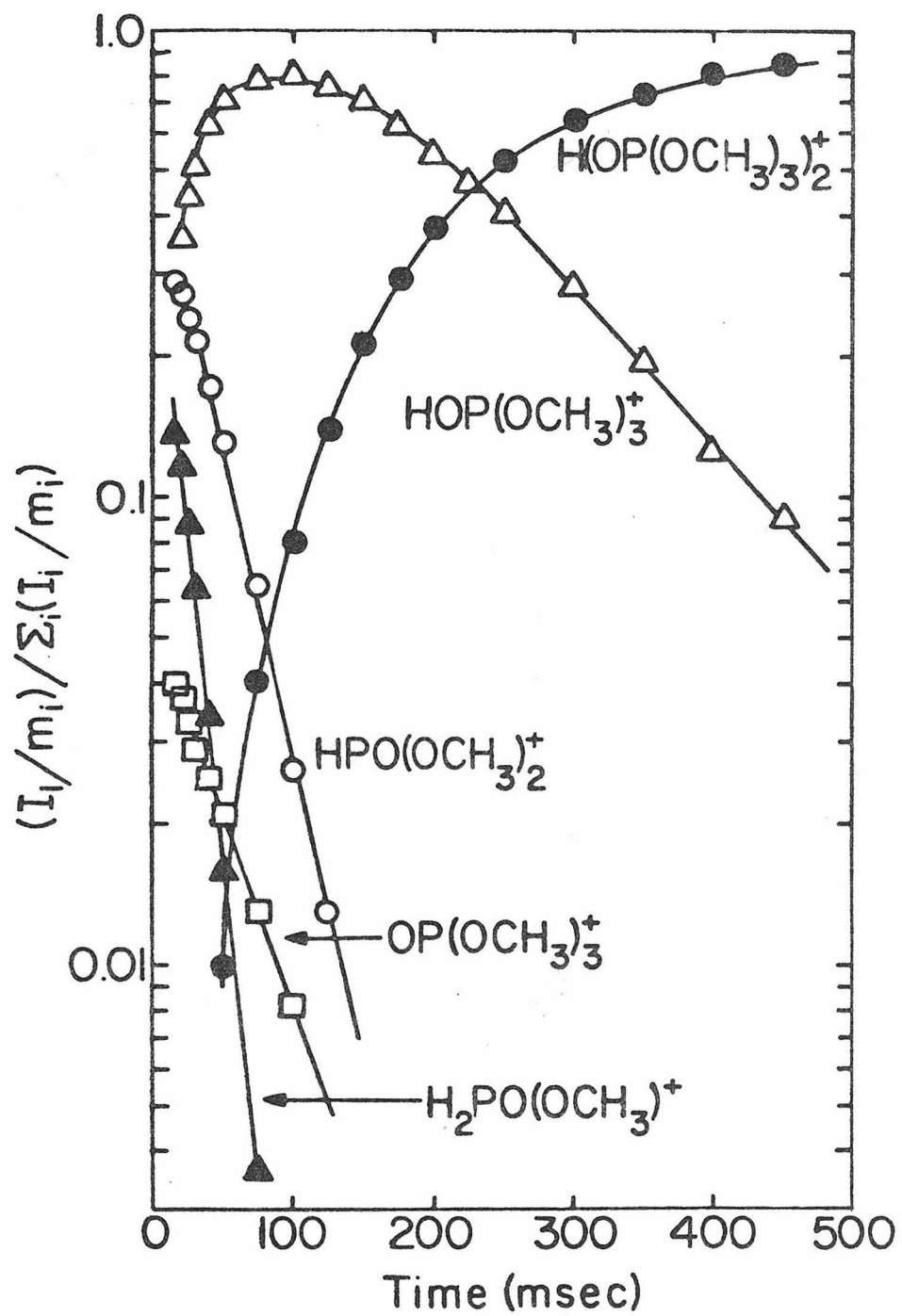
Table III. Proton Affinities of Phosphorus Esters Derived from Equilibrium Constants for Proton Transfer Reactions

$\text{HXP(OR)}_3^+ + \text{B} \rightleftharpoons \text{BH}^+ + \text{XP(OR)}_3$	$K^a$	$\Delta G^b$	$\Delta H^b$	$\text{PA(B)}^{c, d}$	$\text{PA(XP(OR)}_3)^d$
$\text{HP(OCH}_3)_3^+ + \text{C}_5\text{H}_5\text{N} \rightleftharpoons \text{C}_5\text{H}_5\text{NH}^+ + \text{P(OCH}_3)_3$	0.55	0.4	0.4	218.1	218.5
$\text{HP(OCH}_3)_3^+ + \text{c-C}_6\text{H}_{11}\text{NH}_2 \rightleftharpoons \text{c-C}_6\text{H}_{11}\text{NH}_3^+ + \text{P(OCH}_3)_3$	0.90	0.1	-0.5	218.5	218.0
$\text{HOP(OCH}_3)_3^+ + \text{C}_6\text{H}_5\text{NH}_2 \rightleftharpoons \text{C}_6\text{H}_5\text{NH}_3^+ + \text{OP(OCH}_3)_3$	0.09	1.4	0.8	208.8	209.6
$\text{HOP(OCH}_3)_3^+ + (\text{C}_6\text{H}_5)_2\text{CCH}_2 \rightleftharpoons (\text{C}_6\text{H}_5)_2\text{CCH}_3^+ + \text{OP(OCH}_3)_3$	0.78	0.1	0.1	209.2	209.3
$\text{HOP(OC}_2\text{H}_5)_3^+ + 1, 3, 5\text{-(CH}_3\text{O)}_3\text{C}_6\text{H}_3 \rightarrow 1, 3, 5\text{-(CH}_3\text{O)}_3\text{C}_6\text{H}_4^+ + \text{OP(OC}_2\text{H}_5)_3$				216.8	< 217.9
$\text{C}_2\text{H}_5\text{NH}_3^+ + \text{OP(OC}_2\text{H}_5)_3 \rightarrow \text{HOP(OC}_2\text{H}_5)_3^+ + \text{C}_2\text{H}_5\text{NH}_2$				214.0	> 213.4
$\text{HOP(OC}_2\text{H}_5)_3^+ + 3\text{-(CH}_3\text{CO)C}_5\text{H}_4\text{N} \rightleftharpoons 3\text{-(CH}_3\text{CO)C}_5\text{H}_4\text{NH}^+ + \text{OP(OC}_2\text{H}_5)_3$	equilibrium not established			214.4	~ 214.4
$\text{HOP(OC}_2\text{H}_5)_3^+ + \text{C}_4\text{H}_4\text{N}_2 \rightleftharpoons \text{C}_4\text{H}_4\text{N}_2\text{H}^+ + \text{OP(OC}_2\text{H}_5)_3$	equilibrium not established			213.8	~ 214.2
$\text{HSP(OCH}_3)_3^+ + 4\text{-CH}_3\text{OC}_6\text{H}_4\text{CHO} \rightleftharpoons 4\text{-CH}_3\text{OC}_6\text{H}_4\text{CHOH}^+ + \text{SP(OCH}_3)_3$	0.15	1.1	1.1	210.8	211.9

<sup>a</sup>Average of at least three independent determinations.<sup>b</sup>In kcal/mol.<sup>c</sup>From a compilation of R. W. Taft. Thesevalues differ slightly from those reported in R. W. Taft, in "Proton-Transfer Reactions," E. Caldin and V. Gold, Eds., Wiley, New York, N. Y., 1975, p. 31. <sup>d</sup>Proton affinity in kcal/mol. All data relative to  $\text{PA(NH}_3) = 202.3$  kcal/mol.

## FIGURE 3

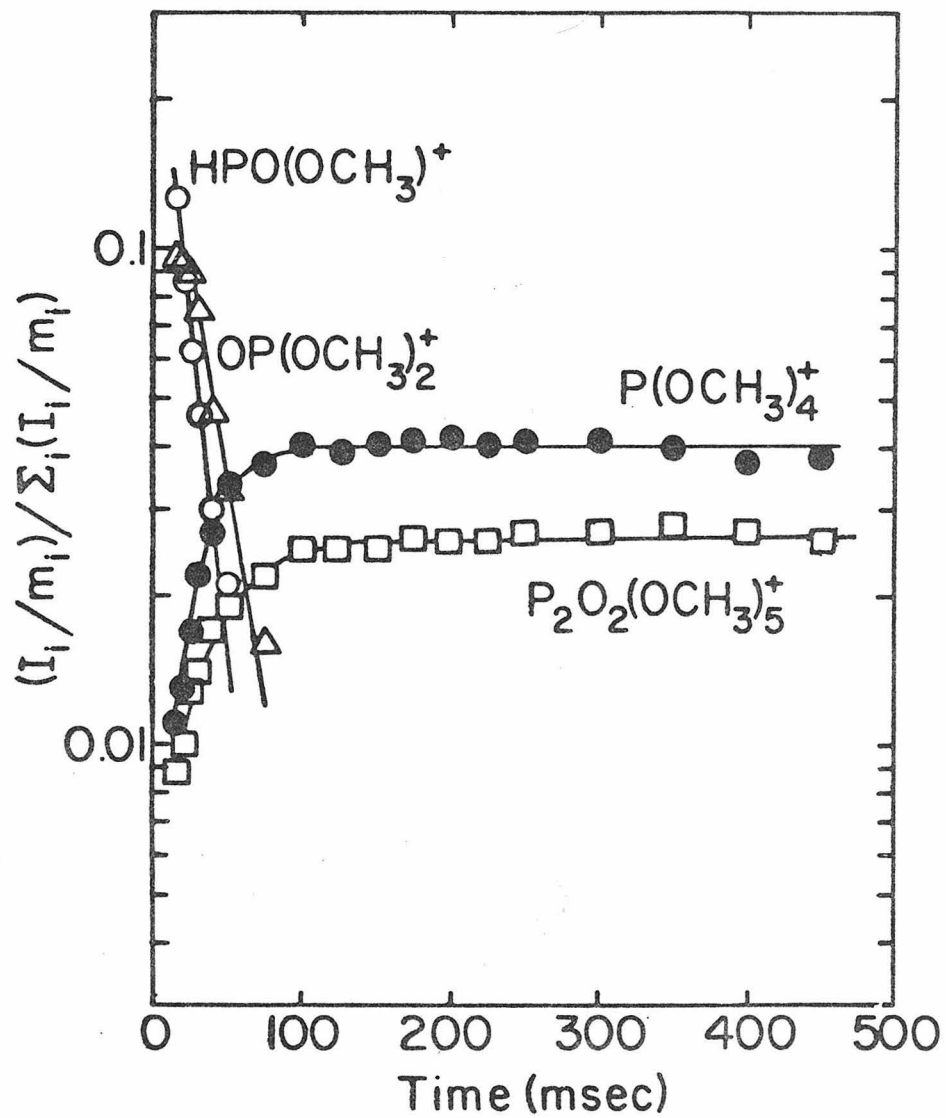
Temporal variation of ion concentrations in trimethyl phosphate at  $3.2 \times 10^{-6}$  Torr pressure and 70 eV electron energy (see Figure 4).





## FIGURE 4

Temporal variation of ion concentrations in trimethyl phosphate at  $3.2 \times 10^{-6}$  Torr pressure and 70 eV electron energy (see Figure 3).

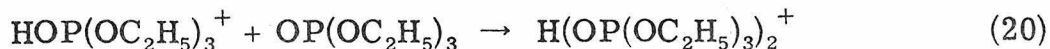
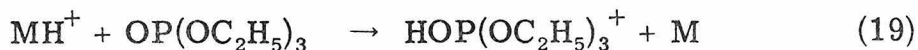


Rate constants for the reactions in trimethyl phosphate are listed in Table IV.

Proton Affinity. Proton transfer equilibria were observed in mixtures of  $\text{OP}(\text{OCH}_3)_3$  with aniline and with 1,1-diphenylethene. Data from these experiments are presented in Table III. The proton affinity of trimethyl phosphate is found to be  $209.5 \pm 0.3$  kcal/mol.

Triethyl Phosphate. Mass Spectrum. The icr mass spectrum agrees with the reported spectrum.<sup>28</sup> The major ions at 70 eV are  $\text{P}(\text{OH})_4^+$  ( $\underline{\text{m/e}}$  99, 30%),  $(\text{HO})_2\text{P}(\text{OC}_2\text{H}_5)_2^+$  ( $\underline{\text{m/e}}$  155, 29%),  $(\text{HO})_3\text{POC}_2\text{H}_5^+$  ( $\underline{\text{m/e}}$  127, 19%),  $\text{OP}(\text{OH})_2^+$  ( $\underline{\text{m/e}}$  81, 13%), and  $\text{OP}(\text{OH})(\text{OC}_2\text{H}_5)^+$  ( $\underline{\text{m/e}}$  109, 9%).

Ion Chemistry. The time evolution of the relative ion abundances in trimethyl phosphate is presented in Figure 5. The only primary process observed is the proton transfer reaction 19, where  $\text{MH}^+$  equals  $\text{P}(\text{OH})_4^+$ ,  $\text{OP}(\text{OH})_2^+$ ,  $\text{OP}(\text{OH})(\text{OC}_2\text{H}_5)^+$ ,  $(\text{HO})_3\text{POC}_2\text{H}_5^+$ , and  $(\text{HO})_2\text{P}(\text{OC}_2\text{H}_5)_2^+$ . The protonated parent rapidly clusters with the neutral, yielding the proton bound dimer  $\text{H}(\text{OP}(\text{OC}_2\text{H}_5)_3)_2^+$  ( $\underline{\text{m/e}}$  365) (reaction 20). The rate



constants for the reactions of the three most abundant primary ions and the protonated parent are listed in Table V.

Proton Affinity. Because of the rapid rate of clustering of the protonated parent both with the triethyl phosphate neutral and with other Lewis bases, proton transfer equilibria between triethyl phosphate and added bases could not be established. The observation that proton

Table IV. Rate Constants for the Ion-Molecule Reactions in Trimethyl Phosphate<sup>a</sup>

Reaction	$k_1^b$	$\Sigma k_1^b$
$\text{HPO}(\text{OCH}_3)^+ + \text{OP}(\text{OCH}_3)_3 \rightarrow \text{HOP}(\text{OCH}_3)_3^+ + \text{OPOCH}_3$	4.9	
$\text{H}_2\text{PO}(\text{OCH}_3)^+ + \text{OP}(\text{OCH}_3)_3 \rightarrow \text{HOP}(\text{OCH}_3)_3^+ + \text{HPO}(\text{OCH}_3)$	6.1	
$\text{HOPO}(\text{OCH}_3)^+ + \text{OP}(\text{OCH}_3)_3 \rightarrow \text{HOP}(\text{OCH}_3)_3^+ + \text{OPO}(\text{OCH}_3)$	3.6	
$\text{OP}(\text{OCH}_3)_2^+ + \text{OP}(\text{OCH}_3)_3 \rightarrow$	$\text{P}(\text{OCH}_3)_4^+ + \text{OPO}(\text{OCH}_3)$	1.9
	$\text{P}_2\text{O}_2(\text{OCH}_3)_5^+$	1.9
		3.8
$\text{HPO}(\text{OCH}_3)_2^+ + \text{OP}(\text{OCH}_3)_3 \rightarrow \text{HOP}(\text{OCH}_3)_3^+ + \text{OP}(\text{OCH}_3)_2$	2.8	
$\text{OP}(\text{OCH}_3)_3^+ + \text{OP}(\text{OCH}_3)_3 \rightarrow \text{HOP}(\text{OCH}_3)_3^+ + \text{OP}(\text{OCH}_2)(\text{OCH}_3)_2$	2.0	
$\text{HOP}(\text{OCH}_3)_3^+ + \text{OP}(\text{OCH}_3)_3 \rightarrow \text{H}(\text{OP}(\text{OCH}_3)_3)_2^+$	0.7	

<sup>a</sup>All data from trapped-ion studies at 70 eV. <sup>b</sup>In units of  $10^{-10} \text{ cm}^3 \text{ molecule}^{-1} \text{ sec}^{-1}$ . All constants except that for  $\text{HOPO}(\text{OCH}_3)^+$  is an average of two determinations. Accuracy in rate constants estimated to be  $\pm 50\%$  due to uncertainties in pressure measurement.

## FIGURE 5

Temporal variation of ion concentrations in triethyl phosphate at  $1.4 \times 10^{-6}$  Torr pressure and 70 eV electron energy.

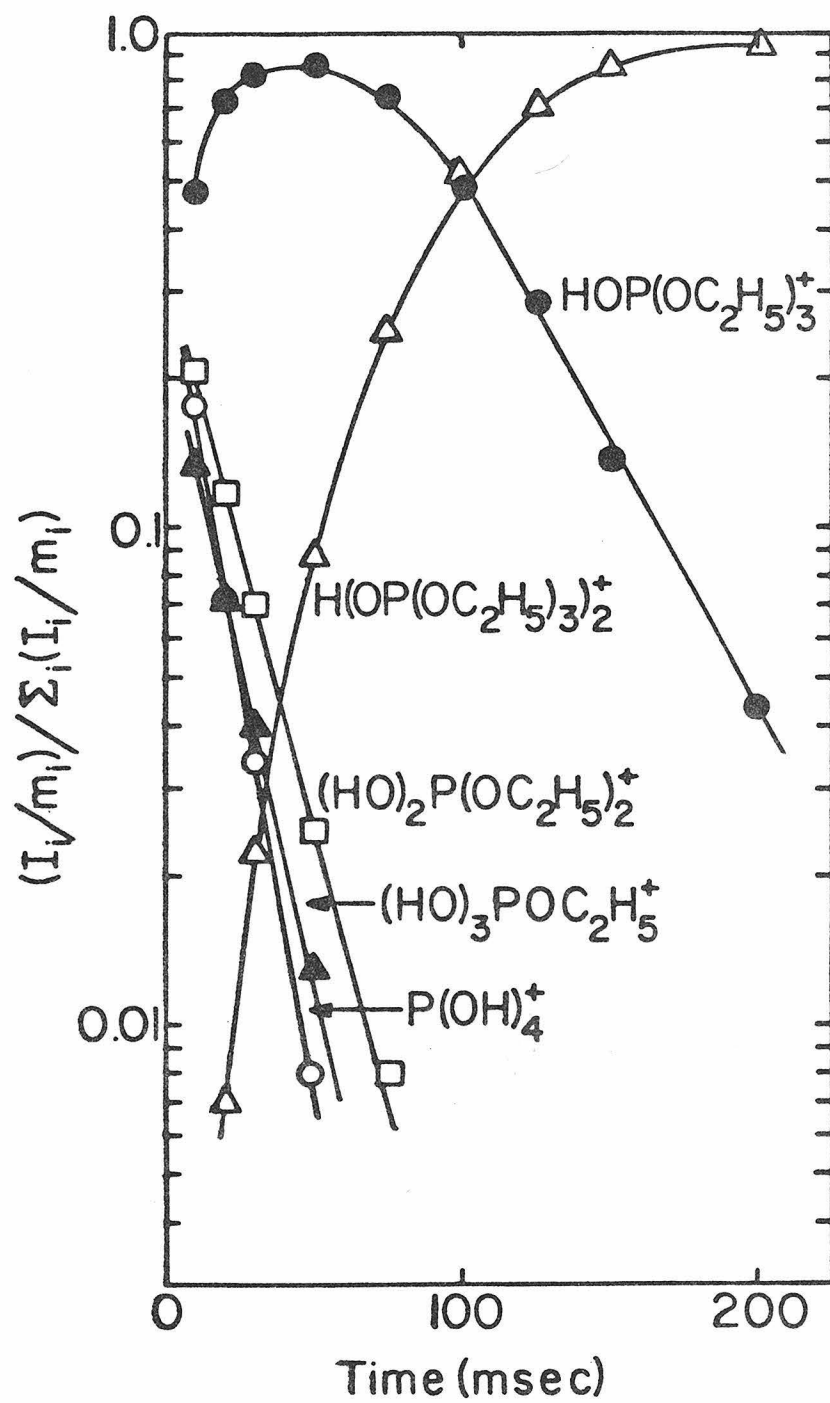


Table V. Rate Constants for the Ion-Molecule Reactions in Triethyl Phosphate<sup>a</sup>

Reactions	$k_i^b$
$P(OH_4)^+ + OP(OC_2H_5)_3 \rightarrow HOP(OC_2H_5)_3^+ + OP(OH)_3$	17
$(HO)_3POC_2H_5 + OP(OC_2H_5)_3 \rightarrow HOP(OC_2H_5)_3^+ + OP(OH)_2OC_2H_5$	15
$(HO)_2P(OC_2H_5)_2^+ + OP(OC_2H_5)_3 \rightarrow HOP(OC_2H_5)_3^+ + OP(OH)(OC_2H_5)_2$	12
$HOP(OC_2H_5)_3^+ + OP(OC_2H_5)_3 \rightarrow H(OP(OC_2H_5)_3)_2^+$	6.0

<sup>a</sup>All data from trapped-ion studies at 70 eV. <sup>b</sup>In units of  $10^{-10}$   $cm^3 molecule^{-1} sec^{-1}$ . Each constant is an average of three determinations. Accuracy in the rate constants estimated to be  $\pm 50\%$  due to uncertainties in pressure measurement.

transfer occurs in one direction in mixtures of triethyl phosphate and certain bases permits the assessment of upper and lower limits for the proton affinity of triethyl phosphate. In mixtures of triethyl phosphate with 3-acetylpyridine and with pyridazine, proton transfer in both directions is detected in double resonance experiments. This indicates that the free energy of protonation of triethyl phosphate is within about 2 kcal/mol of that of these compounds. The results of these experiments are summarized in Table III. The proton affinity of triethyl phosphate is estimated to be  $214 \pm 2$  kcal/mol.

Trimethyl Phosphorothionate. Mass Spectrum. The mass spectrum of trimethyl phosphorothionate has not been previously reported. The ions observed in the 70 eV icr mass spectrum are listed in Table VI. The mass spectrum closely resembles that of  $\text{SP}(\text{SCH}_3)(\text{OCH}_3)_2$ .<sup>27</sup> A major difference between the spectra is the decreased abundance of  $\text{SP}(\text{OCH}_3)_2^+$  ( $\underline{\text{m/e}}$  125) in the spectrum of  $\text{SP}(\text{OCH}_3)_3$ . This is due to the greater strength of the P-OR bond relative to the P-SR bond in the radical cation.

Ion Chemistry. Trapped ion experiments were performed at electron energies of 14 and 19 eV. The major primary ions present at these electron energies are  $\text{P}(\text{OCH}_3)_2^+$  ( $\underline{\text{m/e}}$  93),  $\text{HSP}(\text{OCH}_3)_2^+$  ( $\underline{\text{m/e}}$  126), and  $\text{SP}(\text{OCH}_3)_3^+$  ( $\underline{\text{m/e}}$  156). Ion abundances are plotted as a function of time in Figures 6, 7, and 8. The three primary ions initiate three complex reaction sequences. The parent ion,  $(\text{CH}_3\text{O})_3\text{PS}^+$  ( $\underline{\text{m/e}}$  156), clusters with the parent neutral (reaction 21).

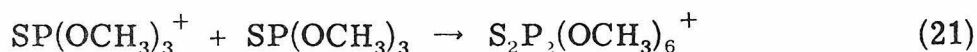


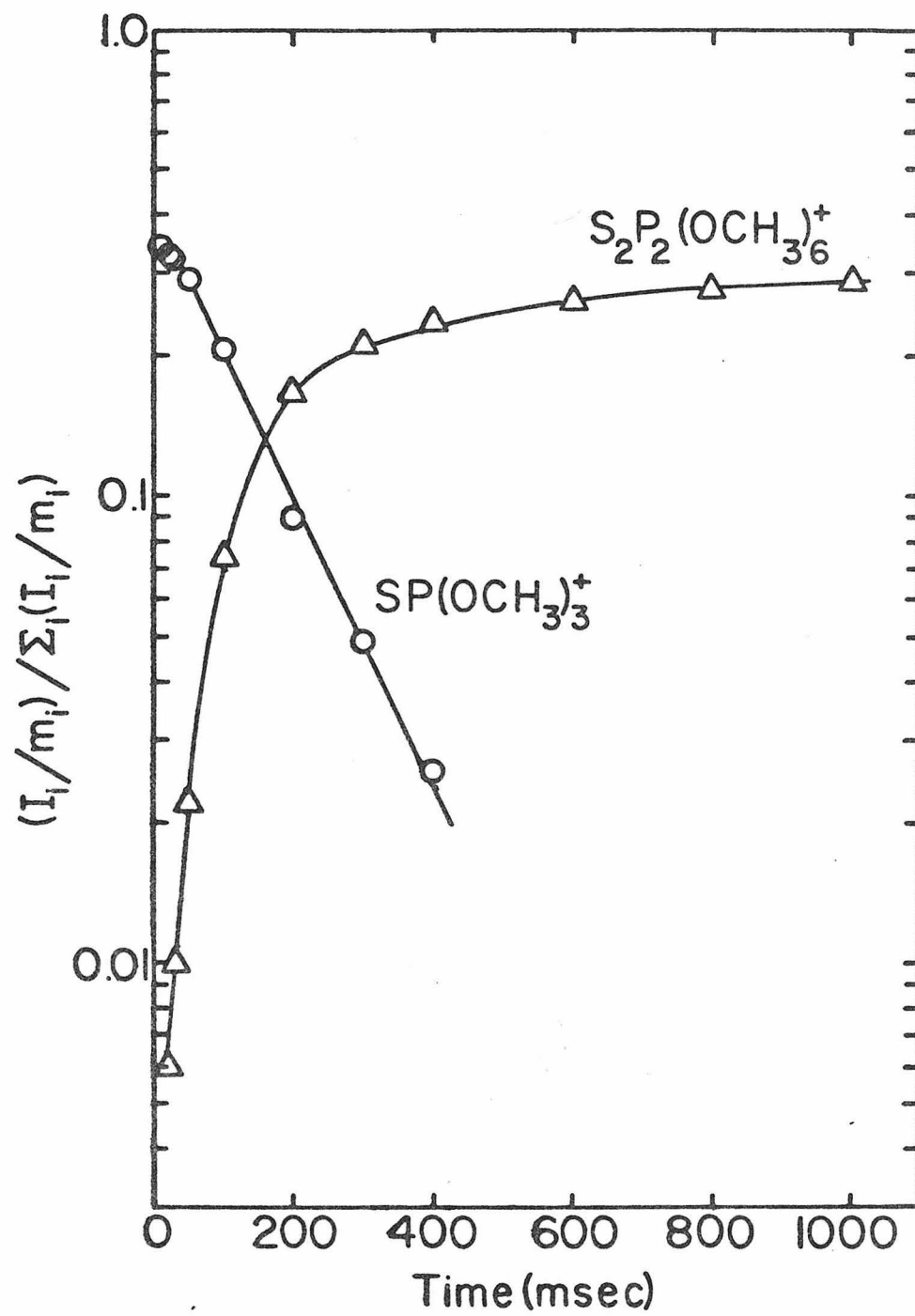


Table VI. The Mass Spectrum of Trimethyl Phosphorothionate at 70 eV

m/e	Ion Assignment	Relative Intensity
15	$\text{CH}_3^+$	12
45	$\text{CHS}^+$ and/or $\text{C}_2\text{H}_5\text{O}^+$	4
47	$\text{PO}^+$ and/or $\text{CH}_3\text{S}^+$	17
62	$\text{CH}_3\text{OP}^+$ and/or $\text{C}_2\text{H}_6\text{S}^+$	5
63	$\text{PS}^+$ and/or $\text{CH}_4\text{OP}^+$	27
79	$\text{CH}_4\text{O}_2\text{P}^+$	13
80	$\text{CH}_5\text{O}_2\text{P}^+$	2
93	$\text{C}_2\text{H}_6\text{O}_2\text{P}^+$	100
94	$\text{CH}_3\text{OPS}^+$	5
109	$\text{C}_2\text{H}_6\text{OPS}^+$	4
111	$\text{CH}_4\text{O}_2\text{PS}^+$	2
125	$\text{C}_2\text{H}_6\text{O}_2\text{PS}^+$	12
126 } 128 }	$\text{C}_2\text{H}_7\text{O}_2\text{PS}^+$	48
		3
156 } 158 }	$\text{C}_3\text{H}_9\text{O}_3\text{PS}^+$	68
		3
157	$\text{C}_3\text{H}_{10}\text{O}_3\text{PS}^+$	8

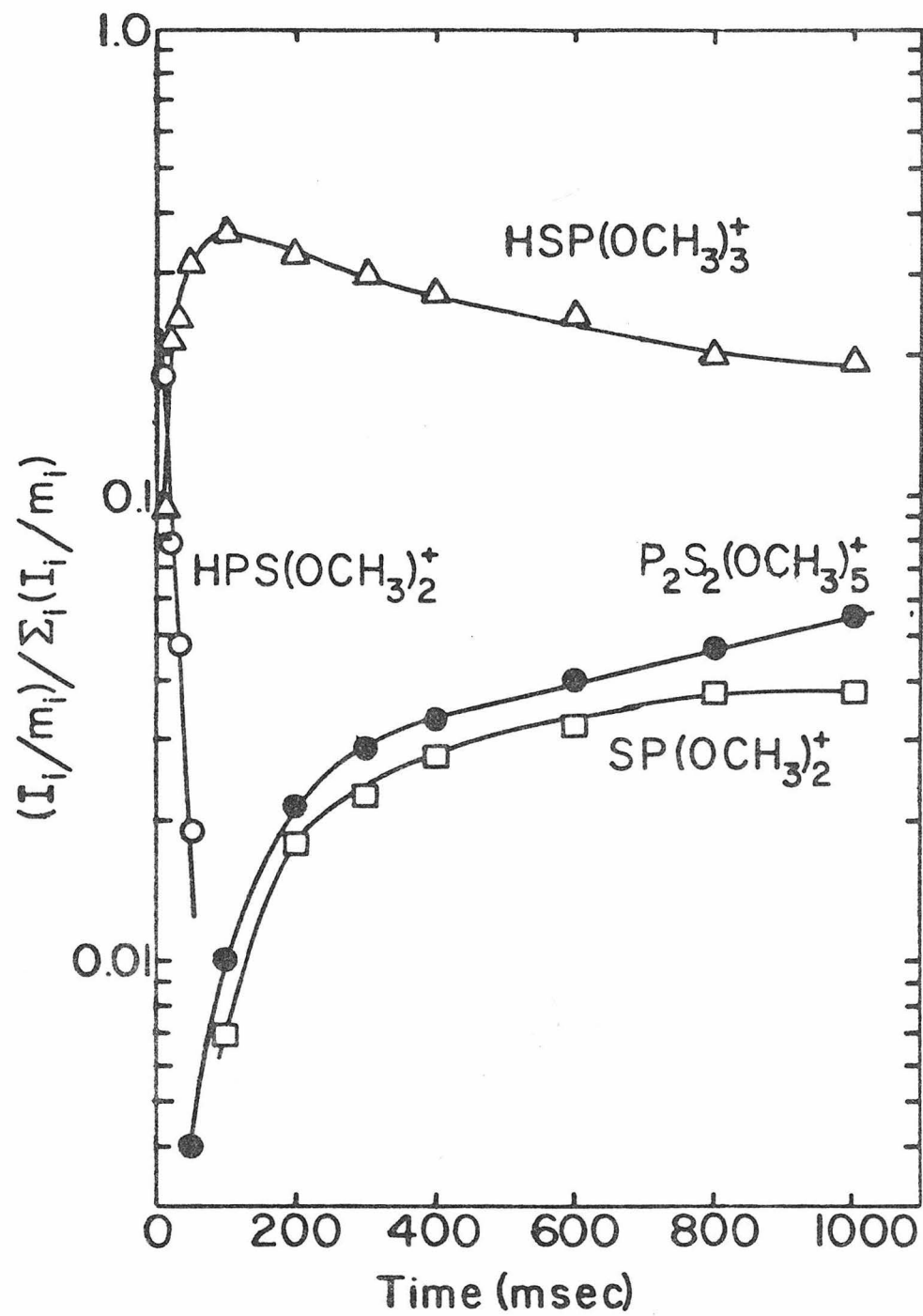
## FIGURE 6

Temporal variation of ion concentrations in trimethyl phosphorothionate at  $1.3 \times 10^{-6}$  Torr pressure and 19 eV electron energy. The primary ion  $\text{SP}(\text{OCH}_3)_3^+$  and the product of its reaction.



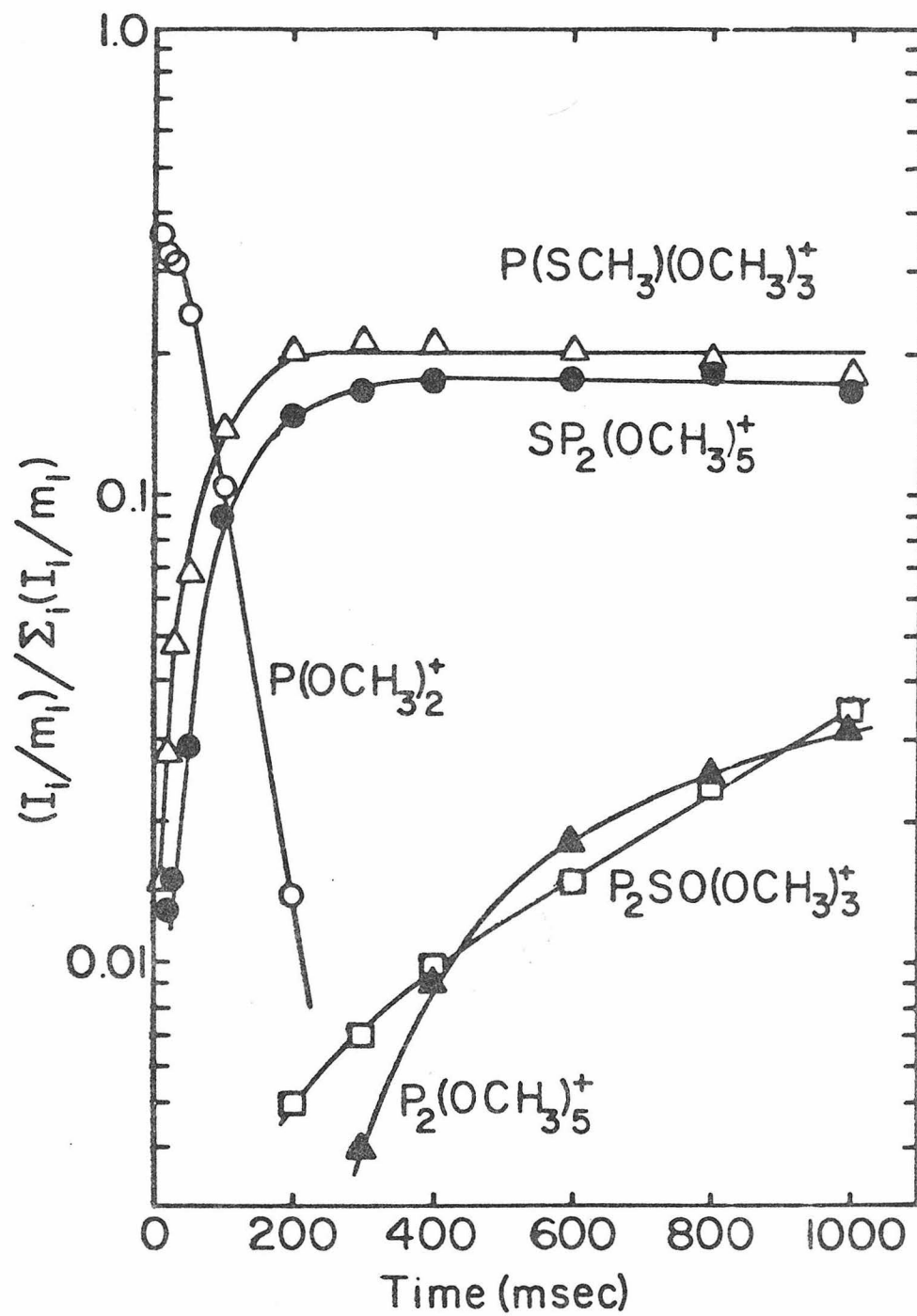
## FIGURE 7

Temporal variation of ion concentrations in trimethyl phosphorothionate at  $1.3 \times 10^{-6}$  Torr pressure and 19 eV electron energy. The primary ion  $\text{HPS}(\text{OCH}_3)_2^+$  and the products of its reactions.

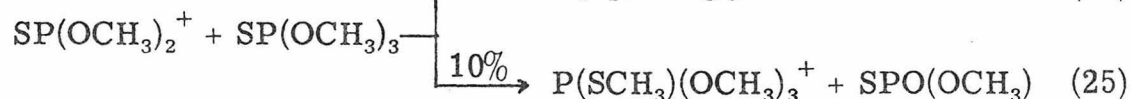
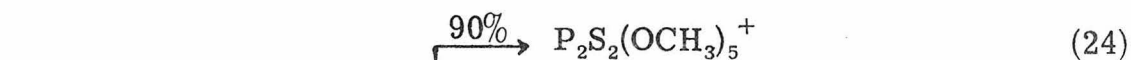
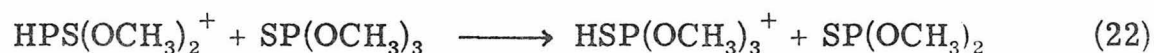


## FIGURE 8

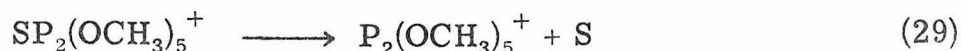
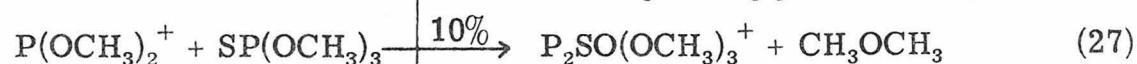
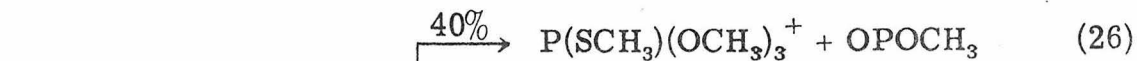
Temporal variation of ion concentrations in trimethyl phosphorothionate at  $1.3 \times 10^{-6}$  Torr pressure and 19 eV electron energy. The primary ion  $\text{P}(\text{OCH}_3)_2^+$  and the products of its reactions.



Rapid proton transfer from  $\text{HPS}(\text{OCH}_3)_2^+$  ( $\underline{\text{m/e}}$  126) to the neutral yields  $\text{HSP}(\text{OCH}_3)_3^+$  (reaction 22). The protonated parent loses methanol to give  $\text{SP}(\text{OCH}_3)_2^+$  ( $\underline{\text{m/e}}$  125) (reaction 23). Loss of S from  $\text{HSP}(\text{OCH}_3)_3^+$  would also result in an ion of  $\underline{\text{m/e}}$  125, however, this process is thermodynamically less favorable. In reaction 24  $\text{SP}(\text{OCH}_3)_2^+$  ( $\underline{\text{m/e}}$  125) forms the cluster ion  $\text{P}_2\text{S}_2(\text{OCH}_3)_5^+$  ( $\underline{\text{m/e}}$  281). A small fraction of  $\text{SP}(\text{OCH}_3)_2^+$  transfers  $\text{CH}_3^+$  to the neutral to give  $\text{P}(\text{SCH}_3)(\text{OCH}_3)_3^+$  ( $\underline{\text{m/e}}$  171) (reaction 25).



The fragment ion  $\text{P}(\text{OCH}_3)_2^+$  ( $\underline{\text{m/e}}$  93) also transfers  $\text{CH}_3^+$  (reaction 26). The minor product ion  $\text{P}_2\text{SO}(\text{OCH}_3)_3^+$  ( $\underline{\text{m/e}}$  203) is formed in the condensation reaction 27. This mass could correspond to  $\text{HP}_2\text{O}(\text{OCH}_3)_4^+$ , which would result from a condensation with loss of  $\text{CH}_2\text{S}$ , rather than  $\text{CH}_3\text{OCH}_3$ . The ion  $\text{P}(\text{OCH}_3)_2^+$  also clusters with the neutral (reaction 28). A portion of the clusters expel a sulfur atom to give  $\text{P}_2(\text{OCH}_3)_5^+$  ( $\underline{\text{m/e}}$  217) (reaction 29). Loss of a sulfur atom is a common





fragmentation pathway observed in the mass spectra of phosphorothionates.<sup>27, 29</sup> The rate constants for the reactions of the primary ions are summarized in Table VII.

Proton Affinity. In mixtures of  $(\text{CH}_3\text{O})_3\text{PS}$  and p-methoxybenzaldehyde equilibrium between the protonated parent ions of the two species was achieved. Processes, such as reaction 23, which involve the protonated parent ion, were sufficiently slow to permit equilibrium to be obtained. Data from these experiments are presented in Table III. The proton affinity of trimethyl phosphorothionate is  $211.9 \pm 0.3$  kcal/mol.

## Discussion

Ion Chemistry. Although the number of ion-molecule reactions of these phosphorus esters is large, they fall with few exceptions into one of two classes: reactions in which a tetracoordinated phosphonium ion is formed and clustering reactions. The phosphonium ions  $\text{P}(\text{OCH}_3)_4^+$ ,  $\text{P}(\text{CH}_3)(\text{OCH}_3)_3^+$  and  $\text{P}(\text{SCH}_3)(\text{OCH}_3)_3^+$  are formed in reactions 8, 10, 17, 25, and 26. The protonated parent ions of each of these esters may also be classified as tetracoordinated phosphonium ions. Solution studies of protonated phosphorus compounds in strongly ionizing media have shown that phosphates<sup>30</sup> and thiophosphates<sup>31</sup> are protonated on the phosphoryl oxygen and sulfur and that phosphites<sup>30</sup> are protonated on phosphorus. There is no expectation that the site of protonation differs in the gas phase. The gas phase proton affinities of phosphorus bases are higher than those of similar oxygen bases.<sup>6, 11</sup> Thus, it is reasonable that phosphites should be protonated on phosphorus.

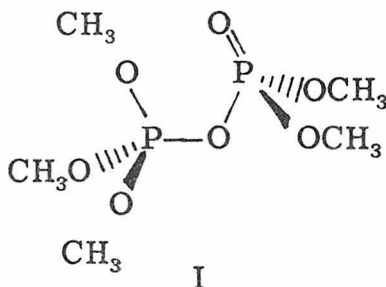
The cluster ions are of two types, proton bound dimers and ions with the formula  $\text{P}_2\text{X}_a(\text{OCH}_3)_b$  ( $\text{X} = \text{O}$  or  $\text{S}$ ,  $a = 0-2$ ,  $b = 3, 5$ , or  $6$ ).

Table VII. Rate Constants for the Primary Ion-Molecule Reactions in Trimethyl Phosphorothionate<sup>a</sup>

Reactions		$k_i^b$	$\Sigma k_i^b$
$P(OCH_3)_2^+ + SP(OCH_3)_3$	$\rightarrow P(SCH_3)(OCH_3)_3^+ + OPOCH_3$	1.1	2.7
	$\rightarrow P_2SO(OCH_3)_3^+ + CH_3OCH_3$	0.3	
	$\rightarrow SP_2(OCH_3)_5^+$	1.3	
$HPS(OCH_3)_2^+ + SP(OCH_3)_3 \rightarrow HSP(OCH_3)_3^+ + SP(OCH_3)_2$		7.0	
$SP(OCH_3)_3^+ + SP(OCH_3)_3 \rightarrow S_2P_2(OCH_3)_6^+$		1.7	

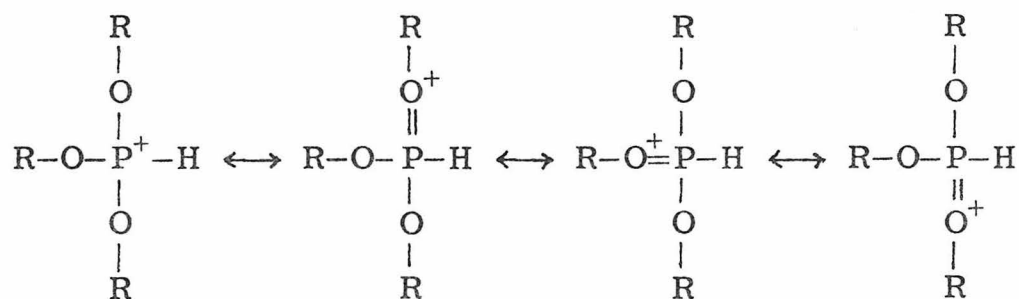
<sup>a</sup>All data from trapped ion studies at 14 eV. <sup>b</sup>In units of  $10^{-10} \text{ cm}^3 \text{ molecule}^{-1} \text{ sec}^{-1}$ . Each constant is an average of three determinations. Accuracy in rate constants is estimated to be  $\pm 50\%$  due to uncertainties in pressure measurement.

The bimolecular rate constants for the clustering reactions remain within  $\pm 20\%$  of their average values over pressures which vary by at least a factor of two in the pressure range  $10^{-7}$ - $10^{-5}$  Torr employed in these experiments. The clustering reactions are, therefore, largely bimolecular at these pressures. Evidence for bimolecular kinetics has also been found for clustering reactions in fluoromethyl silanes.<sup>32</sup> Formation of the proton bound dimers occurs in the phosphates. Reasonable structures for the other cluster ions can be suggested by considering that the ion results from donation of lone pair electrons from the neutral to the phosphorus atom of the ion. For example, structure I can be proposed for the product ion  $P_2O_2(OCH_3)_5^+$  ( $m/e$  249) formed in reaction 18.



Proton Affinities, Adiabatic Ionization Potentials and Homolytic Bond Dissociation Energies. The proton affinities, adiabatic ionization potentials and homolytic bond dissociation energies of the phosphorus esters and related compounds are listed in Table I. A number of trends in these quantities are noteworthy. The proton affinity order  $PA(SP(OCH_3)_3) > PA(OP(OCH_3)_3)$  reflects the decreased electronegativity<sup>33</sup> and increased polarizability<sup>34</sup> of sulfur compared to oxygen. The same order applies to other related sulfur and oxygen compounds, e.g.,  $PA(H_2S) > PA(H_2O)$ .<sup>11</sup>

The proton affinities of tervalent compounds in Table I decrease with increasing electron withdrawing ability of the substituents in the series  $\text{P}(\text{CH}_3)_3$ ,  $\text{P}(\text{OCH}_3)_3$ ,  $\text{PF}_3$ . The same substituent effect is present in the solution basicity order  $\text{PA}(\text{OP}(\text{CH}_3)_3) > \text{PA}(\text{OP}(\text{OCH}_3)_3)$ .<sup>35</sup> The  $^{31}\text{P}$  nmr chemical shift of  $\text{P}(\text{OCH}_3)_3$  lies 202 ppm downfield from that of  $\text{P}(\text{CH}_3)_3$  (Table VIII). The deshielding effect of  $-\text{OCH}_3$  relative to  $-\text{CH}_3$  can also be understood on the basis of the relative inductive effects of these groups. However, protonation of  $\text{P}(\text{OCH}_3)_3$  results in a remarkably large shielding effect on the  $^{31}\text{P}$  nmr shift whereas the phosphorus of  $\text{P}(\text{CH}_3)_3$  is deshielded upon protonation (Table VIII). Shielding of the phosphorus atom has been attributed to the ability of the alkoxy groups to disperse the positive charge in phosphonium ions by the formation of  $\text{d}\pi\text{-p}\pi$  bonds to phosphorus.<sup>30</sup>



Such charge dispersal should increase the proton affinity of phosphates relative to phosphines. The observed proton affinity order, though, indicates that the inductive effect is dominant.

The homolytic bond dissociation energies of  $\text{OP}(\text{OCH}_3)_3$ ,  $\text{OP}(\text{OC}_2\text{H}_5)_3$ , and  $\text{OPF}_3$  are large in comparison with those of the most common oxygen bases (e.g.,  $\text{D}((\text{CH}_3)_2\text{CO}^+-\text{H}) = 104 \text{ kcal/mol}$ <sup>36</sup>). Substitution of  $\text{CH}_3\text{O}$  for  $\text{CH}_3$  in  $\text{R}_2\text{CO}$  to give the carbonyl analog of

Table VIII.  $^{31}\text{P}$  nmr Chemical Shifts in  $\text{P}(\text{CH}_3)_3^{\text{a}}$  and  $\text{P}(\text{OCH}_3)_3^{\text{b}}$  and Their Conjugate Acids

Base	$\delta_{^{31}\text{P}}^{\text{c}}$	Conjugate Acid	$\delta_{^{31}\text{P}}^{\text{c}}$
$\text{P}(\text{CH}_3)_3$	+ 62.2	$\text{HP}(\text{CH}_3)_3^+$	+ 3.2
$\text{P}(\text{OCH}_3)_3$	-139.7	$\text{HP}(\text{OCH}_3)_3^+$	-24.7

<sup>a</sup>G. A. Olah and C. W. McFarland, J. Org. Chem., 34, 1832 (1969).

<sup>b</sup>Reference 30. <sup>c</sup>ppm relative to 85%  $\text{H}_3\text{PO}_4$ .

$\text{OP}(\text{OCH}_3)_3$  results in a marked increase in homolytic bond dissociation energy to  $D((\text{CH}_3\text{O})_2\text{CO}^+ - \text{H}) = 128 \text{ kcal/mol}$ .<sup>37</sup> The substituents  $\text{CH}_3\text{O}$  and  $\text{F}$  are probably responsible for the large bond energies in the phosphoryl compounds. These substituents must stabilize the conjugate acid relative to the molecular ion. The mechanism of the stabilization may involve both inductive and resonance effects. Clarification of the role of these effects requires data for systems in which the effects are separable or quantum mechanical calculations of the ions.

The proton affinity of triethyl phosphate exceeds that of trimethyl phosphate by  $4.5 \text{ kcal/mol}$ . This methyl substituent effect appears to be large, considering that the additional substitution occurs three bonds distant from the site of protonation. The difference in the proton affinities of tripropyl and tributyl amine is only  $1.4 \text{ kcal/mol}$ .<sup>38</sup> In the protonated phosphates considerable positive charge is located on the alkoxy oxygens and phosphorus, which are one and two bonds distant from the alkyl groups. Thus, charge dispersal enhances the substituent effect of the alkyl group.

The difference in the heats of protonation of trimethyl and triethyl phosphate in  $\text{HSO}_3\text{F}$  is quite small, only  $0.2 \text{ kcal/mol}$ . The inductive effect of the larger alkyl groups is almost completely neutralized by opposing effects in the enthalpies of solvation. The difference in the heats of solvation of  $\text{OP}(\text{OCH}_3)_3$  and  $\text{OP}(\text{OC}_2\text{H}_5)_3$  is  $1.6 \text{ kcal/mol}$ .<sup>39</sup> Using the thermodynamic cycle previously described,<sup>40</sup> a difference in the heats of solvation of the conjugate acids ( $\Delta H_S((\text{CH}_3\text{O})_3\text{POH}^+) - \Delta H_S((\text{C}_2\text{H}_5\text{O})_3\text{POH}^+)$ ) of  $-2.6 \text{ kcal/mol}$  is obtained. This value is similar to the difference of  $-1.9 \text{ kcal/mol}$  between the heats of solvation of  $(\text{CH}_3)_3\text{NH}^+$  and  $(\text{C}_2\text{H}_5)_2\text{NH}^+$ .<sup>40</sup>

Assignment of the Photoelectron Spectrum of  $\text{P}(\text{OCH}_3)_3$ . Correlations of the homolytic bond dissociation energies of homologous compounds can aid in the assignment of their photoelectron spectra.<sup>12</sup> The first ionization potential of trimethyl phosphite has been assigned to the phosphorus lone pair<sup>41</sup> and, more recently, to oxygen lone pairs.<sup>42</sup> Using an estimated adiabatic ionization potential of the band assigned by the latter authors to the phosphorus lone pair yields a correlated homolytic bond dissociation energy for  $\text{P}(\text{OCH}_3)_3$  of 151 kcal/mol. This value is unreasonably high in comparison with other values in Table I. This discrepancy could be resolved by assuming that the phosphite is protonated on oxygen. However, for reasons given above, this possibility seems unlikely. The more acceptable alternative is to assign the first ionization potential to the phosphorus lone pair.

Chemical Ionization Mass Spectrometry. An optimum system for chemical ionization mass spectrometric analysis of a class of compounds is one in which the desired compounds are selectively ionized and give spectra with prominent molecular or quasimolecular ions. Chemical ionization of the phosphorus esters dioxathan and phosphamidon using the reagent gas isobutane yielded a quasimolecular ion only for the latter compound.<sup>43</sup> The relatively high proton affinities of the phosphorus esters in the present work suggest that these compounds would be amenable to ionization by selective protonation. Selective protonation is accomplished by using a reagent gas of high proton affinity. This technique has two advantages: (1) contaminants in the sample which have lower proton affinities than the reagent gas are not represented in the chemical ionization mass spectrum and

(2) protonation of sample molecules is "softer" (less exothermic) than protonation by ions in more traditional reagent gases ( $\text{CH}_4$ ,  $\text{C}_4\text{H}_{10}$ ) with the result that fragmentation is reduced. Reagent gases consisting of mixtures of hydrocarbons and amines have been used to produce chemical ionization mass spectra of alkyl diphenyl phosphine oxides<sup>44</sup> and tri-(2-butoxyethyl) phosphate<sup>45</sup> which contain abundant  $[\text{M} + \text{H}]^+$  and other quasimolecular ions.



References and Notes

- (1) For an overview of organophosphorus chemistry, see A. J. Kirby and S. G. Warren, "The Organic Chemistry of Phosphorus," Elsevier, New York, N.Y., 1967.
- (2) D. Holtz and J. L. Beauchamp, J. Am. Chem. Soc., 91, 5913 (1969).
- (3) J. R. Eyler, Inorg. Chem., 9, 98 (1970).
- (4) D. Holtz, J. L. Beauchamp, and J. R. Eyler, J. Am. Chem. Soc., 92, 7045 (1970).
- (5) J. W. Long and J. L. Franklin, J. Am. Chem. Soc., 96, 2320 (1974).
- (6) R. H. Staley and J. L. Beauchamp, J. Am. Chem. Soc., 96, 6252 (1974).
- (7) R. R. Corderman and J. L. Beauchamp, Inorg. Chem., submitted for publication.
- (8) S. A. Sullivan and J. L. Beauchamp, Inorg. Chem., submitted for publication.
- (9) D. A. Dixon and J. L. Beauchamp, unpublished results.
- (10) T. C. Rhyne and J. G. Dillard, Int. J. Mass Spectrom. Ion Phys., 7, 371 (1971).
- (11) J. F. Wolf, R. H. Staley, I. Koppel, M. Taagepera, R. T. McIver, Jr., J. L. Beauchamp, and R. W. Taft, J. Am. Chem. Soc., 99, 5417 (1977).
- (12) R. H. Staley, J. E. Kleckner, and J. L. Beauchamp, J. Am. Chem. Soc., 98, 2081 (1976).
- (13) D. W. Hutchinson, Organophosphorus Chem., 6, 124 (1974).

- (14) J. Matheja and E. T. Degens, "Structural Biology of Phosphates, " Gustav Fischer Verlag, Stuttgart, Germany, 1971.
- (15) H. G. Khorana, "Some Recent Developments in the Chemistry of Phosphate Esters of Biological Interest, " Wiley, New York, N.Y., 1961.
- (16) R. D. O'Brien, "Toxic Phosphorus Esters, Chemistry, Metabolism and Biological Effects, " Academic Press, New York, N.Y., 1960.
- (17) Ibid., pp. 329-334.
- (18) Ibid., p. 336.
- (19) G. W. A. Milne and M. J. Lacey, CRC Crit. Rev. Anal. Chem., 4, 45 (1974).
- (20) J. L. Beauchamp, Ann. Rev. Phys. Chem., 22, 527 (1971).
- (21) T. B. McMahon and J. L. Beauchamp, Rev. Sci. Instrum., 43, 509 (1972).
- (22) J. L. Occolowitz and G. L. White, Anal. Chem., 35, 1179 (1963).
- (23) The neutral products of all reactions are inferred.
- (24) R. V. Hodges and J. L. Beauchamp, Inorg. Chem., 14, 2887 (1975).
- (25) L. Hellner and L. W. Sieck, Int. J. Chem. Kin., 5, 177 (1973).
- (26) S. W. Benson, "Thermochemical Kinetics, " 2nd Ed., Wiley, New York, N.Y., 1976, p. 47.
- (27) E. Santoro, Org. Mass Spectrom., 7, 589 (1973).
- (28) D. A. Bafus, E. J. Gallegos, and R. W. Kiser, J. Phys. Chem., 70, 2614 (1966).
- (29) R. G. Cooks and A. F. Gerrard, J. Chem. Soc. (B), 1327 (1968).
- (30) G. A. Olah and C. W. McFarland, J. Org. Chem., 36, 1374 (1971).

- (31) G. A. Olah and C. W. McFarland, J. Org. Chem., 40, 2582 (1975).
- (32) M. K. Murphy and J. L. Beauchamp, J. Am. Chem. Soc., 98, 578 (1976).
- (33) R. T. Sanderson, "Inorganic Chemistry," Reinhold, New York, N.Y., 1967, p. 78
- (34) Ibid., p. 54.
- (35) E. M. Arnett, E. J. Mitchell, and T. S. S. R. Murty, J. Am. Chem. Soc., 96, 3875 (1974).
- (36) Calculated from  $PA((CH_3)_2CO) = 193.9$  kcal/mol, Reference 11, and  $IP((CH_3)_2CO) = 224$  kcal/mol, B. J. Cocksey, J. H. D. Eland, and C. J. Danby, J. Chem. Soc. (B), 790 (1971).
- (37) Calculated from  $PA((CH_3O)_2CO) = 197.2$  kcal/mol, Reference 11, and  $IP((CH_3O)_2CO) = 244$  kcal/mol, estimated from the photo-electron spectrum published in S. P. McGlynn and J. L. Meeks, J. El. Spectrosc. Rel. Phen., 8, 85 (1976).
- (38) D. H. Aue, H. M. Webb, and M. T. Bowers, J. Am. Chem. Soc., 98, 311 (1976).
- (39) The heats of solution of the gaseous phosphates are calculated from heats of solution for the liquid phosphates in Reference 35 and heats of vaporization in D. P. Evans, W. C. Davies, and W. J. Jones, J. Chem. Soc., 1310 (1930).
- (40) D. H. Aue, H. M. Webb, and M. T. Bowers, J. Am. Chem. Soc., 98, 318 (1976).
- (41) D. Betteridge, M. Thompson, A. D. Baker, and N. R. Kemp, Anal. Chem., 44, 2005 (1972).
- (42) A. H. Cowley, D. W. Goodman, N. A. Kuebler, M. Sanchez, and J. G. Verkade, Inorg. Chem., 16, 854 (1977).

- (43) H. M. Fales, G. W. A. Milne, H. U. Winkler, H. D. Beckez, J. N. Damico, and R. Barron, Anal. Chem., 47, 207 (1975).
- (44) S. D. Goff, B. L. Jelus, and E. E. Schweizer, Org. Mass. Spectrom., 12, 33 (1977).
- (45) D. V. Bowen and F. H. Field, Org. Mass Spectrom., 9, 195 (1974).

CHAPTER II

Nucleophilic Reactions of Anions with Trimethyl Phosphate  
in the Gas Phase by Ion Cyclotron Resonance Spectroscopy

by

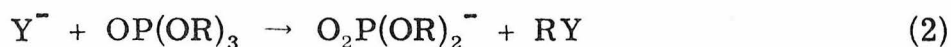
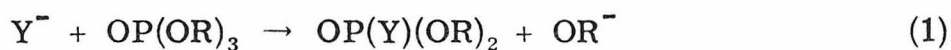
Ronald V. Hodges, S. A. Sullivan, and J. L. Beauchamp

Contribution No. 5690 from the Arthur Amos Noyes  
Laboratory of Chemical Physics, California Institute of  
Technology, Pasadena, California 91125

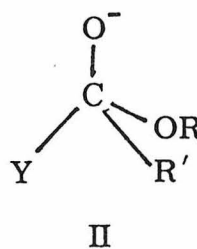
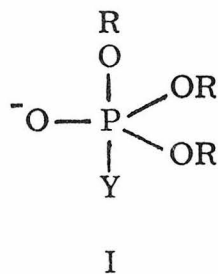
## ABSTRACT

The gas phase ion-molecule reactions of several negative ions ( $\text{SF}_6^-$ ,  $\text{SF}_5^-$ ,  $\text{SO}_2\text{F}^-$ ,  $\text{F}_2^-$ ,  $\text{F}^-$ ,  $\text{CF}_3\text{Cl}^-$ ,  $\text{Cl}^-$ ,  $\text{CD}_3\text{O}^-$ ,  $\text{DNO}^-$ ,  $\text{OH}^-$ , and  $\text{NH}_2^-$ ) with trimethyl phosphate are investigated using ion cyclotron resonance techniques. Nucleophilic attack on  $\text{OP}(\text{OCH}_3)_3$  occurs chiefly at carbon, resulting in displacement of  $\text{O}_2\text{P}(\text{OCH}_3)_2^-$ . This behavior contrasts with that observed in solution, where attack at phosphorus is favored for hard nucleophiles. This difference is ascribed to solvation energetics for the intermediates involved in the two reactions. The failure of  $\text{SF}_6^-$  to transfer  $\text{F}^-$  to  $\text{OP}(\text{OCH}_3)_3$  places an upper limit of  $11 \pm 8$  kcal/mol on the fluoride affinity of  $\text{OP}(\text{OCH}_3)_3$ . The significance of the results for the negative chemical ionization mass spectrometry of phosphorus esters is briefly discussed.

Bimolecular nucleophilic substitution reactions occupy an important place in the chemistry of phosphorus compounds.<sup>1</sup> All classes of phosphorus compounds are susceptible to nucleophilic attack. The esters of phosphoric acid are of special interest because of their biological significance. Some are essential to life processes, while the toxicology of others has commanded attention.<sup>2</sup> The site of nucleophilic attack may be the phosphorus atom or the  $\alpha$  carbon of the ester group.<sup>3, 4</sup> Attack at phosphorus results in transesterification (reaction 1), while attack at carbon displaces the phosphate diester anion (reaction 2). The



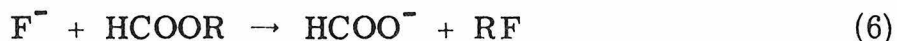
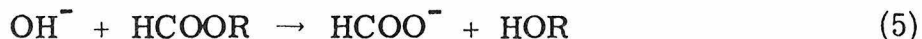
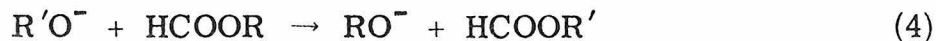
site of attack follows predictions of the theory of hard and soft reagents.<sup>3,5,6</sup> Hard nucleophiles (e.g.,  $OH^-$ ,  $F^-$ ) attack at phosphorus, while soft nucleophiles (e.g.,  $Cl^-$ ,  $H_2O$ ) attack at carbon. Reaction 1 is first order in nucleophile and substrate and occurs with inversion of configuration.<sup>4, 7</sup> The pentacoordinate species I is proposed to exist during the course of the reaction.<sup>8</sup> This species is analogous to the tetrahedral intermediate II, formed by nucleophilic attack on carboxylic esters.



Earlier opinion<sup>10</sup> that species such as I are unstable transition states has given way to the view that in many cases they are intermediates.<sup>8,11-13</sup> reaction 2 is considered to be an S<sub>N</sub>2 displacement at carbon.<sup>4, 14</sup>

Studies of gas phase ion-molecule reactions can provide information about the reactivity of ionic and neutral species in the absence of solvent effects. Gas phase nucleophilic attack of anions on various substrates has been the subject of a number of recent studies.<sup>15-23</sup>

Riveros and coworkers have examined reactions of alkoxide anions, F<sup>-</sup> and OH<sup>-</sup> with alkyl formates.<sup>16, 22</sup> Among the reactions observed are transesterification (for R larger than R', (reaction 4)<sup>22</sup> and formation of the formate anion (reactions 5 and 6).<sup>16</sup> Mechanisms for these



reactions were proposed in which the nucleophile adds to the ester to give the intermediate II, which decomposes to products.

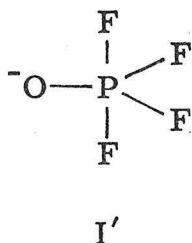
Ions similar to species II have been generated at low pressure in an ion cyclotron resonance (icr) spectrometer by halide transfer from a donor anion to a carbonyl compound (e.g., reaction 7).<sup>18</sup>



An analogous adduct with a phosphorus compound has recently been prepared. SF<sub>6</sub><sup>-</sup> and SF<sub>5</sub><sup>-</sup> transfer F<sup>-</sup> to OPF<sub>3</sub> to give the pentacoordinate anion I'.<sup>24</sup> The binding energy of F<sup>-</sup> to OPF<sub>3</sub> was determined by icr



techniques to be  $59 \pm 1$  kcal/mol.<sup>24</sup>



This paper reports icr investigations of the reactions of a number of anions with trimethyl phosphate. Mechanisms are proposed and compared with those of other gas phase nucleophilic reactions. Differences between the solution and gas phase reactivities of trimethyl phosphate are discussed in terms of solvation effects. The implications of these results for negative chemical ionization mass spectrometry of phosphorus esters are discussed.

### Experimental Section

Experiments were performed using an icr spectrometer built in this laboratory. The general features of icr instrumentation and experimental techniques have been described previously.<sup>25, 26</sup> All reaction pathways were verified in double resonance experiments.<sup>25</sup>

Pressure measurements were made using a Schulz-Phelps gauge located adjacent to the icr cell. This gauge is calibrated for each gas for a given emission current (5  $\mu$ A) and magnetic field (6 kG) against an MKS Instruments Baratron Model 90H1-E capacitance manometer in the region  $10^{-5}$ - $10^{-3}$  Torr where linear variation of gauge current with pressure is observed. Pressures in the trapped ion experiments were in the range  $10^{-7}$ - $10^{-6}$  Torr. Experiments in

the drift mode were carried out at pressures of  $\sim 10^{-5}$  Torr. The uncertainty in the rate constants, estimated to be  $\pm 20\%$ , is due principally to uncertainties in pressure measurement.

Negative ions were generated by electron capture or dissociative electron capture from the following neutral species:  $\text{SF}_6$  ( $\text{SF}_6^-$ ,  $\text{SF}_5^-$ , 70 eV),  $\text{SO}_2\text{F}_2$  ( $\text{SO}_2\text{F}^-$ ,  $\text{F}_2^-$  and  $\text{F}^-$ , 3 eV),  $\text{NF}_3$  ( $\text{F}^-$ , 70 eV),  $\text{CCl}_4$  ( $\text{Cl}^-$ , 70 eV),  $\text{CF}_3\text{COCl}$  ( $\text{Cl}^-$  and  $\text{CF}_3\text{Cl}^-$ , 70 eV),  $\text{CD}_3\text{ONO}$  ( $\text{CD}_3\text{O}^-$  and  $\text{DNO}^-$ , 70 eV),  $\text{H}_2\text{O}$  ( $\text{OH}^-$ , 5 eV) and  $\text{NH}_3$  ( $\text{NH}_2^-$ , 4 eV). The major ions produced from each species and the electron energies employed are given in parentheses.

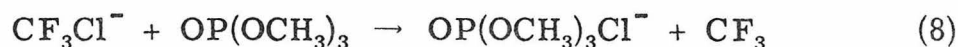
Methyl nitrite was prepared by literature methods.<sup>27</sup> All other chemicals were commercial, reagent grade materials and were used as supplied.

## Results

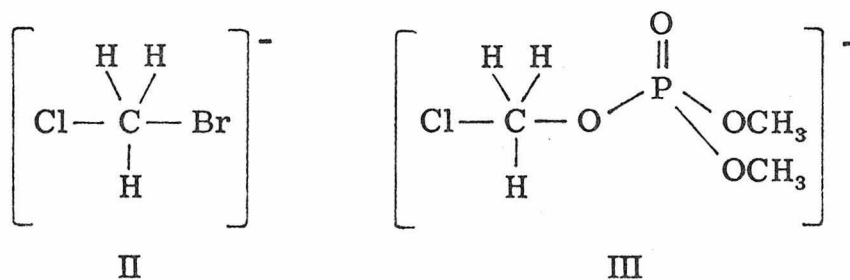
Electron impact of trimethyl phosphate alone at electron energies varying from 0-70 eV produced no abundant negative ions at the pressures employed in these experiments ( $10^{-6}$ - $10^{-5}$  Torr).

The ions  $\text{SF}_6^-$ ,  $\text{SF}_5^-$ ,  $\text{SO}_2\text{F}^-$  and  $\text{F}_2^-$  gave no reaction with  $\text{OP}(\text{OCH}_3)_3$ . In particular, no halide transfer or direct attachment processes to give ion I were observed. Failure to observe  $\text{F}^-$  transfer from  $\text{SF}_5^-$ ,  $\text{SO}_2\text{F}^-$ ,  $\text{F}_2^-$  and  $\text{SF}_6^-$  to  $\text{OP}(\text{OCH}_3)_3$  permits the assignment of upper limits on the fluoride affinity of  $\text{OP}(\text{OCH}_3)_3$  of  $54 \pm 12$ , 45,  $29 \pm 3$ , and  $11 \pm 8$  kcal/mol, respectively.<sup>24</sup>

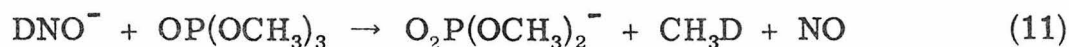
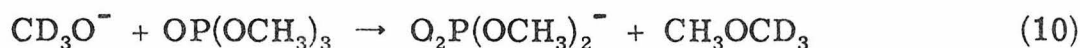
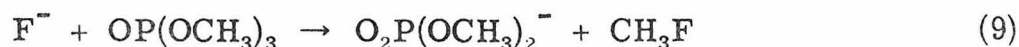
The ion  $\text{CF}_3\text{Cl}^-$  transfers  $\text{Cl}^-$  to  $\text{OP}(\text{OCH}_3)_3$  (reaction 8). Therefore, the chloride affinity of  $\text{OP}(\text{OCH}_3)_3$  is greater than that of  $\text{CF}_3$ .



The chloride affinity of  $\text{CF}_3$  is very low. Even methyl bromide will accept a chloride ion from  $\text{CF}_3\text{Cl}^-$  to form ion II.<sup>15</sup> It is possible that the adduct of  $\text{Cl}^-$  with  $\text{OP}(\text{OCH}_3)_3$  does not assume structure I, but rather structure III or possibly a species where the bonding is even less specific than in I or III.



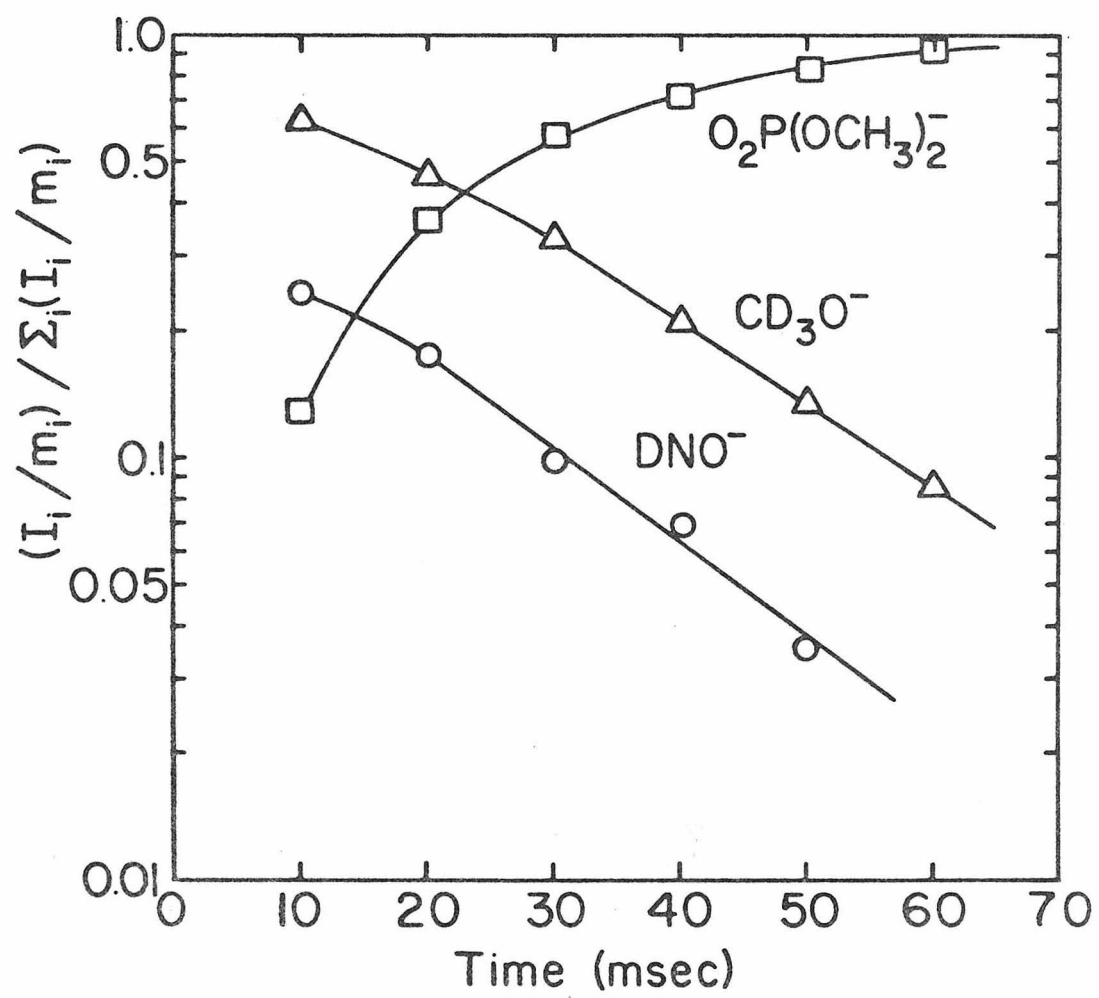
The ions  $\text{F}^-$ ,  $\text{CD}_3\text{O}^-$ , and  $\text{DNO}^-$  displace the phosphate diester anion from trimethyl phosphate (reactions 9, 10 and 11).<sup>28</sup> Figures 1



and 2 illustrate the variation of the abundances of these ions with time. The rate constants determined for these reactions are  $k_9 = 1.6 \times 10^{-9}$ ,  $k_{10} = 1.4 \times 10^{-9}$ , and  $k_{11} = 1.6 \times 10^{-9} \text{ cm}^3 \text{ molecule}^{-1} \text{ sec}^{-1}$ . No deuterium incorporation into the phosphate diester anion formed in reaction 10 occurs. The site of attack in this reaction must, therefore, be the carbon atom. If attack at phosphorus were to occur, giving the intermediate I, pseudorotation<sup>29</sup> in the chemically activated intermediate

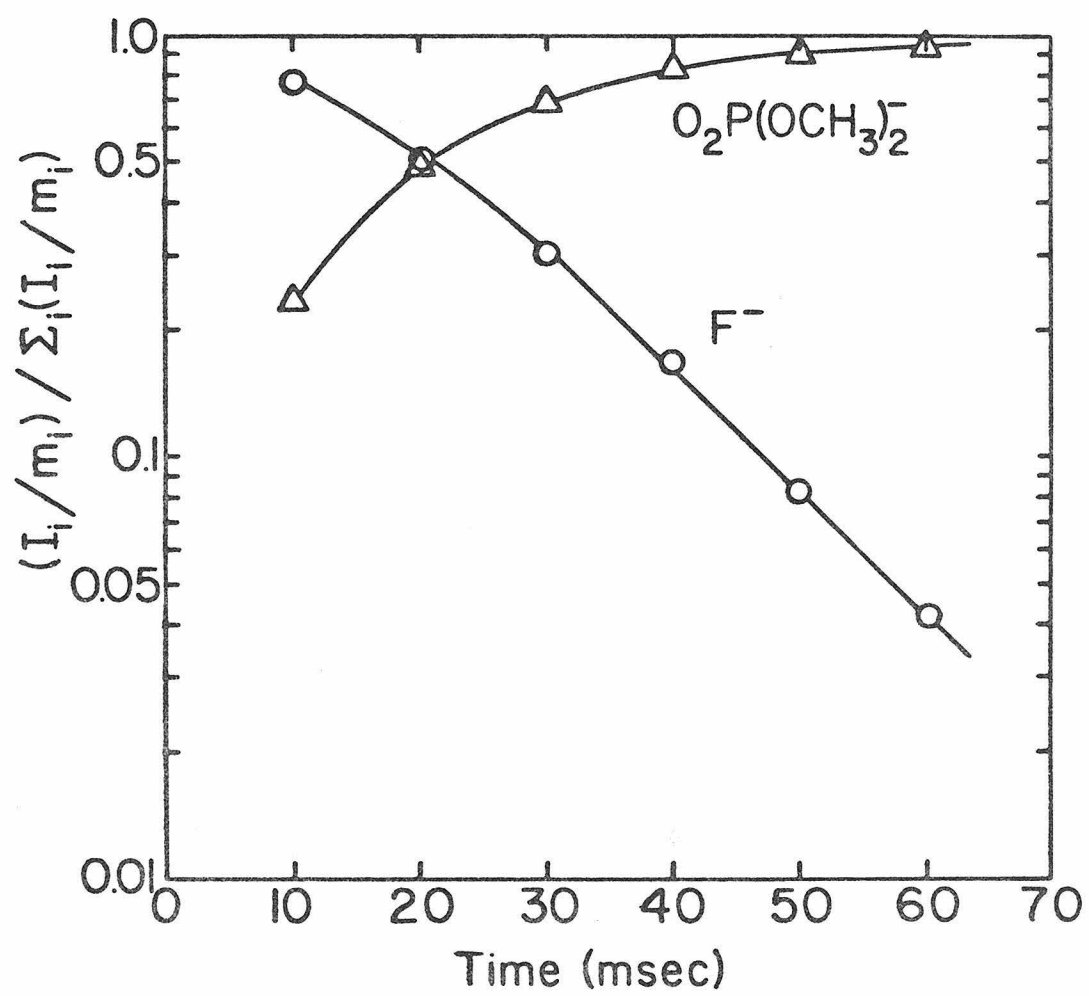
## FIGURE 1

The temporal variation of ion abundances in a mixture of  $\text{OP}(\text{OCH}_3)_3$  (partial pressure  $9.0 \times 10^{-7}$  Torr) and  $\text{CD}_3\text{ONO}$  following a 10 msec, 70 eV electron pulse.



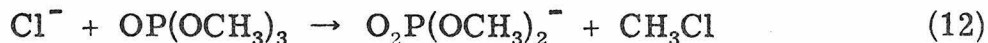
## FIGURE 2

The temporal variation of ion abundances in a mixture of  $\text{OP}(\text{OCH}_3)_3$  (partial pressure  $1.35 \times 10^{-6}$  Torr) and  $\text{NF}_3$  following a 10 msec, 70 eV electron pulse.



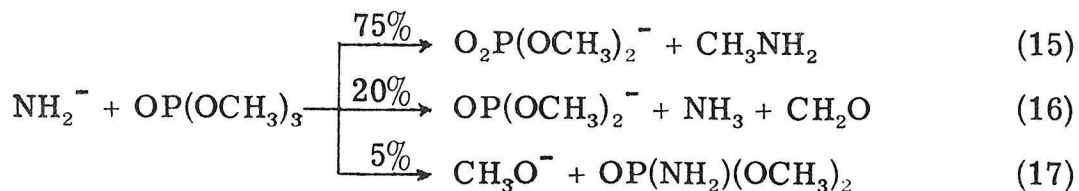
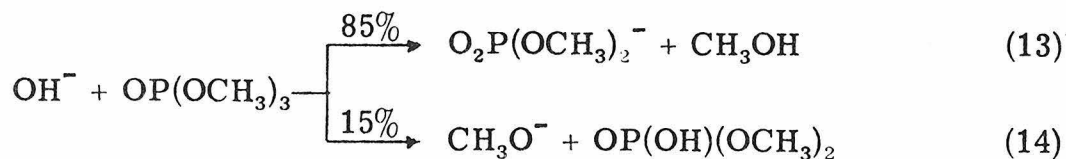
would very likely scramble the methoxy groups in a time much shorter than the lifetime of the intermediate toward loss of dimethyl ether, such that deuterium incorporation into the ionic product would be observed.

$\text{Cl}^-$  produced in a mixture of  $\text{CCl}_4$  and  $\text{OP}(\text{OCH}_3)_3$  was non-reactive. However, when the signal intensity of  $\text{O}_2\text{P}(\text{OCH}_3)_2^-$  in a mixture of  $\text{OP}(\text{OCH}_3)_3$  and  $\text{CD}_3\text{ONO}$  was monitored, a positive double resonance signal from  $\text{Cl}^-$ , which was present as a contaminant, was observed. This suggests that the displacement of  $\text{O}_2\text{P}(\text{OCH}_3)_2^-$  from  $\text{OP}(\text{OCH}_3)_3$  by  $\text{Cl}^-$  (reaction 12) is slightly endothermic, but can occur with translationally excited  $\text{Cl}^-$ .



The phosphate diester anion is the major product ion observed in drift mode mass spectra of mixtures of  $\text{OP}(\text{OCH}_3)_3$  with  $\text{H}_2\text{O}$  and with  $\text{NH}_3$ . Double resonance experiments established that this ion is formed by reaction of  $\text{OH}^-$  and  $\text{NH}_2^-$  (reactions 13 and 15).  $\text{OH}^-$  and  $\text{NH}_2^-$  also displace  $\text{CH}_3\text{O}^-$  from  $\text{OP}(\text{OCH}_3)_3$  (reactions 14 and 17). The amount of  $\text{CH}_3\text{O}^-$  formed in these reactions is uncertain, because  $\text{CH}_3\text{O}^-$  subsequently reacts rapidly to form  $\text{O}_2\text{P}(\text{OCH}_3)_2^-$  (reaction 10). The percentages given for  $\text{CH}_3\text{O}^-$  represent lower limits. However, reaction times in the drift mode are short (a few milliseconds) and the product distribution should, therefore, depend principally on the rate constants of the primary reactions. Double resonance experiments failed to produce any evidence for reaction 10 under these low conversion conditions. The product ion  $\text{OP}(\text{OCH}_3)_2^-$  also results from reaction of  $\text{NH}_2^-$  (reaction 16). This reaction probably occurs by proton transfer from



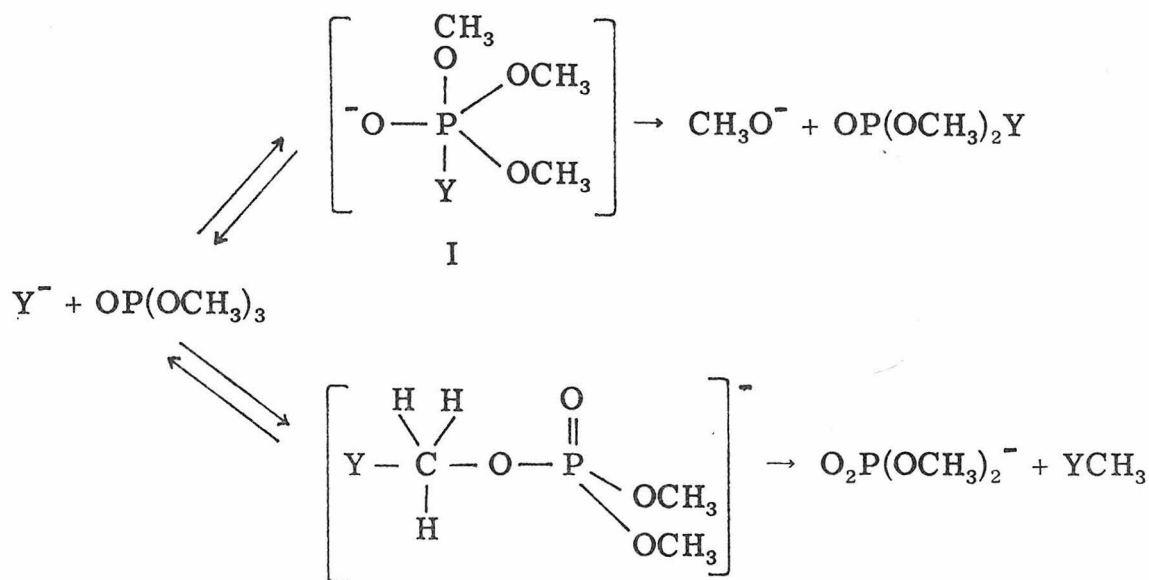


$\text{OP}(\text{OCH}_3)_3$  followed by loss of  $\text{CH}_2\text{O}$  from  $\text{OP}(\text{OCH}_3)_2(\text{OCH}_2)^-$ .

The observation of reaction 16 and the failure of  $\text{OH}^-$  to undergo a similar reaction suggests that the proton affinity of  $\text{OP}(\text{OCH}_3)_2(\text{OCH}_2)^-$  lies between  $\text{PA}(\text{OH}^-) = 390.7 \text{ kcal/mol}^{30, 31}$  and  $\text{PA}(\text{NH}_2^-) = 403.8 \text{ kcal/mol}^{30, 31}$ .

### Discussion

Reaction Mechanism. As in solution the reactions of anions with trimethyl phosphate in the gas phase can be accommodated by a mechanism in which the nucleophile attacks at phosphorus or at carbon (Scheme I). Attack at phosphorus yields a pentacoordinate intermediate I, which can decompose to the reactants or expel  $\text{CH}_3\text{O}^-$ , if displacement of  $\text{CH}_3\text{O}^-$  by  $\text{Y}^-$  is exothermic. Displacement of  $\text{CH}_3\text{O}^-$  is observed for two of the anions in this study,  $\text{OH}^-$  and  $\text{NH}_2^-$ , but not for  $\text{Cl}^-$  and  $\text{F}^-$ . This suggests that the heterolytic bond dissociation energy,  $D(\text{OP}(\text{OCH}_3)_2^+ - \text{Y}^-)$  increases in the order  $\text{Cl}^-, \text{F}^- < \text{CH}_3\text{O}^- < \text{OH}^-$ ,  $\text{NH}_2^-$ . This order parallels the proton affinity order  $\text{Cl}^- < \text{F}^- < \text{CH}_3\text{O}^- < \text{OH}^- < \text{NH}_2^-$ .<sup>30-33</sup>



Scheme I

Attack at carbon leads to displacement of  $\text{O}_2\text{P}(\text{OCH}_3)_2^-$ . This reaction appears to be analogous to the reactions of  $\text{F}^-$  and  $\text{OH}^-$  with alkyl formates to give  $\text{HCOO}^-$  (reactions 5 and 6). Riveros and co-workers, however, interpret their results as supporting attack at carbonyl carbon rather than  $\text{S}_{\text{N}}2$  displacement at the ester carbon.<sup>22</sup> In the case of trimethyl phosphate, though, attack at carbon is clearly shown by the lack of deuterium incorporation in the phosphate diester anion (see above). There is no expectation that  $\text{F}^-$ ,  $\text{OH}^-$  and  $\text{NH}_2^-$  react differently.

Perhaps the most noteworthy result in this study is the fact that even  $\text{OH}^-$  and  $\text{NH}_2^-$ , which are able to displace  $\text{CH}_3\text{O}^-$ , react principally at carbon to displace  $\text{O}_2\text{P}(\text{OCH}_3)_2^-$ . This stands in contrast to the behavior of phosphate esters in solution, where hard nucleophiles react at phosphorus.<sup>3, 5</sup> Differences in the relative importance of the two reaction pathways in the gas phase and in solution may be due to

differences in the solvation energies of the reaction intermediates. The intermediate arising from attack at phosphorus (species I) has a relatively localized charge on the phosphoryl oxygen and may benefit from solvation more than the  $S_N2$  transition state, which has a more delocalized charge distribution. This reasoning suggests that the energetics of attack at phosphorus will be improved by solvation relative to that of attack at carbon.

PA( $O_2P(OCH_3)_2^-$ ). The observation of reaction 9 permits an upper limit of -246 kcal/mol to be placed on the heat of formation of  $O_2P(OCH_3)_2^-$ . If reaction 12 is endothermic, a lower limit of -275 kcal/mol may be set for this heat of formation.<sup>34</sup> Combining a heat of formation of  $O_2P(OCH_3)_2^-$  of  $-260 \pm 15$  kcal/mol with an estimated heat of formation for  $HOPO(OCH_3)_2$  of  $-243 \pm 15$  kcal/mol<sup>35</sup> yields a proton affinity of  $O_2P(OCH_3)_2^-$  of  $350 \pm 30$  kcal/mol. This is in the same range as the proton affinities of other resonance stabilized anions (e.g.,  $PA(CH_3CO_2^-) = 345.8$  kcal/mol).<sup>36</sup>

Fluoride Affinity. The large difference in the fluoride affinities of  $OP(OCH_3)_3$  [ $D(OP(OCH_3)_3-F^-) < 11 \pm 8$  kcal/mol] and  $OPF_3$  [ $D(OPF_3-F^-) = 59 \pm 1$  kcal/mol] is an illustration of the ability of highly electronegative substituents to promote valence expansion of second row elements. The fluoride affinities of the fluoromethyl silanes, which increase in the order  $(CH_3)_3SiF \ll (CH_3)_2SiF_2 < CH_3SiF_3 < SiF_4$ , provide another example.<sup>37</sup> Most stable neutral penta- and hexa-coordinate compounds of phosphorus and sulfur are also substituted with highly electronegative substituents (e.g.,  $PF_5$ ,  $SF_6$ ,  $SOF_4$ ). The ability

of elements below the first row to form more bonds than are permitted by the octet rule has been attributed to the involvement of d orbitals in bond formation<sup>38, 39</sup> or to the formation of a three-center, four-electron bond.<sup>40-42</sup> The stabilization of hypervalent compounds by highly electronegative substituents is accounted for by both of these bonding descriptions. It has been proposed<sup>38, 39</sup> that electronegative substituents contract the otherwise diffuse d orbitals more than s and p valence orbitals and thus improve their overlap with other bonding orbitals. Electronegative substituents are also expected to stabilize the resonance structures of a three-center, four-electron bond.<sup>42</sup>



Negative Chemical Ionization Mass Spectrometry. The development of analytical techniques for phosphorus esters is important, because of the biological significance of these molecules. The results presented here are relevant to the design of negative chemical ionization mass spectrometric<sup>43, 44</sup> schemes for the detection of phosphorus esters. It is desirable to produce peaks in a mass spectrum which indicate the molecular weight of the sample and which provide structural information. Chloride ion attachment has been used to produce the quasimolecular ion  $[\text{M} + \text{Cl}]^-$  with a variety of substrates.<sup>44-46</sup> The adduct of  $\text{Cl}^-$  and trimethyl phosphate was observed in this study (reaction 8). No bimolecular pathway for formation of the  $\text{F}^-$  adduct was discovered, but

formation of this adduct by direct attachment at higher pressure may be possible. However, the formation of halide-phosphorus ester adducts under chemical ionization conditions requires a reagent gas with a halide affinity less than that of the phosphorus ester.

The most prominent process observed with trimethyl phosphate, displacement at carbon, could be used to obtain ions which provide structural information. Reaction of an appropriate reagent ion (e.g.,  $\text{CH}_3\text{O}^-$ )<sup>43</sup> with a phosphorus compound with different ester groups,  $\text{OP}(\text{OR})(\text{OR}')(\text{OR}'')$ , is expected to give phosphate diester anions, whose masses are characteristic of the molecular weights of the ester groups.

### References and Notes

- (1) A. J. Kirby and S. G. Warren, "The Organic Chemistry of Phosphorus," Elsevier, New York, N.Y., 1967, p. 25.
- (2) R. D. O'Brien, "Toxic Phosphorus Esters: Chemistry, Metabolism, and Biological Effects," Academic Press, New York, N.Y., 1960.
- (3) C. A. Bunton, Acc. Chem. Res., 3, 257 (1970).
- (4) N. T. Thuong, Bull Soc. Chim. Fr., 928 (1971).
- (5) K. E. DeBruin and S. Chandrasekaran, J. Am. Chem. Soc., 95, 974 (1973).
- (6) R. G. Pearson, ed., "Hard and Soft Acids and Bases," Dowden, Hutchinson and Ross, Inc., Stroudsburg, Pa., 1973.
- (7) Reference 1, p. 307.
- (8) P. Gillespie, F. Ramirez, I. Ugi, and D. Marquarding, Angew. Chem. Int. Ed., 12, 91 (1973).
- (9) M. L. Bender, Chem. Rev., 60, 53 (1960).
- (10) Reference 1, p. 277.
- (11) R. F. Hudson and R. Greenhalgh, J. Chem. Soc. B, 325 (1969).
- (12) T. Koizumi and P. Haake, J. Am. Chem. Soc., 95, 8073 (1973).
- (13) R. D. Cook, C. E. Diebert, W. Schwarz, P. C. Turley, and P. Haake, J. Am. Chem. Soc., 95, 8088 (1975).
- (14) Reference 1, p. 210.
- (15) W. N. Olmstead and J. I. Brauman, J. Am. Chem. Soc., 99, 4219 (1977).
- (16) J. F. G. Faigle, P. C. Isolani, and J. M. Riveros, J. Am. Chem. Soc., 98, 2049 (1976).

- (17) P. C. Isolani and J. M. Riveros, Chem. Phys. Lett., 33, 362 (1975).
- (18) O. I. Asubiojo, L. K. Blair, and J. I. Brauman, J. Am. Chem. Soc., 97, 6685 (1975).
- (19) R. C. Dougherty, Org. Mass Spectrom., 8, 77 (1974).
- (20) R. C. Dougherty and J. D. Roberts, Org. Mass Spectrom., 8, 81 (1974).
- (21) R. C. Dougherty, Org. Mass Spectrom., 8, 85 (1974).
- (22) L. K. Blair, R. C. Isolani, and J. M. Riveros, J. Am. Chem. Soc., 95, 1057 (1973).
- (23) D. K. Bohme and L. B. Young, J. Am. Chem. Soc., 92, 7354 (1970).
- (24) S. A. Sullivan and J. L. Beauchamp, Inorg. Chem., submitted for publication.
- (25) J. L. Beauchamp, Ann. Rev. Phys. Chem., 22, 527 (1972).
- (26) T. B. McMahon and J. L. Beauchamp, Rev. Sci. Instrum., 43, 509 (1972).
- (27) W. A. Noyes, Org. Synthesis, 2, 108 (1943).
- (28) In several mixtures of  $\text{OP}(\text{OCH}_3)_3$  and  $\text{CD}_3\text{ONO}$  the ion  $\text{CH}_3\text{O}^-$  was observed. No double resonance signal linking the formation of  $\text{CH}_3\text{O}^-$  to reactions of  $\text{CD}_3\text{O}^-$  or  $\text{DNO}^-$  was found.
- (29) F. Ramirez and I. Ugi, Adv. Phys. Org. Chem., 9, 25 (1971).
- (30) D. K. Bohme, E. L. Ruff, and L. B. Young, J. Am. Chem. Soc., 94, 5153 (1972).
- (31) J. I. Brauman, J. R. Eyler, L. K. Blair, M. J. White, M. B. Comisarow, and K. C. Smith, J. Am. Chem. Soc., 93, 6360 (1971).

- (32) R. T. McIver and J. S. Miller, J. Am. Chem. Soc., 96, 4323 (1974).
- (33) J. I. Brauman and L. K. Blair, J. Am. Chem. Soc., 93, 4315 (1971).
- (34) Calculated using  $\Delta H_f(\text{OP}(\text{OCH}_3)_3) = -239$  kcal/mol in E. Santoro, Org. Mass Spectrom., 7, 589 (1973).
- (35) This value is  $\Delta H_f(\text{OP}(\text{OCH}_3)_3) - 4$ . Carboxylic acids typically have heats of formation 4 kcal/mol below their methyl esters, J. D. Cox and G. Pilcher, "Thermochemistry of Organic and Organometallic Compounds," Academic Press, New York, N.Y., 1970.
- (36) R. Yamdagni and P. Kebarle, J. Am. Chem. Soc., 95, 4050 (1973).
- (37) M. K. Murphy and J. L. Beauchamp, J. Am. Chem. Soc., 99, 4992 (1977).
- (38) K. A. R. Mitchell, Chem. Rev., 69, 157 (1969).
- (39) C. A. Coulson, Nature, 221, 1106 (1969).
- (40) R. E. Rundle, J. Am. Chem. Soc., 85, 112 (1963).
- (41) R. Hoffmann, J. M. Howell, and E. L. Muetterties, J. Am. Chem. Soc., 94, 3047 (1972).
- (42) F. Keil and W. Kutzelnigg, J. Am. Chem. Soc., 97, 3623 (1975).
- (43) D. F. Hunt, G. C. Stafford, Jr., F. W. Crow, and J. W. Russell, Anal. Chem., 48, 2098 (1976).
- (44) H. P. Tannenbaum, J. D. Roberts, and R. C. Dougherty, Anal. Chem., 47, 49 (1975).
- (45) R. C. Dougherty, J. D. Roberts, and F. J. Biros, Anal. Chem., 47, 54 (1975).
- (46) R. C. Dougherty, J. Dalton, and F. J. Biros, Org. Mass Spectrom., 6, 1171 (1972).



## CHAPTER III

Effects of Molecular Structure on Basicity.

The Gas Phase Proton Affinities of Cyclic Phosphites

by

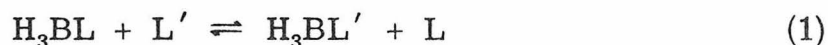
Ronald V. Hodges,<sup>1a</sup> F. A. Houle,<sup>1a</sup> J. L. Beauchamp<sup>\*1a</sup>  
and J. G. Verkade<sup>1b</sup>

Contribution No. 5701 from the Arthur Amos Noyes  
Laboratory of Chemical Physics, California Institute of  
Technology, Pasadena, California 91125  
and the Department of Chemistry,  
Iowa State University, Ames, Iowa 50010

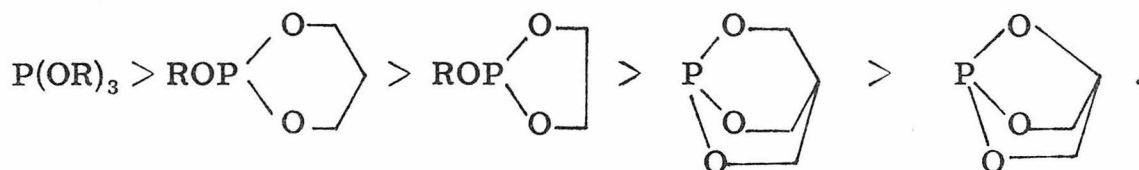
## ABSTRACT

The proton affinities of several monocyclic and bicyclic phosphites are determined by ion cyclotron resonance spectroscopy. The order of proton affinities is identical to the solution basicity order. Increasing steric constraint decreases the proton affinity of phosphites. The phosphorus lone pair in monocyclic six-membered ring phosphites is more basic in the axial than in the equatorial position. Adiabatic ionization potentials are obtained from photoelectron spectra of the phosphites. Decreases in ionization potential parallel increases in proton affinity. This relationship between the ionization potential and proton affinity suggests that the first ionization potential of the phosphites corresponds to ionization from the phosphorus lone pair orbital. These trends are rationalized in terms of changes in the interactions of the oxygen lone pair orbitals with the phosphorus lone pair and d orbitals.

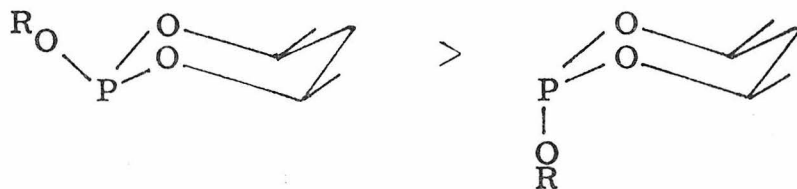
Considerable evidence has been accumulated which indicates that increasing steric constraint reduces the Lewis basicity of tri-alkyl phosphites.<sup>2</sup> The displacement equilibrium 1, where L and L'



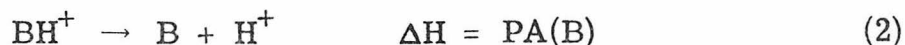
are phosphite esters,<sup>3</sup> nmr  $^1\text{JPH}$  values of protonated phosphites,<sup>4, 5</sup> and ir frequencies of adducts of phosphites with borane<sup>3, 6</sup> and phenol<sup>7</sup> have been investigated. These studies suggest the basicity order<sup>2</sup>



Similar experiments suggest that the basicity of monocyclic six-membered ring phosphites is conformation dependent.<sup>8, 9</sup> The phosphorus lone pair is more basic when placed in the axial rather than the equatorial position.<sup>2, 4</sup>



These experiments yield only basicity orders and are subject to solvent effects. Gas phase proton affinities provide a quantitative measure of base strength in the absence of solvent effects. The proton affinity of a base B is defined as the heterolytic bond dissociation energy for removing a proton from the conjugate acid  $\text{BH}^+$  (reaction 2).

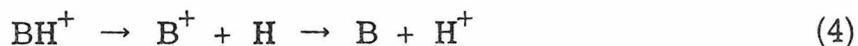


For two bases  $B_1$  and  $B_2$ , a knowledge of the preferred direction of the proton transfer reaction 3 establishes the sign of the free energy change for the reaction,  $\Delta G$ . Gas phase proton transfer reactions can



be observed by ion cyclotron resonance (icr) techniques.<sup>10</sup> If the proton affinities differ by no more than 3 kcal/mol, equilibrium between  $B_1H^+$  and  $B_2H^+$  can often be established in an icr trapped ion experiment.<sup>11, 12</sup> The free energy change for reaction 3 is calculated from the measured equilibrium constant according to  $\Delta G = -RT \ln K$ . If it is assumed that entropy effects are small and are limited to changes in rotational symmetry numbers, then the relative proton affinity  $\Delta H = PA(B_1) - PA(B_2)$ , is readily calculated.<sup>11, 13</sup> If the absolute proton affinity of one of the bases is known, then measurement of their relative proton affinity establishes the proton affinity of the other base.

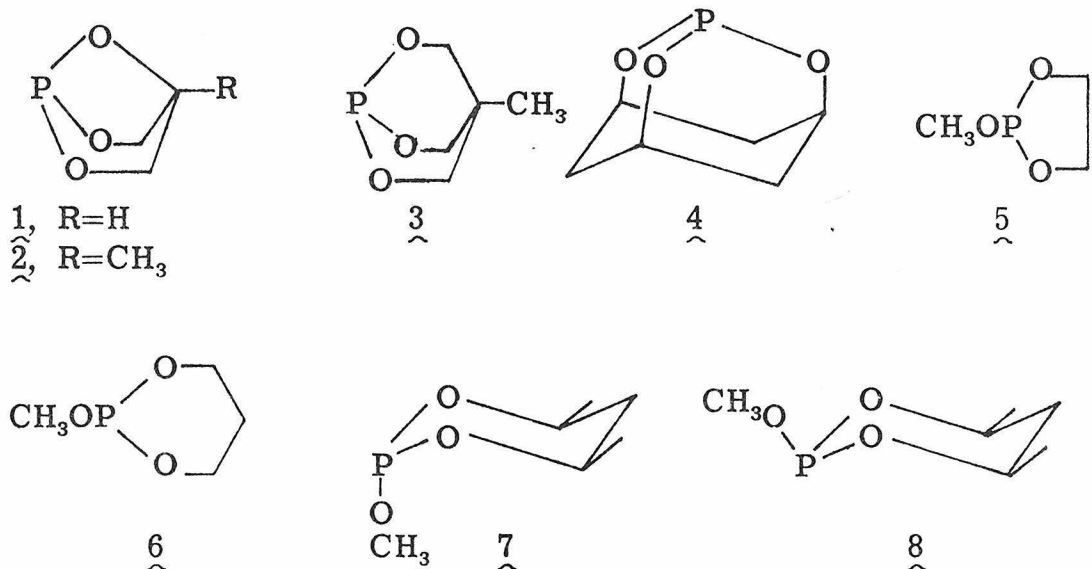
For the purpose of thermodynamic analysis, the removal of a proton from  $BH^+$  can be divided into two steps, homolytic cleavage of the  $B-H^+$  bond and charge transfer between  $B^+$  and H (reaction 4). The proton affinity is then given by the sum of the enthalpies of these two processes (eq 5). For a series of homologous compounds the proton



$$PA(B) = D(B^+-H) + IP(H) - IP(B) \quad (5)$$

affinity is often found to be a linear function of the adiabatic ionization potential of the orbital which becomes the bonding orbital in  $BH^+$ .<sup>14-16</sup>

This paper reports determinations of the proton affinities of the constrained phosphites 1-8 by icr techniques. The adiabatic ionization



potentials of these phosphites were measured by photoelectron spectroscopy and are used to calculate  $D(B^+-H)$  homolytic bond dissociation energies.

### Experimental Section

The general features of icr instrumentation and its operation in trapped ion experiments have been previously described.<sup>10, 17</sup> All experiments were performed at room temperature.

Pressure measurements were made using a Schulz-Phelps gauge located adjacent to the icr cell. This gauge is calibrated for each gas for a given emission current (5  $\mu$ A) and magnetic field (6 kG) against an MKS Instruments Baratron Model 90H1-E capacitance manometer in the region  $10^{-5}$ - $10^{-3}$  Torr. Pressures in the trapped ion experiments were in the range  $10^{-7}$ - $10^{-5}$  Torr. Pressure calibrations were not performed for 3, piperidine or diethylamine, but were assumed

to be equal to those for 2, aniline, and 7, respectively. An uncertainty of  $\pm 0.3$  kcal/mol in the proton affinity is estimated due to uncertainties in pressure measurement. In some cases establishment of equilibrium conditions was hindered by low proton transfer reaction rates or competing reactions. In these cases the reported uncertainty is appropriately increased.

Photoelectron spectra were obtained using a photoelectron spectrometer of standard design built in the Caltech shops. The instrument comprises a helium discharge lamp,  $127^\circ$  electrostatic analyzer and Channeltron electron multiplier. Spectra were accumulated in a Tracor-Northern NS-570A multichannel scaler with 4 K memory. Argon was used to calibrate all spectra. The ionization potentials reported here have error limits of  $\pm 0.02$  eV as determined from the width of the argon peaks.

The cyclic phosphites were prepared by literature methods.<sup>4, 18-21</sup> The mass spectra of all of the phosphites contained an abundant molecular ion. Other chemicals were reagent grade materials from commercial sources and were used as supplied.

## Results

$P(O)(OCH_2)_2CH$  (1). In mixtures of 1 and  $c\text{-C}_3\text{H}_5\text{CN}$  or  $n\text{-C}_3\text{H}_7\text{CN}$ , the ratio of protonated parent ion abundances reached a constant value. Double resonance experiments established that proton transfer was occurring in both directions, thus demonstrating that proton transfer equilibria had been achieved. The equilibrium constants, free energies, and enthalpies for proton transfer are presented in Table I.

Table I. Proton Transfer Equilibrium Constants, Free Energies, and Enthalpies

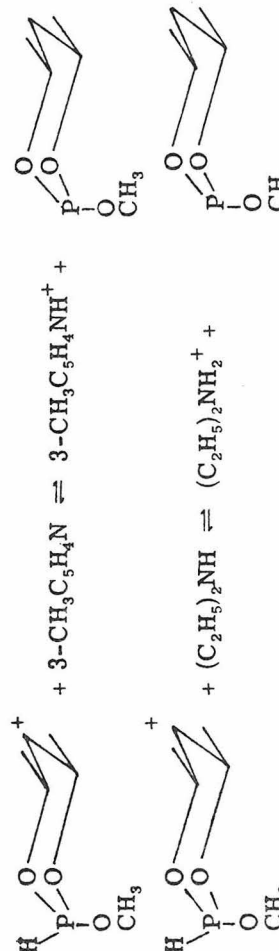
Phosphite $H^+ + B \rightleftharpoons BH^+ + \text{Phosphite}$	$K^a$	$\Delta G^b$	$\Delta H^b$	$PA(B)^{b, c, d}$	$PA(\text{phosphite})^{b, c}$
$HP(O)(OCH_2)_2CH^+ + c-C_3H_5CN \rightleftharpoons c-C_3H_5CNH^+ + P(O)(OCH_2)_2CH$	10.6	-1.4	-1.4	193.2 <sup>e</sup>	191.8
$HP(O)(OCH_2)_2CH^+ + n-C_3H_7CN \rightleftharpoons n-C_3H_7CNH^+ + P(O)(OCH_2)_2CH$	0.51	0.4	0.4	191.4 <sup>e</sup>	191.8
$HP(O)(OCH_2)_2CCH_3^+ + \overline{CH_2CH_2CH_2CH_2O} \rightleftharpoons \overline{CH_2CH_2CH_2CH_2OH^+} + P(O)(OCH_2)_2CCH_3$	4.7	-0.9	-0.6	196.4 <sup>e</sup>	195.9
$HP(O)(OCH_2)_2CCH_3^+ + CH_3COOCH_3 \rightleftharpoons (CH_3COOCH_3)H^+ + P(O)(OCH_2)_2CCH_3$	0.75	0.2	0.2	195.4 <sup>e</sup>	195.6
$CF_2HCH_2NH_3^+ + P(OCH_2)_3CCH_3 \rightarrow HP(OCH_2)_3CCH_3^+ + CF_2HCH_2NH_2$				205.9	>205.3
$HP(OCH_2)_3CCH_3^+ + (t-C_4H_9)_2S \rightarrow (t-C_4H_9)_2SH^+ + P(OCH_2)_3CCH_3$				210.4	<210.8
$HP(OCH_2)_3CCH_3^+ + HCON(CH_3)_2 \rightleftharpoons (HCON(CH_3)_2)H^+ + P(OCH_2)_3CCH_3$	9	-1.3	-1.3	$209.0 \pm 0.03$	207.7
$HP(OCH)_3(CH_2)_3^+ + 2-ClC_5H_4N \rightleftharpoons 2-ClC_5H_4NH^+ + P(OCH)_3(CH_2)_3$	1.1	-0.1	-0.1	211.8	211.7
$HP(OCH)_3(CH_2)_3^+ + (t-C_4H_9)_2S \rightleftharpoons (t-C_4H_9)_2SH^+ + P(OCH)_3(CH_2)_3$	0.9	0.1	0.5	210.4	210.9
$(CH_3OPOCH_2CH_2O)H^+ + 2-ClC_5H_4N \rightleftharpoons 2-ClC_5H_4NH^+ + CH_3OPOCH_2CH_2O$	27	-2.0	-2.0	211.8	209.8
$(CH_3OPOCH_2CH_2O)H^+ + (t-C_4H_9)_2S \rightleftharpoons (t-C_4H_9)_2SH^+ + CH_3OPOCH_2CH_2O$	0.80	0.1	0.5	210.4	210.9
$n-C_3H_7NH_3^+ + CH_3OPOCH_2CH_2CH_2O \rightleftharpoons (CH_3OPOCH_2CH_2CH_2O)H^+ + n-C_3H_7NH_2$				215.5	>214.9
$(CH_3OPOCH_2CH_2CH_2O)H^+ + C_5H_5N \rightleftharpoons C_5H_5NH^+ + CH_3OPOCH_2CH_2CH_2O$	8.8	-1.3	-1.3	218.1	216.8
					
$+ 3-CH_3C_5H_4N \rightleftharpoons 3-CH_3C_5H_4NH^+ +$	0.08	1.5	1.5	220.8	222.3
$+ (C_2H_5)_2NH \rightleftharpoons (C_2H_5)_2NH_2^+ +$	13	-1.5	-1.9	222.7	220.8

Table I. (continued)

Phosphite $H^+ + B \rightleftharpoons BH^+ + \text{Phosphite}$		$K^a$	$\Delta G^b$	$\Delta H^b$	$PA(B)^{b, c, d}$	$PA(\text{phosphite})^{b, c}$
$+ 2-CH_3C_5H_4N \rightleftharpoons 2-CH_3C_5H_4NH^+ +$		11	-1.4	-1.4	221.6	220.2
$+ 4-CH_3C_5H_4N \rightleftharpoons 4-CH_3C_5H_4NH^+ +$		0.36	0.6	0.6	222.1	222.7
$+ \overline{CH_2(CH_2)_4NH} \rightleftharpoons \overline{CH_2(CH_2)_4NH_2^+} +$		0.69	0.2	-0.2	223.1	222.9

<sup>a</sup> Average of at least three independent determinations. <sup>b</sup> kcal/mol. <sup>c</sup> Proton affinity relative to  $PA(NH_3) = 202.3$  kcal/mol.

<sup>d</sup> Except as noted proton affinities are from a compilation by R. W. Taft. A number of values are slightly modified from those given in R. W. Taft in "Proton-Transfer Reactions," E. Caldin and V. Gold, Eds., Wiley, New York, N.Y., 1975. <sup>e</sup> Reference 11.



These data yield  $PA(P(O)(OCH_2)_2CH) = 191.8 \pm 0.3$  kcal/mol.

$P(O)(OCH_2)_2CCH_3$  (2). Proton transfer equilibria were observed in mixtures of 2 with tetrahydrofuran and with  $CH_3COOCH_3$ . The free energies and enthalpies of proton transfer calculated from the measured equilibrium constants are listed in Table I. These data yield  $PA(P(O)(OCH_2)_2CCH_3) = 195.7 \pm 0.3$  kcal/mol.

$P(OCH_2)_3CCH_3$  (3). In a mixture of 3 and  $CF_2HCH_2NH_2$  proton transfer from the protonated amine to the phosphite occurs, but the reverse is not observed. This implies that the free energy of protonation of the phosphite is greater than that for the amine and, thus,  $PA(P(OCH_2)_3CCH_3) > 205.3$  kcal/mol. Similarly, the observation of proton transfer from the protonated phosphite to  $(t-C_4H_9)_2S$  establishes an upper limit for  $PA(P(OCH_2)_3CCH_3)$  of 210.8 kcal/mol. In a mixture of 3 and  $HCON(CH_3)_2$  proton transfer in both directions was detected. Measurement of the equilibrium constant in this system was difficult because a competing reaction, which was not identified, removes the protonated species. An approximate equilibrium constant, free energy and enthalpy of proton transfer are listed in Table I along with the results of the other experiments with 3. From these data a proton affinity for  $P(OCH_2)_3CCH_3$  equal to  $207.7 \pm 0.6$  kcal/mol is calculated.

$P(OCH)_3(CH_2)_3$  (4). Double resonance experiments established that proton transfer occurs in both directions in a mixture of 4 and 2-chloropyridine. An unidentified reaction of a protonated species competes with proton transfer in this system also. An approximate equilibrium constant and the resulting free energy and enthalpy of proton transfer are given in Table I. Proton transfer equilibria were

observed in mixtures of 4 and  $(t\text{-C}_4\text{H}_9)_2\text{S}$ . Data from these mixtures are presented in Table I. Using the latter data,  $\text{PA}(\text{P}(\text{OCH})_3(\text{CH}_2)_3) = 210.9 \pm 0.3 \text{ kcal/mol}$  is calculated.

$\text{CH}_3\text{OPOCH}_2\text{CH}_2\text{O}$  (5). Proton transfer in both directions in mixtures of 5 with 2-chloropyridine and  $(t\text{-C}_4\text{H}_9)_2\text{S}$  is observed. Data from these experiments are given in Table I. A reaction which competes with proton transfer occurs in the mixtures of 2-chloropyridine and 5. The equilibrium constant determined for the mixtures with  $(t\text{-C}_4\text{H}_9)_2\text{S}$  is judged to be more reliable. From this equilibrium constant  $\text{PA}(\text{CH}_3\text{OPOCH}_2\text{CH}_2\text{O}) = 210.9 \pm 0.3$  is obtained.

$\text{CH}_3\text{OPOCH}_2\text{CH}_2\text{CH}_2\text{O}$  (6). In mixtures of  $n\text{-C}_3\text{H}_7\text{NH}_2$  and 6, proton transfer from the protonated amine to the phosphite occurs. This implies that  $\text{PA}(\text{CH}_3\text{OPOCH}_2\text{CH}_2\text{CH}_2\text{O}) > 214.9 \text{ kcal/mol}$ . Proton transfer equilibria in mixtures of 6 with pyridine was observed. These experiments are summarized in Table I. The proton affinity of  $\text{CH}_3\text{OPOCH}_2\text{CH}_2\text{CH}_2\text{O}$  is determined to be  $216.8 \pm 0.7 \text{ kcal/mol}$ .

$\text{CH}_3\text{OPOCH}(\text{CH}_3)\text{CH}_2\text{CH}(\text{CH}_3)\text{O}$  (7). Proton transfer in both directions was observed in mixtures of 7 with 3-methylpyridine, diethylamine and 2-methylpyridine. In the mixtures with the first two compounds a competing reaction removed the protonated species, rendering accurate determination of the equilibrium constant difficult. This problem was much less severe in the mixtures with 2-methylpyridine. Using data from the latter experiments, a proton affinity for 7 of  $220.2 \pm 0.5 \text{ kcal/mol}$  is calculated. The results of these experiments are summarized in Table I.

$\overline{\text{CH}_3\text{OPOCH}(\text{CH}_3)\text{CH}_2\text{CH}(\text{CH}_3)\text{O}}$  (8). Proton transfer equilibria were observed in mixtures of 8 with 4-methylpyridine and piperidine. The proton transfer equilibrium constants, free energies and enthalpies are presented in Table I. From these data a proton affinity for 8 of  $222.8 \pm 0.3$  kcal/mol is calculated.

Photoelectron Spectra. Adiabatic ionization potentials for the phosphites were estimated from their photoelectron spectra and are given in Table II. The first ionization bands were generally smooth and bell-shaped. The adiabatic ionization potentials were picked by extrapolating the approximately straight edge of the bands to the baseline of the spectra. This did not always correspond to the onset of the band due to instrumental factors; however, it was considered to be the most consistent method of choosing adiabatic values for the purposes of the present work. The difference between the vertical and adiabatic ionization potentials of the phosphites is approximately constant in the series and equals  $\sim 0.6$  eV.

### Discussion

The proton affinities, adiabatic ionization potentials and  $D(\text{B}^+-\text{H})$  homolytic bond dissociation energies for the phosphites and other trivalent phosphorus compounds are presented in Table II. The gas phase proton affinity order of the phosphites is the same as the basicity order in solution. Thus, this order is a result of differences in the intrinsic properties of the isolated molecules. The significant difference in the proton affinities of 7 and 8 (2.6 kcal/mol) represents the first purely conformational effect on basicity observed in the gas phase.

Table II. Proton Affinities, Adiabatic Ionization Potentials and  $D(B^+-H)$  Homolytic Bond Dissociation Energies of Tervalent Phosphorus Compounds

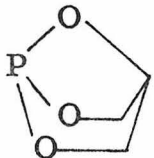
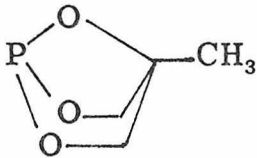
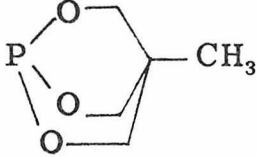
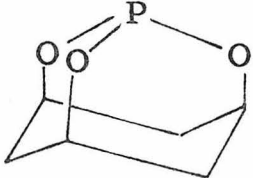
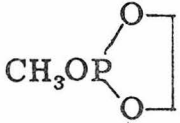
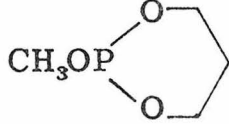
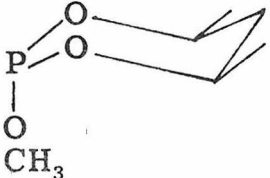
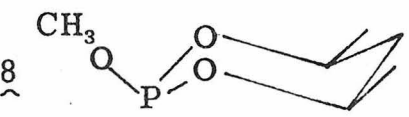
Compound	PA <sup>a</sup>	IP <sup>a</sup>	$D(B^+-H)^a$
1 	191.8		
2 	195.7	224 (9.72) <sup>b</sup>	106
3 	207.7	216 (9.35) <sup>c</sup>	110
4 	210.9	217 (9.42) <sup>b</sup>	115
5 	210.9	209 (9.06)	106
6 	216.8	202 (8.74)	105
$P(OCH_3)_3$	218.2	196 (8.50) <sup>c</sup>	101
7 	220.2	200 (8.69)	107

Table II. (continued)

Compound	PA <sup>a</sup>	IP <sup>a</sup>	D(B <sup>+</sup> -H) <sup>a</sup>
<sup>8</sup> 	222.8	192 (8.34)	102
PF <sub>3</sub>	160 ± 5 <sup>d</sup>	269 (11.66) <sup>e</sup>	116
PH <sub>3</sub>	187.4 <sup>f</sup>	230 (9.96) <sup>f</sup>	103
CH <sub>3</sub> PH <sub>2</sub>	201.8 <sup>f</sup>	210 (9.12) <sup>f</sup>	98
(CH <sub>3</sub> ) <sub>2</sub> PH	214.0 <sup>f</sup>	195 (8.47) <sup>f</sup>	96
(CH <sub>3</sub> ) <sub>3</sub> P	223.5 <sup>f</sup>	187 (8.11)	97

<sup>a</sup>kcal/mol. Values in parentheses in eV. <sup>b</sup>Reference 23.

<sup>c</sup>Reference 22. <sup>d</sup>R. R. Corderman and J. L. Beauchamp, Inorg. Chem., submitted for publication. <sup>e</sup>P. J. Bassett and D. R. Lloyd, J. Chem. Soc. Dalton, 248 (1972). <sup>f</sup>Reference 11.

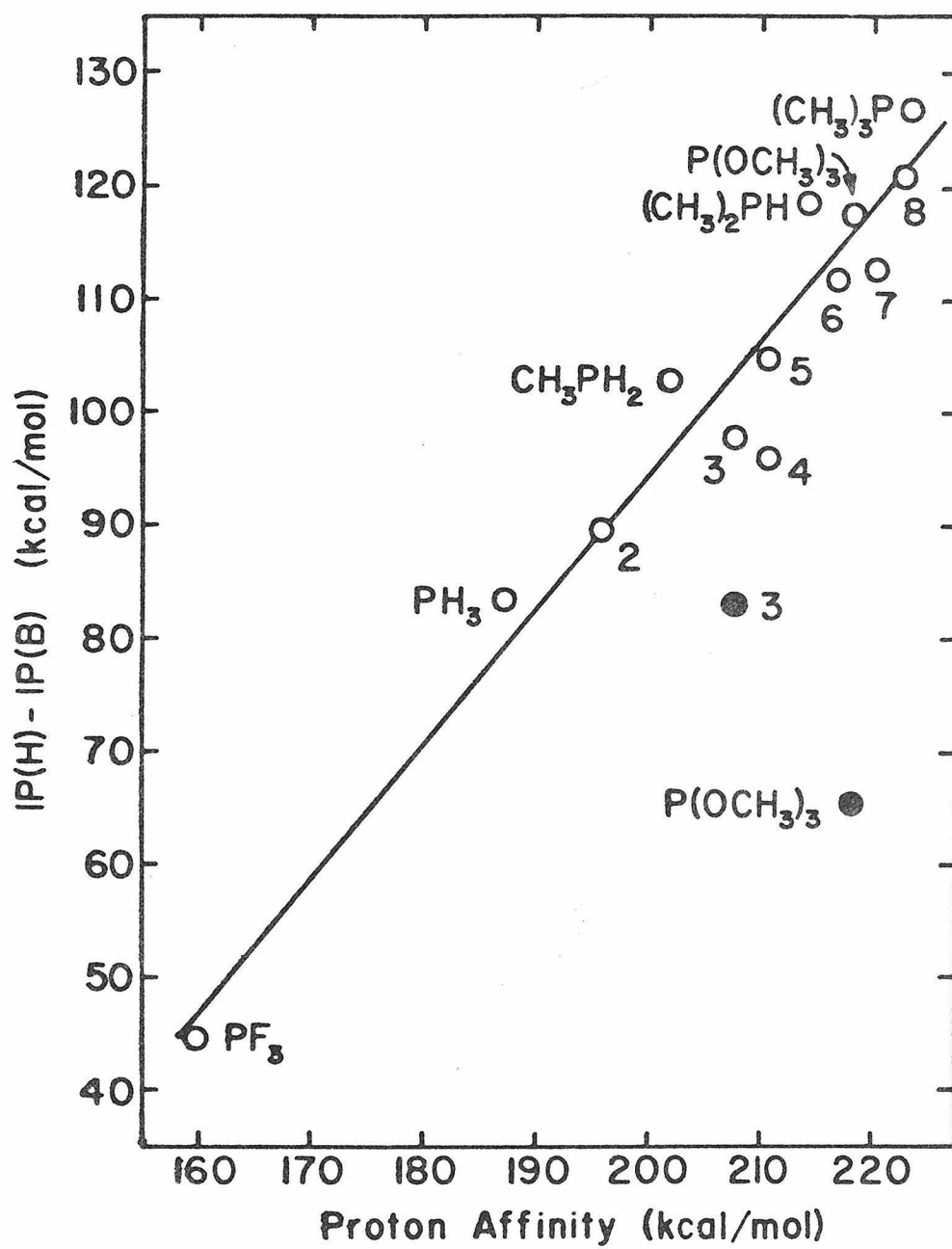
The proton affinity reflects changes in the ionization potential and homolytic bond dissociation energy according to eq 5. The homolytic bond dissociation energies of the phosphites exhibit some variation, but do not follow a consistent trend. The decrease in proton affinity with increasing constraint parallels an increase in ionization potential. Figure 2 illustrates the correlation between the ionization potential and the proton affinity for the tervalent phosphorus compounds studied to date. From this plot the proton affinities of other tervalent phosphorus compounds can be estimated, if their ionization potentials are known.

In a study of the proton affinities and photoelectron spectra of nitriles a correlation between the proton affinity and the adiabatic ionization potential of the nitrogen lone pair orbital was observed.<sup>14</sup> No correlation was found with the first ionization potential, which corresponds to ionization from the  $C\equiv N$   $\pi$  orbitals. This suggests that the ionization potential of the orbital which becomes the bonding orbital in  $B-H^+$  is the one, which is expected to correlate with the proton affinity. The existence of a correlation between the proton affinity and first ionization potential of the phosphites is evidence that this ionization occurs from the phosphorus lone pair orbital. This assignment is in conflict with a previous assignment of this ionization potential to oxygen lone pairs.<sup>22</sup> However, these authors are revising their assignment on the basis of evidence from the photoelectron spectra of additional compounds.<sup>23</sup>

The relationship between the proton affinity and ionization potential revealed in the present study indicates that the proton affinity order is determined by differences in the abilities of the phosphites to assume a positive charge. This conclusion supports previous

## FIGURE 2

The quantity  $IP(H)-IP(B)$  plotted vs.  $PA(B)$  for tervalent phosphorus compounds (values from Table II). Filled circles are points calculated using estimated adiabatic ionization potentials of the band assigned to the phosphorus lone pair in reference 22.





rationalizations of the basicity order, in which the order is ascribed to differences in the interaction of the oxygen lone pairs with phosphorus.<sup>2, 4, 24</sup> The repulsive interaction of the phosphorus and oxygen lone pairs destabilizes the phosphorus lone pair in the neutral,<sup>2, 25</sup> while  $\pi$  bonding between oxygen and phosphorus in the protonated phosphite and the molecular ion delocalizes the positive charge.<sup>2, 24, 26</sup> Both of these interactions serve to decrease the ionization potential and increase the proton affinity. The changes in geometry which accompany increasing constraint of the phosphite alter the spatial orientation and hybridization of the oxygen lone pair orbitals such that their interactions with the phosphorus lone pair and d orbitals are weakened.<sup>2</sup> The decrease in the basicity of an equatorial vs. an axial phosphorus lone pair in 7 and 8 may also be ascribed to a weakening of these interactions.<sup>2, 24, 25</sup>

The 5 kcal/mol increase in proton affinity upon methyl substitution in 1 is large in comparison with the effect of methyl substitution remote from the site of protonation in other compounds. For example, substitution of  $\text{CH}_3$  for H in  $\text{RCH}_2\text{CHO}$  and  $\text{RCH}_2\text{CN}$  raises the proton affinity by about 3 kcal/mol.<sup>11</sup> A satisfactory understanding of this methyl effect must await the determination of the proton affinities of analogous compounds, such as the hydrogen substituted analog of 3. Tentatively, it may be suggested that the existence of three pathways for through-bond interactions between the methyl group and the phosphorus atom in the bicyclic molecule augments the methyl effect relative to that in acyclic compounds.

### References and Notes

- (1) (a) California Institute of Technology; (b) Iowa State University.
- (2) J. G. Verkade, Phosphorus Sulfur, 2, 251 (1976).
- (3) D. W. White and J. G. Verkade, Phosphorus, 3, 9 (1973).
- (4) L. J. Vande Griend J. G. Verkade, J. F. M. Pennings, and H. M. Buck, J. Am. Chem. Soc., 99, 2459 (1977).
- (5) L. J. Vande Griend and J. G. Verkade, Phosphorus, 3, 13 (1973).
- (6) C. W. Heitsch and J. G. Verkade, Inorg. Chem., 1, 863 (1962).
- (7) L. J. Vande Griend, D. W. White, and J. G. Verkade, Phosphorus, 3, 5 (1973).
- (8) D. W. White and J. G. Verkade, Phosphorus, 3, 15 (1973).
- (9) L. J. Vande Griend and J. G. Verkade, Inorg. Nucl. Chem. Lett., 9, 1137 (1973).
- (10) J. L. Beauchamp, Ann. Rev. Phys. Chem., 22, 527 (1971).
- (11) J. F. Wolf, R. H. Staley, I. Koppel, M. Taagepera, R. T. McIver, Jr., J. L. Beauchamp, and R. W. Taft, J. Am. Chem. Soc., 99, 5417 (1977).
- (12) M. T. Bowers, D. H. Aue, H. M. Webb, and R. T. McIver, Jr., J. Am. Chem. Soc., 93, 4314 (1971).
- (13) S. W. Benson, "Thermochemical Kinetics," 2nd ed., Wiley, New York, N.Y., 1976, p. 47.
- (14) R. H. Staley, J. E. Kleckner, and J. L. Beauchamp, J. Am. Chem. Soc., 98, 2081 (1976).
- (15) W. G. Henderson, M. Taagepera, D. Holtz, R. T. McIver, Jr., J. L. Beauchamp, and R. W. Taft, J. Am. Chem. Soc., 94, 4729 (1972).

- (16) D. H. Aue, H. M. Webb, and M. T. Bowers, J. Am. Chem. Soc., 94, 4726 (1972).
- (17) T. B. McMahon and J. L. Beauchamp, Rev. Sci. Instrum., 43, 509 (1972).
- (18) D. B. Denney and S. C. Varga, Phosphorus, 2, 245 (1973).
- (19) J. G. Verkade, T. J. Hutteman, M. K. Fung, and R. W. King, Inorg. Chem., 4, 83 (1965).
- (20) K. Moedritzer, L. Maier, and L. C. D. Groenweghe, J. Chem. Eng. Data, 7, 307 (1962).
- (21) J. A. Mosbo and J. G. Verkade, J. Am. Chem. Soc., 95, 4659 (1973).
- (22) A. H. Cowley, D. W. Goodman, N. A. Kuebler, M. Sanchez, and J. G. Verkade, Inorg. Chem., 16, 854 (1977).
- (23) A. H. Cowley, M. Sattman, and J. G. Verkade, unpublished results.
- (24) J. G. Verkade, Bioinorg. Chem., 3, 165 (1974).
- (25) R. F. Hudson and J. G. Verkade, Tetrahedron Lett., 3231 (1975).
- (26) J. G. Verkade, Coord. Chem. Rev., 9, 1 (1972).

## CHAPTER IV

The Proton Affinities of Pyridine, Phosphabenzene  
and Arsabenzene

by

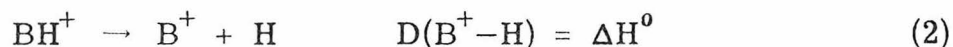
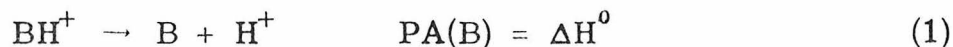
Ronald V. Hodges,<sup>1a</sup> J. L. Beauchamp,<sup>\*1a</sup> and  
Arthur J. Ashe III<sup>1b</sup>

Contribution No. 5680 from the Arthur Amos Noyes  
Laboratory of Chemical Physics, California Institute of  
Technology, Pasadena, California 91125, and the  
Department of Chemistry, University of Michigan,  
Ann Arbor, Michigan 48104

## ABSTRACT

The proton affinities of the P and As analogs of pyridine, phosphabenzene and arsabenzene, are determined by ion cyclotron resonance techniques to be 194.5 kcal/mol and 188.0 kcal/mol, respectively, relative to  $PA(NH_3) = 202.3$  kcal/mol. These values are compared to those of pyridine, 218.1 kcal/mol and other Group V compounds. Deuterium labeling experiments demonstrate that phosphabenzene is protonated on the phosphorus atom. The decrease in proton affinity in the series pyridine, phosphabenzene, arsabenzene is ascribed to the decreasing p character of heteroatom lone pair in this series.

Gas phase proton affinities provide a quantitative measure of base strength in the absence of solvent effects. The proton affinity of a base B is defined as the heterolytic bond dissociation energy for removing a proton from the conjugate acid  $BH^+$  (reaction 1). The homolytic bond dissociation energy of the conjugate acid is defined as the standard enthalpy change for reaction 2. These two bond energies are related by the adiabatic ionization potentials of B and H according to eq 3. Comparisons of the proton affinities, ionization potentials and homolytic bond dissociation energies of related compounds permit evaluations of the effects of changes in molecular and electronic structure on these quantities.<sup>2, 3</sup>



The proton affinities of a large number of amines,<sup>2-8</sup> pyridines,<sup>4, 6, 8, 9</sup> and nitriles<sup>2, 6, 10</sup> are now known. Recently, the proton affinities of phosphine,<sup>2</sup> the methylphosphines,<sup>11</sup> arsine<sup>2</sup> and trimethylarsine<sup>12</sup> have become available for comparison with the analogous amines (Figure 1 and Table I). Successive methyl substitution increases the proton affinity in each series. In general, the proton affinities of compounds with identical substitution decrease in the order  $N > P > As$ . An exception occurs in the trimethyl series, where  $PA[(CH_3)_3P] > PA[(CH_3)_3N]$ . The differences in proton affinity between the amines and the phosphines have been explained by considering the character of the lone pair to which the proton binds.<sup>11</sup>

## FIGURE 1

Proton affinities of group V bases. Data from  
Table I.

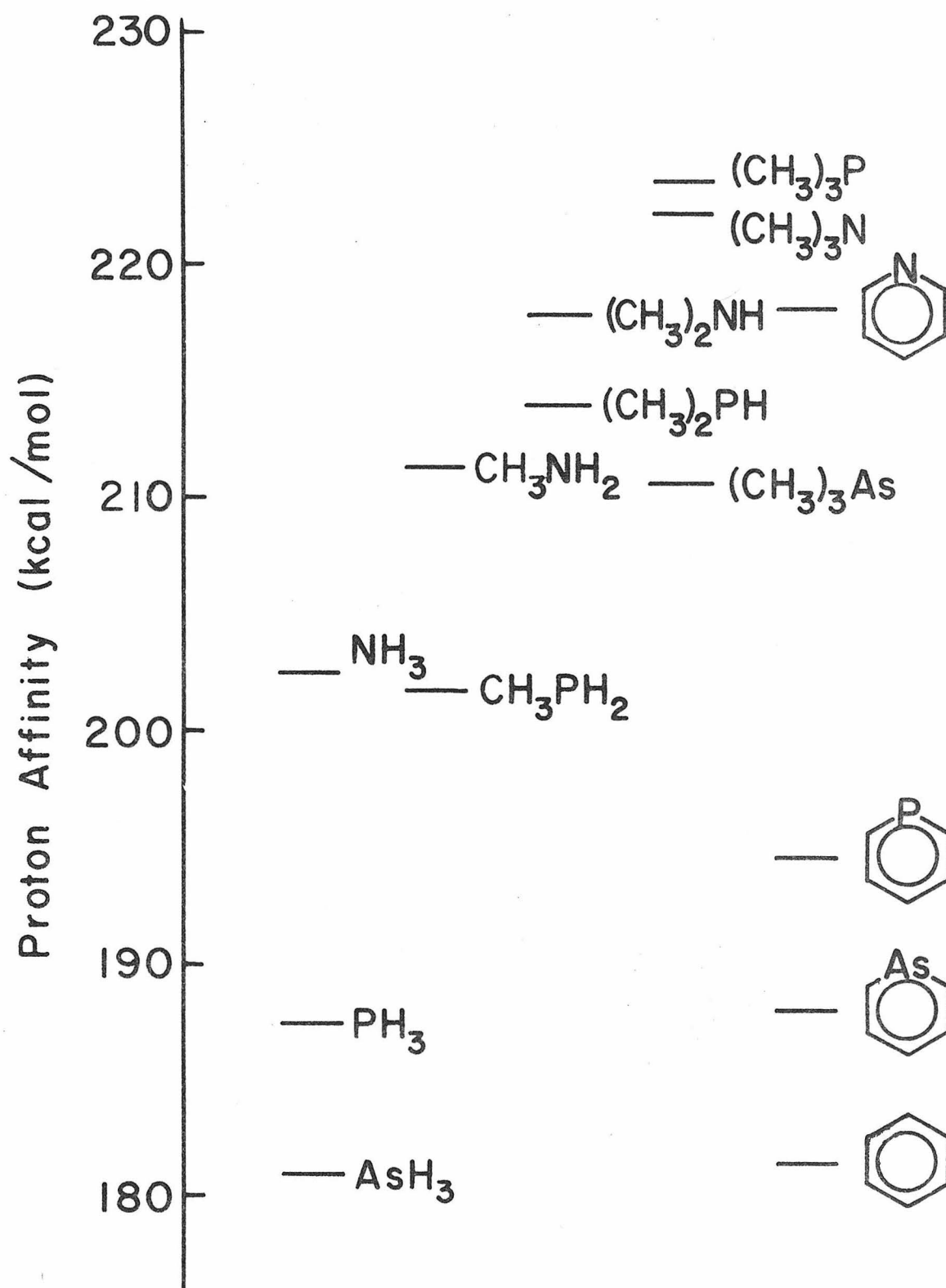

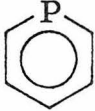






Table I. Proton Affinities, Adiabatic Ionization Potentials, and  $D(B^+-H)$  Homolytic Bond Dissociation Energies of Group V Bases<sup>a</sup>

Molecule	PA <sup>b</sup>	IP <sup>b, c</sup>	$D(B^+-H)^{b, d}$
	218.1 <sup>e</sup>	210 <sup>f</sup>	114
	194.5 <sup>g</sup>	208 (217) <sup>f</sup>	89 (98)
	188.0 <sup>g</sup>	199 (214) <sup>f</sup>	73 (88)
	181.4	213.1 <sup>h</sup>	80.9
NH <sub>3</sub>	202.3	234.3	122.9
CH <sub>3</sub> NH <sub>2</sub>	211.3	206.8	104.5
(CH <sub>3</sub> ) <sub>2</sub> NH	217.9	190.0	94.3
(CH <sub>3</sub> ) <sub>3</sub> N	222.1	181.5	90.0
PH <sub>3</sub>	187.4	229.6	103.4
CH <sub>3</sub> PH <sub>2</sub>	201.8	210.2	98.4
(CH <sub>3</sub> ) <sub>2</sub> PH	214.0	195.3	95.7
(CH <sub>3</sub> ) <sub>3</sub> P	223.5	184.7	94.6
AsH <sub>3</sub>	180.9	228	95
(CH <sub>3</sub> ) <sub>3</sub> As	210.7	182	79

<sup>a</sup>Except as noted, data are from Reference 2. <sup>b</sup>kcal/mol.

<sup>c</sup>Values in parentheses are lone pair adiabatic ionization potentials, where these are not the first ionization potentials. <sup>d</sup>Values in

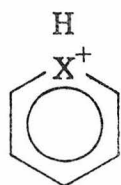
Table I. (Continued)

---

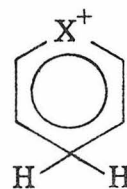
parentheses are the correlated homolytic bond dissociation energies  
(see discussion in text). <sup>e</sup>Reference 16. <sup>f</sup>Estimated from the  
photoelectron spectrum published in Reference 26. <sup>g</sup>Present work.  
<sup>h</sup>L. Asbrink, E. Lindholm, and O. Edqvist, Chem. Phys. Lett., 5,  
609 (1970).

Protonation of the phosphines requires a rehybridization of the phosphorus lone pair from largely  $s$  ( $\angle \text{H}-\text{P}-\text{H} = 93^\circ$  in  $\text{PH}_3$ <sup>13</sup>) to  $sp^3$  character. Ammonia, which is  $sp^3$  hybridized ( $\angle \text{H}-\text{N}-\text{H} = 107^\circ$ <sup>14</sup>), requires no rehybridization energy upon protonation and is 14.9 kcal/mol more basic than phosphine.<sup>15</sup> Successive methyl substitution in the amines increases the  $s$  character of the lone pair and introduces an increasing rehybridization energy. This acts in opposition to the inductive effect of the methyl groups, so that the increase in proton affinity with methyl substitution in the amines is attenuated relative to the increase in the phosphines with the result that the proton affinity of  $(\text{CH}_3)_3\text{P}$  is 1.4 kcal/mol greater than that of  $(\text{CH}_3)_3\text{N}$ .

The phosphorus and arsenic compounds studied to date are similar, in that the heteroatom forms  $\sigma$  bonds to three substituents. This paper reports ion cyclotron resonance (icr) investigations of the energetics and site specificity of the protonation of phosphabenzene and arsabenzene, compounds in which the heteroatom is involved in  $\pi$  bonding. The proton affinity of pyridine has been previously determined to be 218.1 kcal/mol.<sup>16</sup> Although it has not been demonstrated experimentally, protonation undoubtedly occurs at the nitrogen atom. Protonation of phosphabenzene and arsabenzene could conceivably occur at the heteroatom to give structure I or at a ring carbon to give structure II.



I



II

## Experimental Section

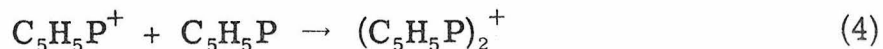
Phosphabenzene and arsabenzene were prepared by the method of Ashe.<sup>17</sup> The icr mass spectra of these materials match the reported spectra.<sup>17</sup>

The general features of icr instrumentation and its operation in trapped-ion experiments have been previously described.<sup>18, 19</sup> All experiments were performed at room temperature.

Pressure measurements were made using a Schulz-Phelps gauge located adjacent to the icr cell. This gauge is calibrated for each gas for a given emission current (5  $\mu$ A) and magnetic field (6 kG) against an MKS Instruments Baratron Model 90H1-E capacitance manometer in the region  $10^{-5}$  -  $10^{-3}$  torr, where linear variation of gauge current with pressure is observed. Pressures in the trapped ion experiments were in the range  $10^{-7}$  -  $10^{-5}$  torr.

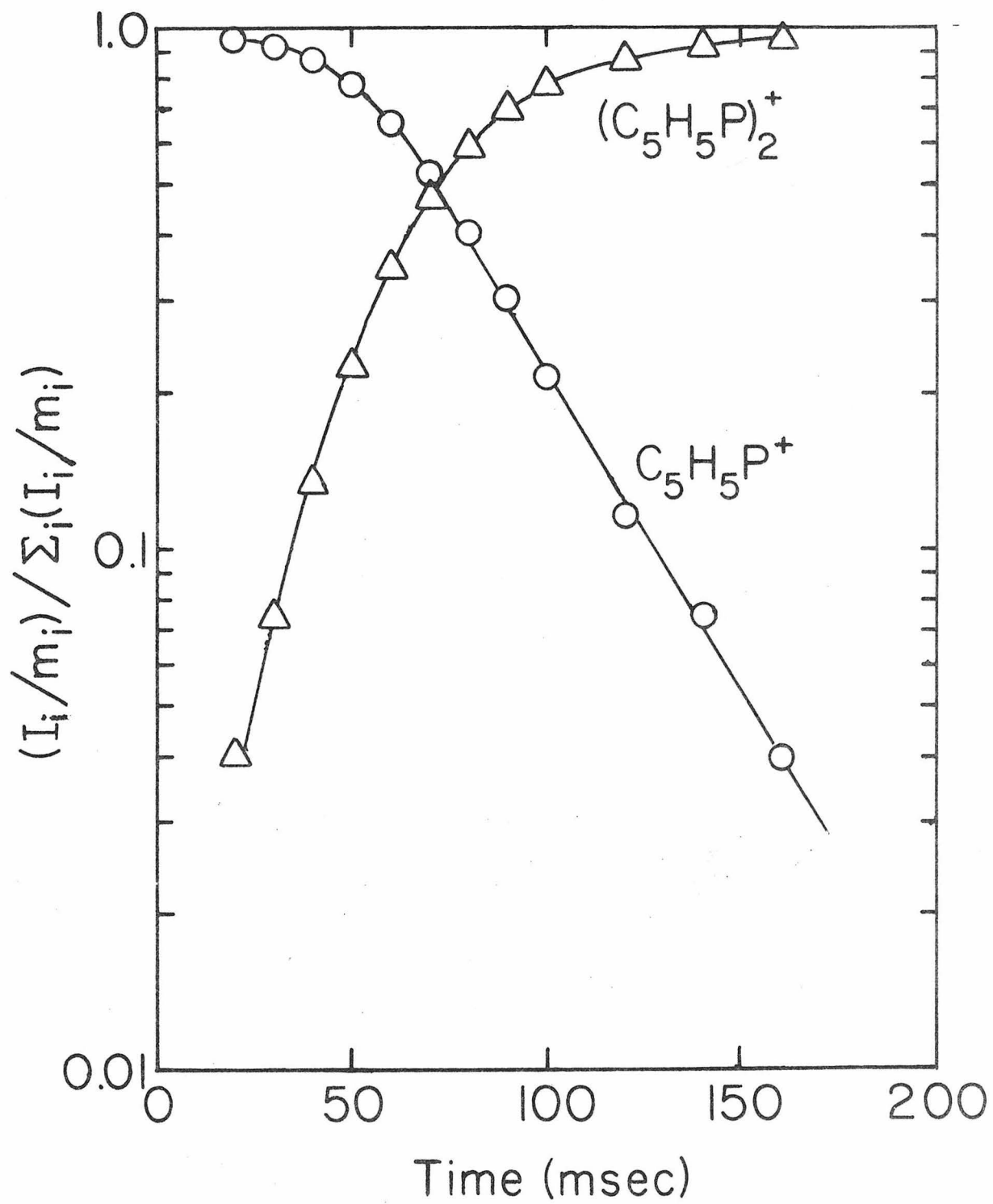
## Results

Phosphabenzene. Ion Chemistry. Icr trapped ion studies of phosphabenzene alone were performed at 14 eV. At this electron energy only the parent ion, m/e 96, is present. The parent ion clusters with the neutral (reaction 4) but is otherwise unreactive. In particular, the conjugate acid, protonated phosphabenzene, m/e 97, is not observed. The variation of ion abundance with time is shown in Figure 2. The parent ion is initially unreactive. It may be formed with



## FIGURE 2

Temporal variation of ion concentrations in phosphabenzene at  $4.0 \times 10^{-6}$  torr pressure and 14 eV electron energy.



excess internal energy and then be collisionally deactivated. The rates of association reactions such as reaction 4 decrease as a function of the internal energy of the reactants.<sup>20</sup> The bimolecular rate constant for reaction 4 is  $2.0 \times 10^{-10} \text{ cm}^3 \text{ molecule}^{-1} \text{ sec}^{-1}$ .<sup>21</sup> This value is constant to within  $\pm 20\%$  over a pressure range of  $1.8 \times 10^{-6}$  to  $4.0 \times 10^{-6}$  torr. Bimolecular ion-molecule clustering at low pressure ( $10^{-6}$  torr) has also been observed to occur with ions in the fluoromethyl silanes.<sup>22</sup>

Proton Affinity. In mixtures of phosphabenzene and acetone or methyl acetate, the ratio of the protonated parent ion abundances reached a constant value. Double resonance experiments established that proton transfer was occurring in both directions, thus demonstrating that proton transfer equilibria had been achieved. The free energies obtained from the equilibrium constants are listed in Table II. The enthalpies are calculated from the free energies with the assumption that entropy effects are small and are limited to changes in rotational symmetry numbers.<sup>2, 23, 24</sup> These data yield a proton affinity of  $194.5 \pm 0.1 \text{ kcal/mol}$ .

Site of Protonation. In a mixture of  $\text{CD}_3\text{CDO}$ , phosphabenzene, and 2-pentanone both protonated and deuterated phosphabenzene and ketone were observed. Double resonance experiments demonstrated that deuterated phosphabenzene reacts to give deuterated, but not protonated ketone. The deuterium is, therefore, not equivalent to the ring hydrogens and must be located on the phosphorus atom.

Arsabenzene. Ion Chemistry. The reactivity of arsabenzene molecular ion is identical to that observed for phosphabenzene.

Table II. Proton Transfer Equilibrium Constants, Free Energies, and Enthalpies

$C_5H_5XH^+ + B \rightleftharpoons BH^+ + C_5H_5X$	$K^a$	$\Delta G^b$	$\Delta H^b$	$PA(B)^{c, d}$	$PA(C_5H_5X)^d$
$C_5H_5PH^+ + (CH_3)_2CO \rightleftharpoons (CH_3)_2COH^+ + C_5H_5P$	0.7	0.2	0.6	193.9	194.5
$C_5H_5PH^+ + CH_3CO_2CH_3 \rightleftharpoons CH_3CO_2CH_3H^+ + C_5H_5P$	4.0	-0.8	-0.8	195.4	194.6
$C_5H_5AsH^+ + HCO_2CH_3 \rightleftharpoons HCO_2CH_3H^+ + C_5H_5As$	0.6	0.3	0.3	187.7	188.0
$C_5H_5AsH^+ + CH_3CN \rightleftharpoons CH_3CNH^+ + C_5H_5As$	0.2	0.9	0.9	187.0	187.9

<sup>a</sup>Average of three independent determinations. <sup>b</sup>In kcal/mol. <sup>c</sup>Reference 2. <sup>d</sup>Proton affinity in kcal/mol. All data relative to  $PA(NH_3) = 202.3$  kcal/mol.



Clustering with the parent neutral is the only observed process (reaction 5).



Proton Affinity. Proton transfer equilibria were achieved in mixtures of arsabenzene with methyl formate and with acetonitrile. The data from these experiments are listed in Table II. The proton affinity of arsabenzene is  $188.0 \pm 0.1$  kcal/mol.

Site of Protonation. Proton transfer reactions with arsabenzene are slow. For this reason experiments to determine the site of protonation in arsabenzene were not successful.

### Discussion

The proton affinities, ionization potentials, and  $D(\text{B}^+-\text{H})$  homolytic bond dissociation energies of the heterobenzenes and several other Group V bases are listed in Table I. The first adiabatic ionization potentials of the bases are used to calculate the homolytic bond dissociation energies as strictly defined according to eq 3. However, for the purpose of comparing the homolytic bond dissociation energies of compounds in a homologous series, the adiabatic ionization potential of the orbital which correlates with the bonding orbital in the conjugate acid should be used in eq 3.<sup>10</sup> The term correlated homolytic bond dissociation energy is suggested for this quantity. In the case of the heterobenzenes the appropriate orbital is the heteroatom lone pair orbital. Calculations suggest that the preferred approach of the proton to pyridine or phosphabenzene is the  $\sigma$  plane along the

symmetry axis of the heteroatom.<sup>25</sup> Experimental and theoretical data for the structure of protonated arsabenzene are lacking. In this discussion, protonation on the arsenic lone pair is assumed. The photoelectron spectra of the heterobenzenes have been assigned.<sup>26</sup> The lone pair and  $a_2(\pi)$  orbitals of pyridine have almost the same energy and are the highest occupied orbitals. However, in phosphabenzene and arsabenzene the lowest energy ionization occurs from the  $b_1(\pi)$  orbital. Ionization from the lone pair orbitals correspond to the third band in the photoelectron spectra. The estimated adiabatic ionization potentials of the lone pairs in phosphabenzene and arsabenzene and the correlated homolytic bond dissociation energies calculated from these values are given in parentheses in Table II.

The proton affinities of the heterobenzenes decrease in the order  $C_5H_5N > C_5H_5P > C_5H_5As$ . This order may be ascribed to differences in the character of the lone pairs in these molecules. The bond angle at the heteroatom decreases from  $116.14^\circ$  in pyridine<sup>27</sup> to  $101.1^\circ$  in phosphabenzene<sup>28</sup> and  $97.3^\circ$  in arsabenzene.<sup>29</sup> Thus, the s character of the lone pair is expected to increase in the series pyridine, phosphabenzene, arsabenzene. CNDO/2 calculations indicate that the lone pair of phosphabenzene does have more s character than that of pyridine.<sup>30</sup> Both ab initio<sup>25, 31</sup> and CNDO/2<sup>30, 32</sup> calculations also show that the nitrogen atom in pyridine withdraws electron density from the adjacent carbons, while the phosphorus and arsenic atoms in phosphabenzene and arsabenzene donate electron density to these carbons. This is not surprising, since the order of

the electronegativities of these elements is  $N > C > P > As$ .<sup>33</sup> These factors indicate that the heteroatom lone pair orbital becomes less directional and more diffuse in proceeding from pyridine to phosphabenzene to arsabenzene.<sup>30</sup> Hence, the strength of the bonding interaction of the proton with the lone pair decreases in this series.

The reduced basicity of phosphabenzenes compared to pyridines is also apparent in solution. The uv spectra of solutions of substituted phosphabenzenes remains unchanged upon addition of trifluoroacetic acid.<sup>34</sup>

The lone pair ionization potentials of the heterobenzenes are relatively constant in this series. Any increase in ionization potential, caused by increasing s character of the lone pair, is approximately cancelled by the decrease due to the change in principal quantum number.<sup>35</sup> Thus, the homolytic bond dissociation energies follow the same trend as the proton affinities.

The reactivity of the parent ions of the heterobenzenes is determined by the  $D(B^+-H)$  homolytic bond dissociation energy. The homolytic bond dissociation energy for pyridine, 114 kcal/mol, is higher than the C-H bond energy of pyridine, if a value equal to the C-H bond energy of benzene  $D(C_6H_5-H) = 110$  kcal/mol,<sup>36</sup> is assumed. Reaction 6 is, therefore, exothermic for pyridine and is observed.<sup>37</sup>



The homolytic bond dissociation energies for phosphabenzene and arsa-benzene, however, are considerably below 110 kcal/mol and reaction 6 is endothermic for  $X = P$  or As. Clustering is the only reaction of the parent ions of these molecules.

References and Notes

- (1) (a) California Institute of Technology; (b) University of Michigan.
- (2) J. F. Wolf, R. H. Staley, I. Koppel, M. Taagepera, R. T. McIver, Jr., J. L. Beauchamp, and R. W. Taft, J. Am. Chem. Soc., 99, 5417 (1977).
- (3) R. H. Staley, M. Taagepera, W. G. Henderson, I. Koppel, J. L. Beauchamp, and R. W. Taft, J. Am. Chem. Soc., 99, 326 (1977).
- (4) D. H. Aue, H. M. Webb, and M. T. Bowers, J. Am. Chem. Soc., 98, 318 (1976).
- (5) D. H. Aue, H. M. Webb, and M. T. Bowers, J. Am. Chem. Soc., 98, 311 (1976).
- (6) D. H. Aue, H. M. Webb, and M. T. Bowers, J. Am. Chem. Soc., 97, 4137 (1975).
- (7) R. H. Staley and J. L. Beauchamp, J. Am. Chem. Soc., 96, 1604 (1974).
- (8) J. P. Briggs, R. Yamdagni, and P. Kebarle, J. Am. Chem. Soc., 94, 5128 (1972).
- (9) M. Taagepera, W. G. Henderson, R. T. C. Brownlee, J. L. Beauchamp, D. Holtz, and R. W. Taft, J. Am. Chem. Soc., 95, 1369 (1972).
- (10) R. H. Staley, J. E. Kleckner, and J. L. Beauchamp, J. Am. Chem. Soc., 98, 2081 (1976).
- (11) R. H. Staley and J. L. Beauchamp, J. Am. Chem. Soc., 96, 6252 (1974).
- (12) R. V. Hodges and J. L. Beauchamp, Inorg. Chem., 14, 2887 (1975).

- (13) M. H. Sirvetz and R. E. Weston, Jr., J. Chem. Phys., 21, 898 (1953).
- (14) G. Herzberg, "Infrared and Raman Spectra of Polyatomic Molecules", D. Van Nostrand, New York, N.Y., 1945, p. 439.
- (15) For a discussion of rehybridization effects see, J. H. Gibbs, J. Chem. Phys., 22, 1460 (1954).
- (16) From a compilation of R. W. Taft. The experimental methods are the same as those in references 2 and 3. This value differs slightly from that reported in reference 4 and reference 8.
- (17) A. J. Ashe III, J. Am. Chem. Soc., 93, 3293 (1971).
- (18) J. L. Beauchamp, Ann. Rev. Phys. Chem., 22, 527 (1971).
- (19) T. B. McMahon and J. L. Beauchamp, Rev. Sci. Instrum., 43, 509 (1972).
- (20) W. A. Chupka in "Interactions Between Ions and Molecules", Pierre Ausloos, Ed., Plenum Press, New York, N.Y., 1974, p. 255.
- (21) This value is an average of three determinations. Accuracy in the rate constant is estimated to be  $\pm 20\%$  due to uncertainties in pressure measurement.
- (22) M. K. Murphy and J. L. Beauchamp, J. Am. Chem. Soc., 98, 5781 (1976).
- (23) S. W. Benson, "Thermochemical Kinetics", 2nd ed., Wiley, New York, N.Y., 1976, p. 47.
- (24) R. Yamdagni and P. Kebarle, J. Am. Chem. Soc., 95, 3504 (1973).

- (25) D. T. Clark and I. W. Scanlan, J. C. S. Faraday 2, 70, 1222 (1974).
- (26) A. J. Ashe III, F. Burger, E. Heilbronner, J. P. Maier, and J. Muller, Helvetica Chimica Acta, 59, 1944 (1976).
- (27) B. Bak, L. Hansen-Nygaard, and J. Rastrup-Andersen, J. Mol. Spectrosc., 2, 36 (1958).
- (28) T. C. Wong and L. S. Bartell, J. Chem. Phys., 61, 2840 (1974).
- (29) T. C. Wong, A. J. Ashe III, and L. S. Bartell, J. Mol. Structure, 25, 65 (1975).
- (30) H. Oehling and A. Schweig, Tetrahedron Lett., 4941 (1970).
- (31) W. von Niessen, G. H. F. Diercksen, and L. S. Cederbaum, Chem. Phys., 10, 345 (1975).
- (32) H. L. Hase, A. Schweig, H. Hahn, and J. Radloff, Tetrahedron, 29, 475 (1973).
- (33) L. Pauling, "The Nature of the Chemical Bond", 3rd ed., Cornell University Press, Ithaca, N.Y., 1960, p. 90.
- (34) K. Dimroth, "Phosphorus-Carbon Double Bonds", Springer-Verlag, New York, N.Y., 1973, p. 39.
- (35) Reference 34, p. 38.
- (36) Reference 23, p. 309.
- (37) D. Holtz, W. G. Henderson, and J. L. Beauchamp, unpublished results.

CHAPTER V

Gas Phase Organometallic Chemistry. Reactions  
of  $\text{Al}^+$  with Alkyl Halides.

by

Ronald V. Hodges and J. L. Beauchamp\*

Contribution No. 5687 from the Arthur Amos Noyes  
Laboratory of Chemical Physics, California Institute of  
Technology, Pasadena, California 91125



## ABSTRACT

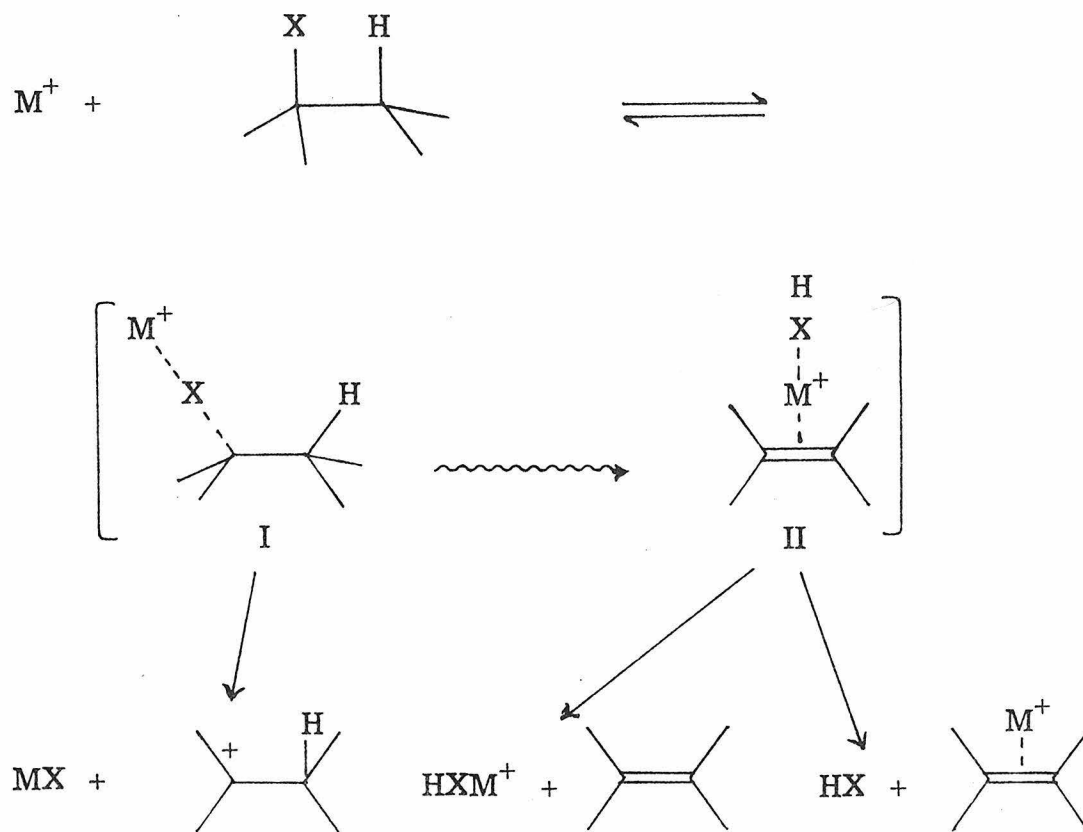
Gas phase ion-molecule reactions of  $\text{Al}^+$  with several alkyl halides have been examined using an ion beam apparatus. Relative product ion abundances are reported as a function of collision energy over the range 0.5 to 5 eV. Three types of reactions are observed: (1) halide transfer, (2) dehydrohalogenation, and (3) oxidation. Halide transfer from dichloroalkanes yields chloronium ions, which may eliminate HCl to give allyl cations. Dehydrohalogenation results in elimination of HX with  $\text{Al}^+$  remaining bound to either HX or the alkene which is concomitantly formed. The relative importance of the halide transfer and dehydrohalogenation products is dependent on the reaction thermodynamics and the collision energy. Reaction of  $\text{Al}^+$  with  $\text{CH}_2\text{ClCH}_2\text{Cl}$  leads to  $\text{AlCl}_2^+$  and  $\text{C}_2\text{H}_4$ , a process in which the metal is formally oxidized from the +1 to the +3 state.

## INTRODUCTION

The area of the gas phase reactions of metal ions is relatively unexplored. Some reactions of alkali ions [1-6],  $U^+$  [7, 8],  $Al^+$  [9], and the transition metal ions  $Co^+$  [4],  $Fe^+$  [4, 10], and  $Ti^+$  [11] have been reported, but at present the data are too meager to reveal general patterns of reactivity which would be useful in predicting gas phase metal ion chemistry.

Alkali ions are easily produced using surface ionization techniques [12] and have received the most attention. Having a noble gas electronic configuration, alkali ions are not easily oxidized and exhibit reactivity characteristic of Lewis acids. The gas phase binding energy of alkali ions to several Lewis bases have been determined [2, 13-16]. Association of an alkali ion  $M^+$  with an alkyl halide  $RX$  leads to an activated intermediate, which may dissociate to  $MX$  and a carbonium ion  $R^+$ , if this reaction is exothermic, or may eliminate  $HX$  to give an alkene, with the alkali ion remaining bound to either species (Scheme I) [1, 4].  $Fe^+$  [4],  $Co^+$  [4], and  $U^+$  [17] also dehydrohalogenate alkyl halides. The dehydrohalogenation of alkyl halides by metal ions and other Lewis acids [18] appears to be a general process.

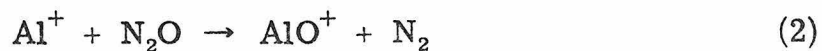
Al atoms in the ground state,  $^2P_{1/2}$ , have the electronic configuration  $Ne3s^23p^1$ . The ionization potential of Al is 6 eV [19]. This value is low enough to permit the use of surface ionization techniques to generate  $Al^+$  in sufficient quantities for mass spectrometric studies [9, 12]. In its ground state electronic configuration,  $Ne3s^2$ ,  $Al^+$  resembles the alkali ions in that it has a filled subshell. Unlike



Scheme I

the alkali ions,  $Al^+$  has vacant orbitals in the valence shell and can assume sp hybridization in compounds in which Al has a formal oxidation state greater than one.

The only ion chemistry involving  $Al^+$  which has been reported in the literature are charge transfer processes and reactions (1) and (2) [9]. Although they were not discussed in such terms, reactions



(1) and (2) represent a formal oxidation of  $\text{Al}^+$  from the +1 to the +3 state. Both reactions (1) and (2) behave as endothermic processes, exhibiting reaction cross sections which rise rapidly from a threshold to a maximum beyond which they decrease with increasing kinetic energy [9].

This paper describes the reactions of low energy (0.5 - 6 eV) aluminum ions with several alkyl halides. The goal of this study was to characterize the range of reactions exhibited by an ionic species whose ground state electronic structure is similar to that of the alkalis, yet which has variable and energetically accessible oxidation states.

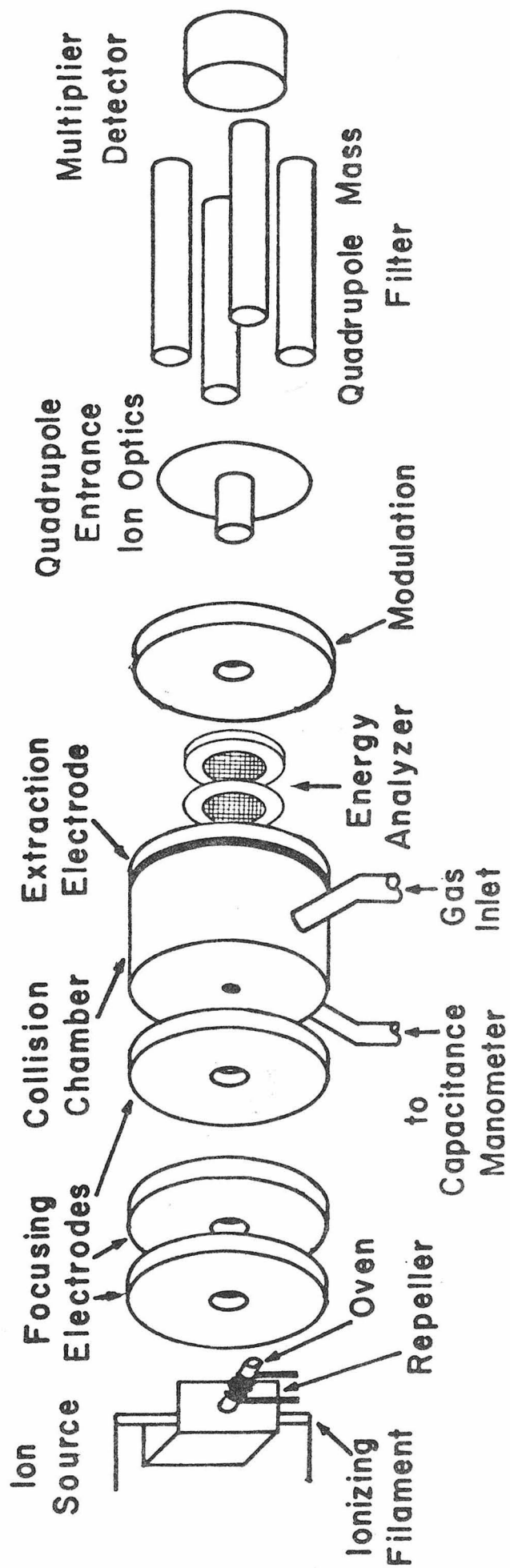
## EXPERIMENTAL SECTION

The apparatus has been previously described [3, 8] and is shown in Fig. 1. Ions from a surface ionization source are focused into a collision chamber containing the reactant gas. The chamber has axial symmetry and is designed to efficiently extract low energy product ions [20]. Ions exit the chamber with the aid of a small extraction field provided by an 0.5 V potential drop across the chamber. They are focused by a final lens element into an EAI Quad 250B quadrupole mass spectrometer for mass analysis and detection. Phase sensitive detection is accomplished by modulating the voltage on the final lens element and directing the output of the Channeltron electron multiplier into a PAR HR-8 lock-in amplifier, referenced to the modulating frequency.

For production of  $\text{Al}^+$  anhydrous  $\text{AlCl}_3$  was placed in the source oven. Hydrated  $\text{AlCl}_3$  and anhydrous  $\text{AlF}_3$  were unsatisfactory for this purpose. The impurities  $\text{Na}^+$  and  $\text{K}^+$  were observed in

**FIGURE 1**

Schematic drawing of the ion beam apparatus and surface ionization source.



abundances varying from  $< 1\%$  of the  $\text{Al}^+$  abundance to slightly greater than the  $\text{Al}^+$  abundance. Traces of  $\text{Cr}^+$ ,  $\text{Ga}^+$ ,  $\text{Fe}^+$ , and  $\text{Cu}^+$  were also noted. No  $\text{AlCl}_x^+$  was present. In control experiments no reaction between  $\text{Na}^+$  and  $\text{K}^+$  and  $\text{CCl}_4$ ,  $\text{CCl}_3\text{F}$  or  $\text{CH}_2\text{ClCH}_2\text{Cl}$  could be detected. No dehydrohalogenation products containing  $\text{Na}^+$  or  $\text{K}^+$  were ever observed.

Ion signal intensities were corrected for the mass discrimination of the mass spectrometer. A mass spectrum of  $\text{C}_3\text{F}_6$  was obtained by allowing  $\text{C}_3\text{F}_6$  into the chamber and biasing the source elements so that the surface ionization filament could be operated as a source of 70 eV electrons. The correction factors were determined by comparing the intensities of the peaks of this mass spectrum with those of the ion cyclotron resonance mass spectrum [21].

A retarding field energy analyzer (Fig. 1) was installed to determine the kinetic energies of reactant and product ions. The analyzer comprises three parallel gold mesh screens (40 lines  $\text{cm}^{-1}$ , 82% transparent) spaced 1 mm apart. The first screen covers the chamber exit aperture. The potential of the final screen is the same as the chamber entrance. A variable retarding potential is applied to the intermediate screen. Retarding potential curves were obtained by monitoring the signal intensity of an ion while varying the potential of the intermediate retarding screen. In some cases the derivative of this curve was obtained by modulating the retarding screen potential and employing phase sensitive detection of the signal. The modulation amplitude was typically 0.1 V. Figure 2 shows a derivative

## FIGURE 2

(a) Derivative of a retarding field potential curve for  $\text{Al}^+$ . (b) Retarding field potential curve for  $\text{CCl}_3^+$  produced by reaction of  $\text{Al}^+$  (3.3 eV LAB energy) with  $\text{CCl}_3\text{F}$ . Dotted line indicates zero signal level.





curve for  $\text{Al}^+$ . The quantity plotted on the abscissa is the difference between the retarding screen potential and the average of the potentials of the chamber entrance and exit. The value of this difference at the maximum of the curve is taken to be the ion energy in the laboratory frame. This value represents only an average of the range of  $\text{Al}^+$  energies in the chamber. The full width at half maximum of this peak is 0.7 eV. The 0.5 V extractor voltage across the chamber introduces an additional uncertainty in the ion energy.

A retarding potential curve for the product ion  $\text{CCl}_3^+$  from the reaction of  $\text{Al}^+$  with  $\text{CCl}_3\text{F}$  is also given in Fig. 2. The signal has both high and low energy components. The high energy component has the same energy as the  $\text{Al}^+$  beam and is attributed to decomposition and surface ionization of  $\text{CCl}_3\text{F}$  on the filament. The signals from all products except  $\text{AlCl}_2^+$  from  $\text{CH}_2\text{ClCH}_2\text{Cl}$  and  $\text{C}_2\text{H}_5^+$  from  $\text{C}_2\text{H}_5\text{Cl}$  exhibited similar high energy components. These components were more significant at higher energies, but never altered product distributions by more than 5%. No corrections for their contribution were made. The low energy components of all product ion signals at all collision energies were less than 1 eV. A detailed analysis of the product ion kinetic energy distributions was not attempted. The wide spread in the reactant ion energy and the uncertainties in the measurement of the low product ion kinetic energies precluded the extraction of information which would be useful in understanding the details of the reactive collision.

Reproducible reaction cross sections could not be obtained. The collection efficiency of the product ions may be significantly less

than one and very sensitive to changes in lens potentials. Relative product ion abundances were reproducible and the data are presented in this form. Some useful qualitative observations about the magnitude and energy dependence of the reaction cross sections are made.

cis-1, 2-Dichlorocyclopentane was synthesized by the method of Filippo [22] and purified by preparative glc. Other chemicals were research grade commercially available reagents and were used as supplied.

## RESULTS

The reactions of  $\text{Al}^+$  and alkyl halides observed in this study are summarized in Table 1. Enthalpies of reaction are given, where appropriate heats of formation are known.

Reactions which are exothermic exhibited cross sections which decreased sharply with increasing collision energy. The upper limit of the energy range which could be examined for each compound depended on the rate at which the reaction cross section decreased with energy.

### Tetrahalomethanes

Chloride ion transfer (reaction 3) is the only significant reaction of  $\text{Al}^+$  and  $\text{CCl}_4$  observed over the collision energy range 1-6 eV. At the



higher end of this range low intensity ions appear at masses corresponding to  $\text{AlCl}_2^+$ ,  $\text{AlCl}^+$ ,  $\text{CCl}_2^+$ , and  $\text{CCl}^+$ . The maximum signal

TABLE 1

Summary of the Ion-Molecule Reactions of  $\text{Al}^+$  and Alkyl Halides and  
Calculated Reaction Enthalpies

Ion-Molecule Reaction		$\Delta H^a$
(3)	$\text{Al}^+ + \text{CCl}_4 \rightarrow \text{CCl}_3^+ + \text{AlCl}$	- 9
(4)	$\text{Al}^+ + \text{CCl}_3\text{F} \begin{cases} \rightarrow \text{CCl}_3^+ + \text{AlF} \\ \rightarrow \text{CCl}_2\text{F}^+ + \text{AlCl} \end{cases}$	-14
(5)		- 6
(6)	$\text{Al}^+ + \text{CCl}_2\text{F}_2 \begin{cases} \rightarrow \text{CCl}_2\text{F}^+ + \text{AlF} \\ \rightarrow \text{CClF}_2^+ + \text{AlCl} \end{cases}$	- 8
(7)		18
	$\text{Al}^+ + \text{CClF}_3 \begin{cases} \not\rightarrow \text{CClF}_2^+ + \text{AlF} \\ \not\rightarrow \text{CF}_3^+ + \text{AlCl} \end{cases}$	19
		33
	$\text{Al}^+ + \text{CF}_4 \not\rightarrow \text{CF}_3^+ + \text{AlF}$	36
	$\text{Al}^+ + \text{CH}_3\text{Cl} \not\rightarrow \text{CH}_3^+ + \text{AlCl}$	51
(8)	$\text{Al}^+ + \text{C}_2\text{H}_5\text{Cl} \begin{cases} \rightarrow (\text{C}_2\text{H}_4)\text{Al}^+ + \text{HCl} \\ \rightarrow (\text{HCl})\text{Al}^+ + \text{C}_2\text{H}_4 \\ \rightarrow \text{C}_2\text{H}_5^+ + \text{AlCl} \end{cases}$	
(9)		
(10)		16
(11)	$\text{Al}^+ + s\text{-C}_3\text{H}_7\text{Cl} \rightarrow s\text{-C}_3\text{H}_7^+ + \text{AlCl}$	- 4
(12)	$\text{Al}^+ + \text{CH}_2\text{ClCH}_2\text{Cl} \begin{cases} \rightarrow \text{C}_2\text{H}_4\text{Cl}^+ + \text{AlCl} \\ \rightarrow \text{AlCl}_2^+ + \text{C}_2\text{H}_4 \end{cases}$	5
(13)		-80
(14)	$\text{Al}^+ + \text{C}_3\text{H}_6\text{Cl}_2 \begin{cases} \rightarrow \text{C}_3\text{H}_6\text{Cl}^+ + \text{AlCl} \\ \rightarrow \text{C}_3\text{H}_5^+ + \text{HCl} + \text{AlCl} \\ \rightarrow (\text{C}_3\text{H}_5\text{Cl})\text{Al}^+ + \text{HCl} \end{cases}$	
(15)		
(16)		

TABLE 1 (continued)

Ion-Molecule Reaction	$\Delta H$
<div style="display: flex; align-items: center;"> <div style="margin-right: 10px;">(17)</div> <div style="margin-right: 10px;"><math>\text{Al}^+ + \text{c-C}_5\text{H}_8\text{Cl}_2</math></div> <div style="margin-right: 10px;">—</div> <div style="display: flex; flex-direction: column; align-items: center;"> <div style="margin-bottom: 5px;">→ <math>\text{C}_5\text{H}_8\text{Cl}^+ + \text{AlCl}</math></div> <div style="margin-top: 5px;">→ <math>\text{C}_5\text{H}_7^+ + \text{HCl} + \text{AlCl}</math></div> </div> </div>	
<div style="display: flex; align-items: center;"> <div style="margin-right: 10px;">(18)</div> <div style="margin-right: 10px;"><math>\text{Al}^+ + \text{c-C}_5\text{H}_8\text{Cl}_2</math></div> <div style="margin-right: 10px;">—</div> <div style="display: flex; flex-direction: column; align-items: center;"> <div style="margin-bottom: 5px;">→ <math>\text{C}_5\text{H}_8\text{Cl}^+ + \text{AlCl}</math></div> <div style="margin-top: 5px;">→ <math>\text{C}_5\text{H}_7^+ + \text{HCl} + \text{AlCl}</math></div> </div> </div>	

<sup>a</sup>Reaction enthalpy in kcal mol<sup>-1</sup>. Data used in calculating this quantity are found in Table 2, Ref. 23, and J. D. Cox and G. Pilcher, Thermochemistry of Organic and Organometallic Compounds, Academic Press, New York, 1970.

TABLE 2

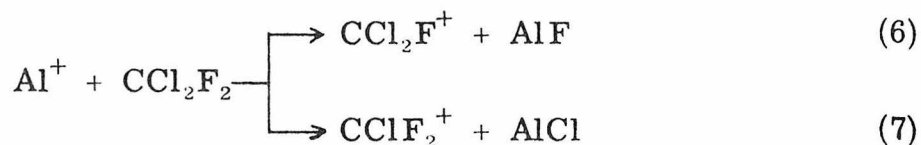
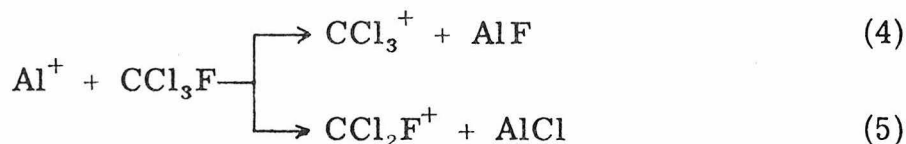
Heats of Formation Used to Calculate Reaction Enthalpies

Species	$\Delta H_{f298}^0$ (kcal mol <sup>-1</sup> )	Reference
Al <sup>+</sup>	217.3 ± 0.5	a
AlCl <sub>2</sub> <sup>+</sup>	94.2 ± 28	b
AlCl	- 12.3 ± 1	a
AlF	- 63.4 ± 0.8	a
CH <sub>3</sub> <sup>+</sup>	261	c
C <sub>2</sub> H <sub>5</sub> <sup>+</sup>	219	c
(CH <sub>3</sub> ) <sub>2</sub> CH <sup>+</sup>	192	c
C <sub>2</sub> H <sub>4</sub> Cl <sup>+</sup>	204	d
CCl <sub>3</sub> <sup>+</sup>	198 ± 7	e
CCl <sub>2</sub> F <sup>+</sup>	155 ± 5	e
CClF <sub>2</sub> <sup>+</sup>	130 ± 4	e
CF <sub>3</sub> <sup>+</sup>	93.8 ± 2	e

<sup>a</sup>JANAF Thermochemical Tables, NSRDS-NBS 37 (1971).<sup>b</sup>J. Phys. Chem. Ref. Data, 3 (1974) 311.<sup>c</sup>F. P. Lossing and G. P. Semeluk, Can J. Chem., 48 (1970) 955.<sup>d</sup>D. W. Berman and J. L. Beauchamp, J. Am. Chem. Soc., to be submitted.<sup>e</sup>Ref. 23.

intensity of these ions never exceeds 0.5% of the maximum signal intensity of  $\text{CCl}_3^+$ . These and similar ions observed in the other halomethanes have been neglected.

Two halide transfer processes are possible with  $\text{CCl}_3\text{F}$  (reactions 4 and 5) and  $\text{CCl}_2\text{F}_2$  (reactions 6 and 7). The ratio



$\text{CCl}_3^+/\text{CCl}_2\text{F}^+$  in  $\text{CCl}_3\text{F}$  decreases with increasing energy until it reaches a value of unity at 4.5 eV (Fig. 3). The ratio  $\text{CCl}_2\text{F}^+/\text{CClF}_2^+$  in  $\text{CF}_2\text{Cl}_2$  behaves similarly but is larger than the product ratio in  $\text{CCl}_3\text{F}$  at a given energy and does not reach a constant value at collision energies up to 5 eV (Fig. 4).

No reaction products were detected with  $\text{CF}_3\text{Cl}$  and  $\text{CF}_4$ .

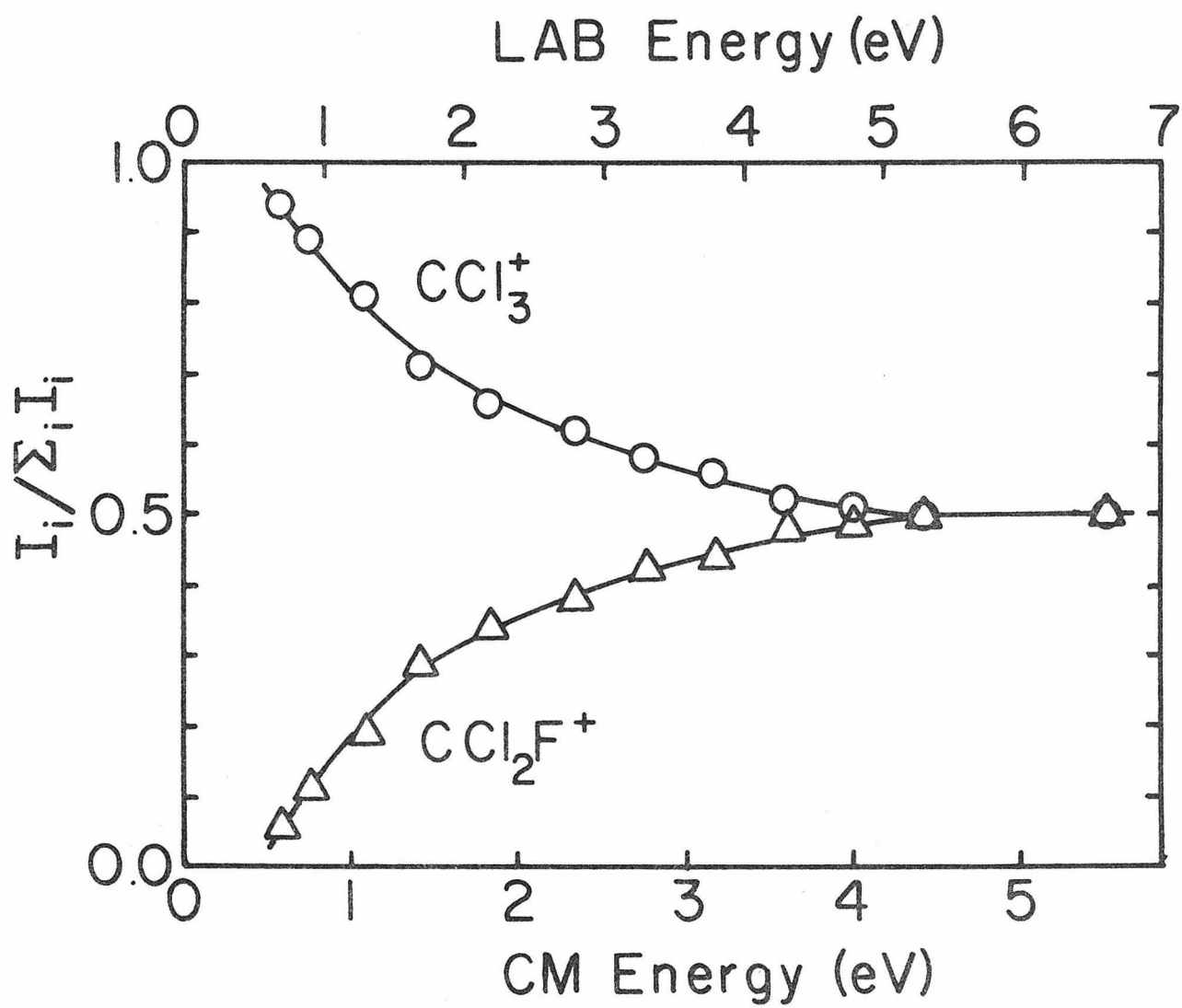
#### Monochloroalkanes. Methyl Chloride

No products were observed when  $\text{Al}^+$  interacted with  $\text{CH}_3\text{Cl}$  at collision energies up to 3.5 eV and a pressure of  $\text{CH}_3\text{Cl}$  of 5.8 mtorr. The smallest product signal that can be detected by this apparatus corresponds to a reaction cross section of about  $0.1 \text{ \AA}^2$ . A cross section for reaction with  $\text{CH}_3\text{Cl}$  less than this value is suggested.

## FIGURE 3

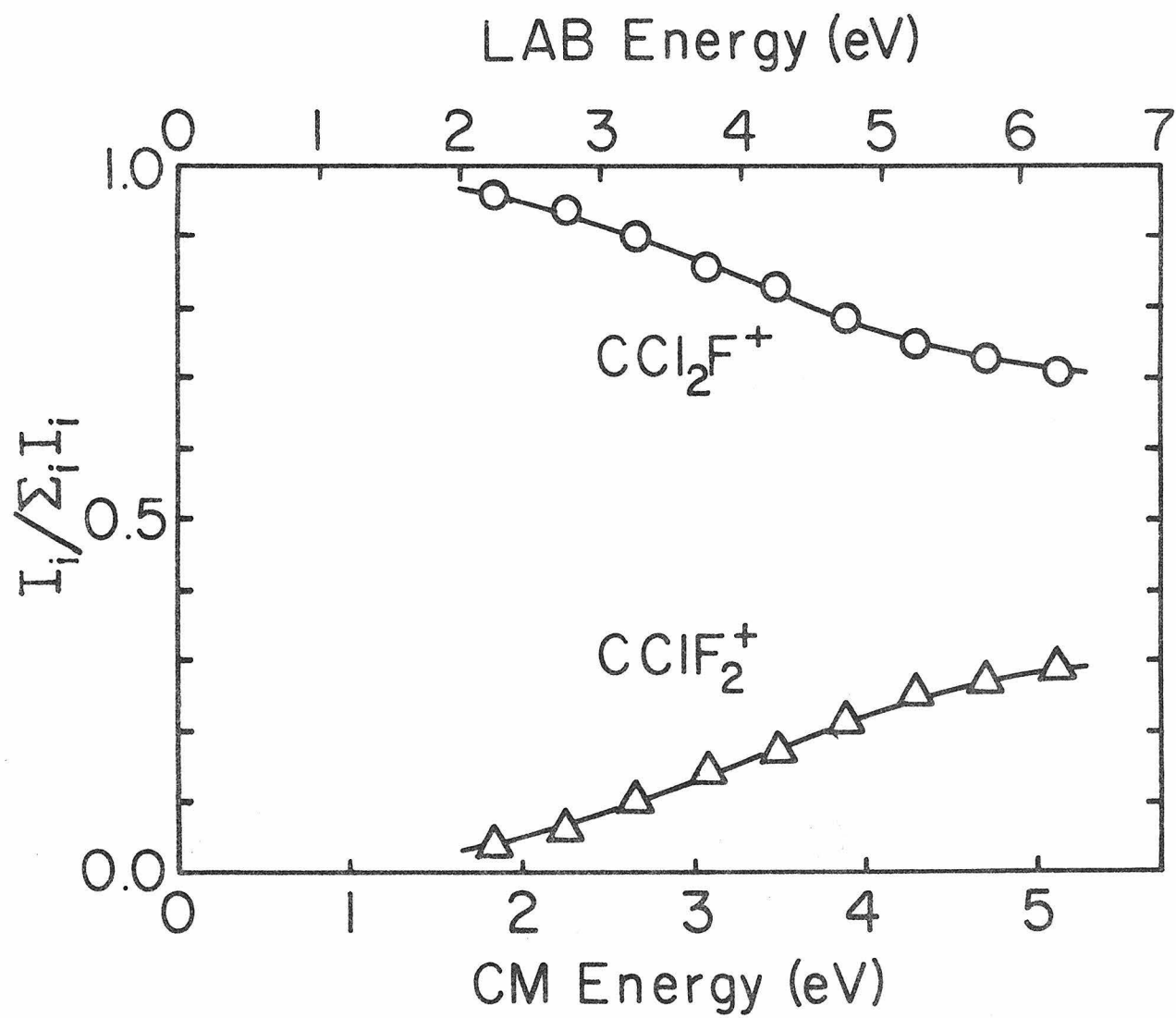
Variation with energy of the relative product ion abundances in the reaction of  $\text{Al}^+$  and  $\text{CCl}_3\text{F}$  at 5.7 mtorr.





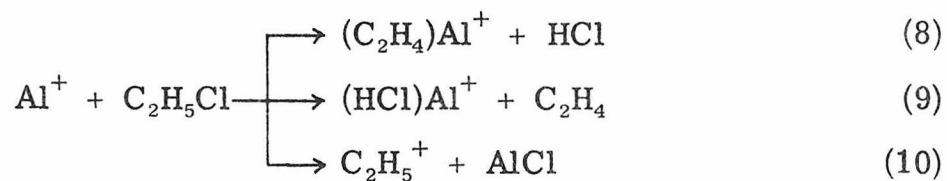
## FIGURE 4

Variation with energy of the relative product ion abundances in the reaction of  $\text{Al}^+$  and  $\text{CCl}_2\text{F}_2$  at 4.7 mtorr.



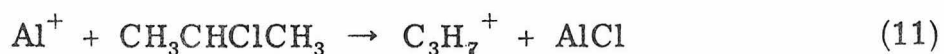
### Ethyl Chloride

The relative product ion abundances observed when  $\text{Al}^+$  reacts with  $\text{C}_2\text{H}_5\text{Cl}$  are shown as a function of collision energy in Fig. 5. The dehydrohalogenation reactions (8) and (9) predominate. The product distribution for these two reactions changes dramatically in favor of  $(\text{HCl})\text{Al}^+$  with increasing energy. Chloride transfer, reaction (10), competes more favorably with dehydrohalogenation as the collision energy increases.



### Isopropyl Chloride

The major reaction of  $\text{Al}^+$  with  $\text{CH}_3\text{CHClCH}_3$  is chloride transfer (reaction 11). Traces of the dehydrohalogenation products



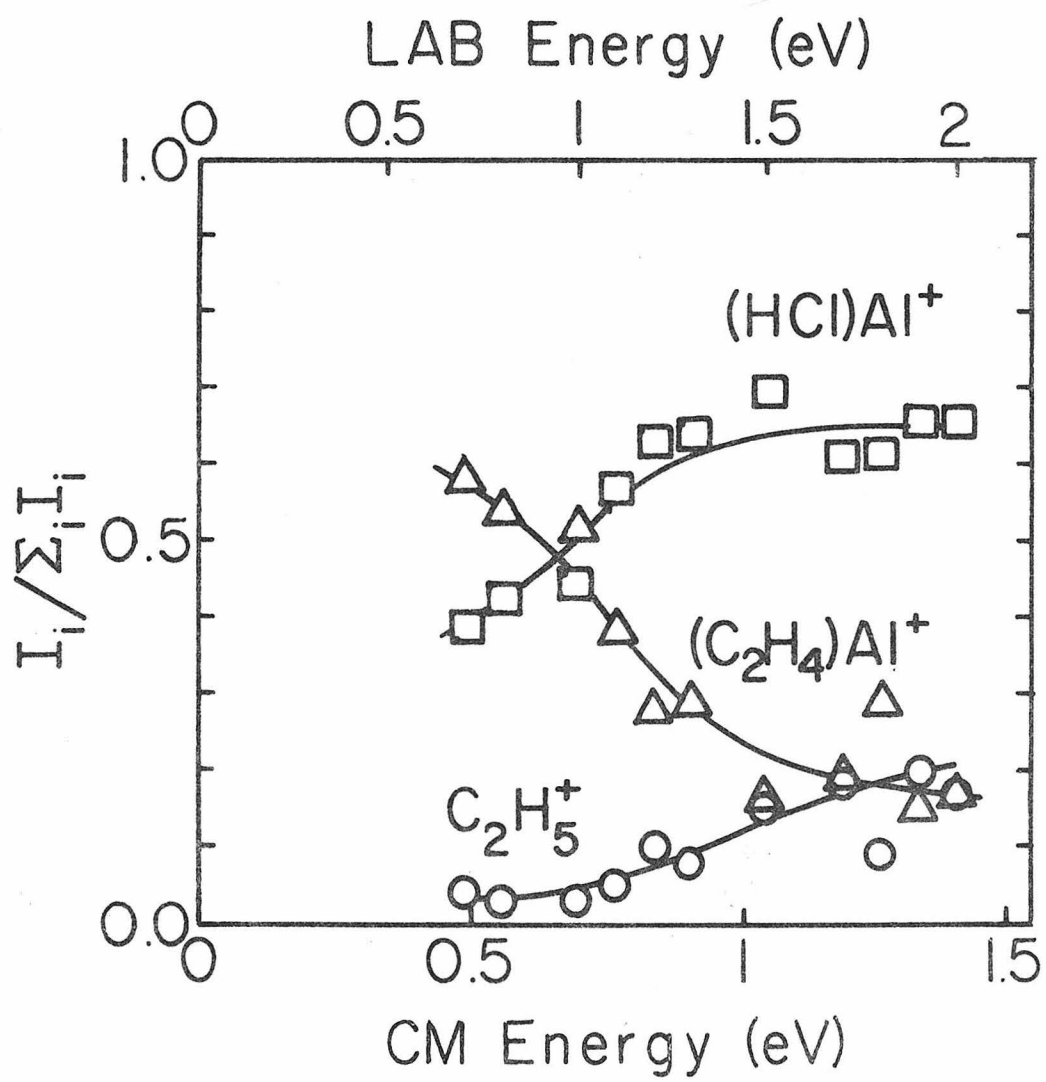
analogous to those formed in reactions (8) and (9) were present, but their abundance was less than 1% of that of  $\text{C}_3\text{H}_7^+$ .

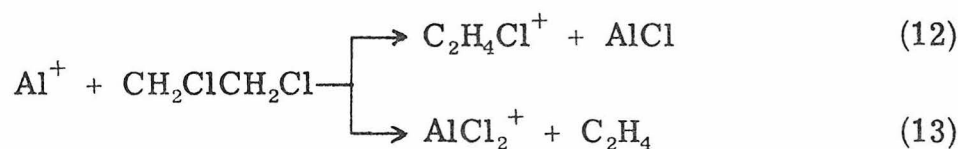
### Dichloroalkanes. 1, 2-Dichloroethane

Chloride transfer is the principal reaction of  $\text{Al}^+$  with  $\text{CH}_2\text{ClCH}_2\text{Cl}$  (reaction 12), but oxidation of  $\text{Al}^+$  to  $\text{AlCl}_2^+$  is also significant (reaction 13). The product of reaction (12),  $\text{C}_2\text{H}_4\text{Cl}^+$ , has the same mass as  $(\text{HCl})\text{Al}^+$  (m/e 63 and 65). Observed patterns of reactivity suggest that  $(\text{C}_2\text{H}_3\text{Cl})\text{Al}^+$  would also be observed, if the

## FIGURE 5

Variation with energy of the relative product ion abundances in the reaction of  $\text{Al}^+$  and  $\text{C}_2\text{H}_5\text{Cl}$ . Combined data from experiments at 5.7, 6.1 and 4.4 mtorr.

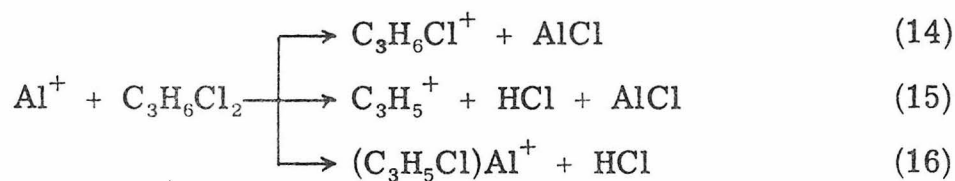




product at  $\underline{m/e}$  63 and 65 were  $(\text{HCl})\text{Al}^+$ .  $(\text{C}_2\text{H}_3\text{Cl})\text{Al}^+$  was not detected and the ions at  $\underline{m/e}$  63 and  $\underline{m/e}$  65 are attributed exclusively to  $\text{C}_2\text{H}_4\text{Cl}^+$ . The relative abundances of the two product ions are plotted as a function of collision energy in Fig. 6. The branching ratio is fairly constant over the energy range examined.

### 1, 2- and 1, 3-Dichloropropane

Dehydrohalogenation (reaction 16) is competitive with chloride transfer (14) in the reaction of  $\text{Al}^+$  with the dichloropropanes at low collision energy (Figs. 7 and 8). As the energy increases the proportion of dehydrohalogenation decreases and a new process appears, loss of HCl from  $\text{C}_3\text{H}_6\text{Cl}^+$  to give allyl cation (reaction 15). Detection

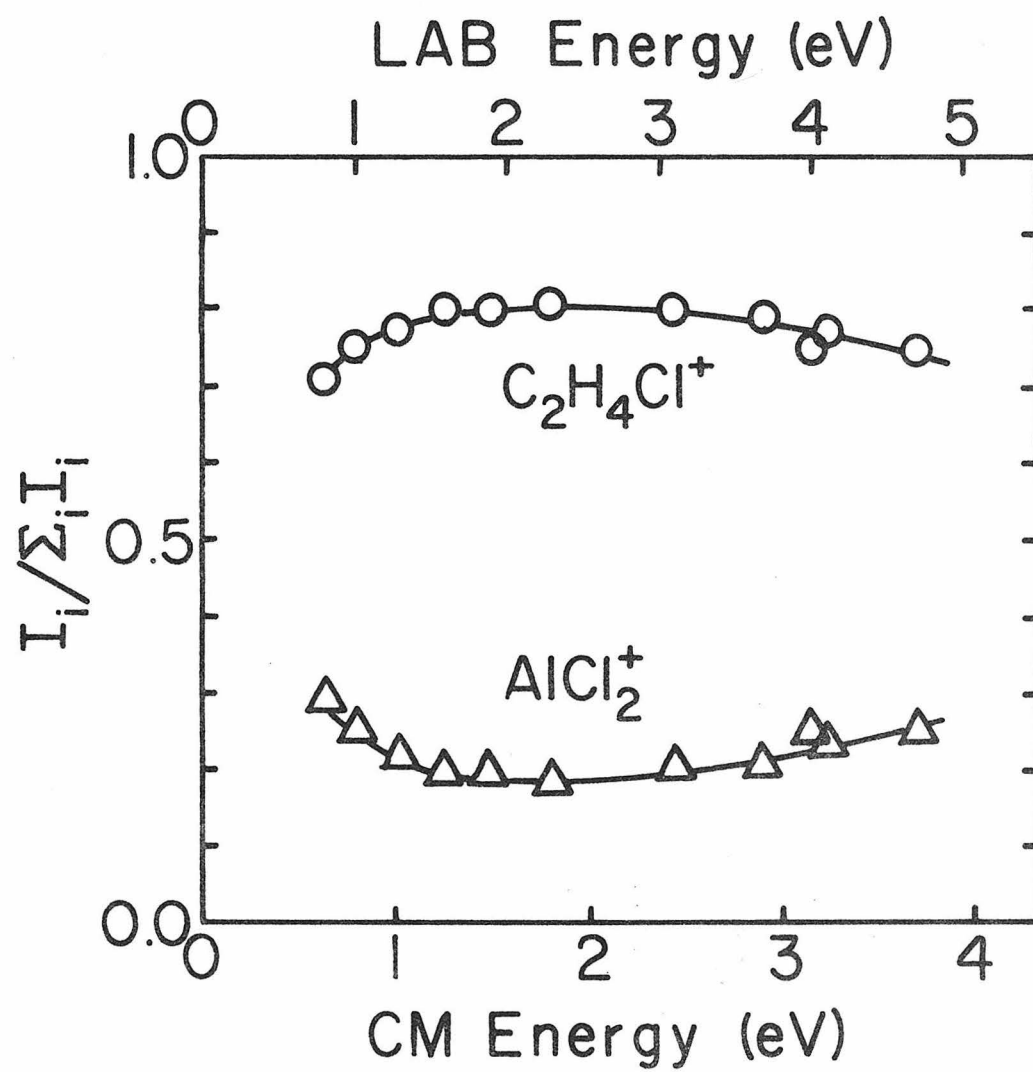


of allyl cation ( $\underline{m/e}$  41) was complicated by the presence of  $\text{K}^+$  ( $\underline{m/e}$  39 and 41) in the reactant ion beam in comparable abundance with allyl cation. The contribution of  $\text{K}^+$  at this mass was calculated using the measured isotope ratio,  $^{41}\text{K}^+ / ^{39}\text{K}^+$ , and subtracted out. As an additional process,  $\text{AlCl}_2^+$  was detected with either 1, 2- or 1, 3-dichloropropane present in the reaction chamber. However, its

## FIGURE 6

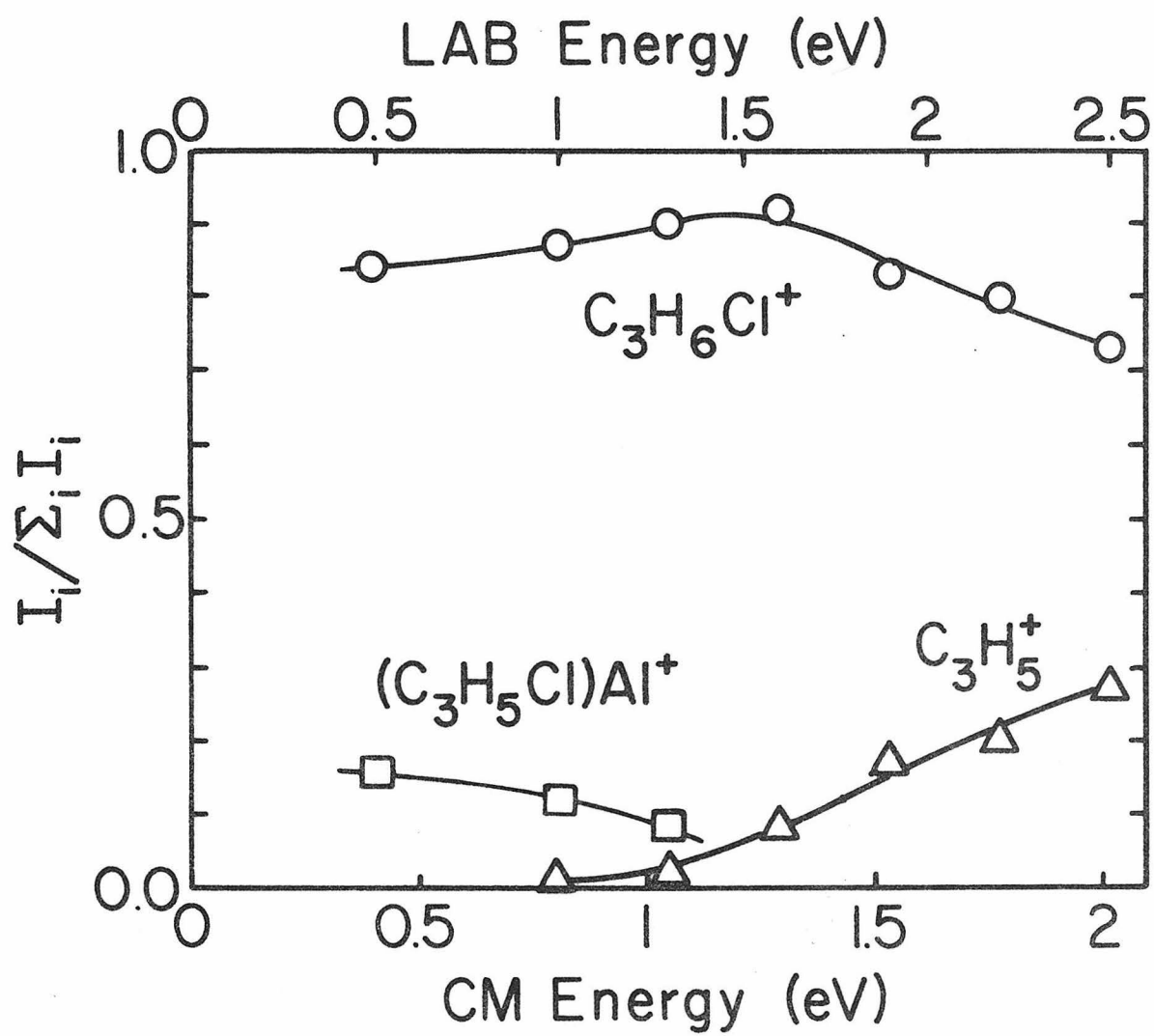
Variation with energy of the relative product ion abundances in the reaction of  $\text{Al}^+$  and  $\text{CH}_2\text{ClCH}_2\text{Cl}$  at 3.7 mtorr.





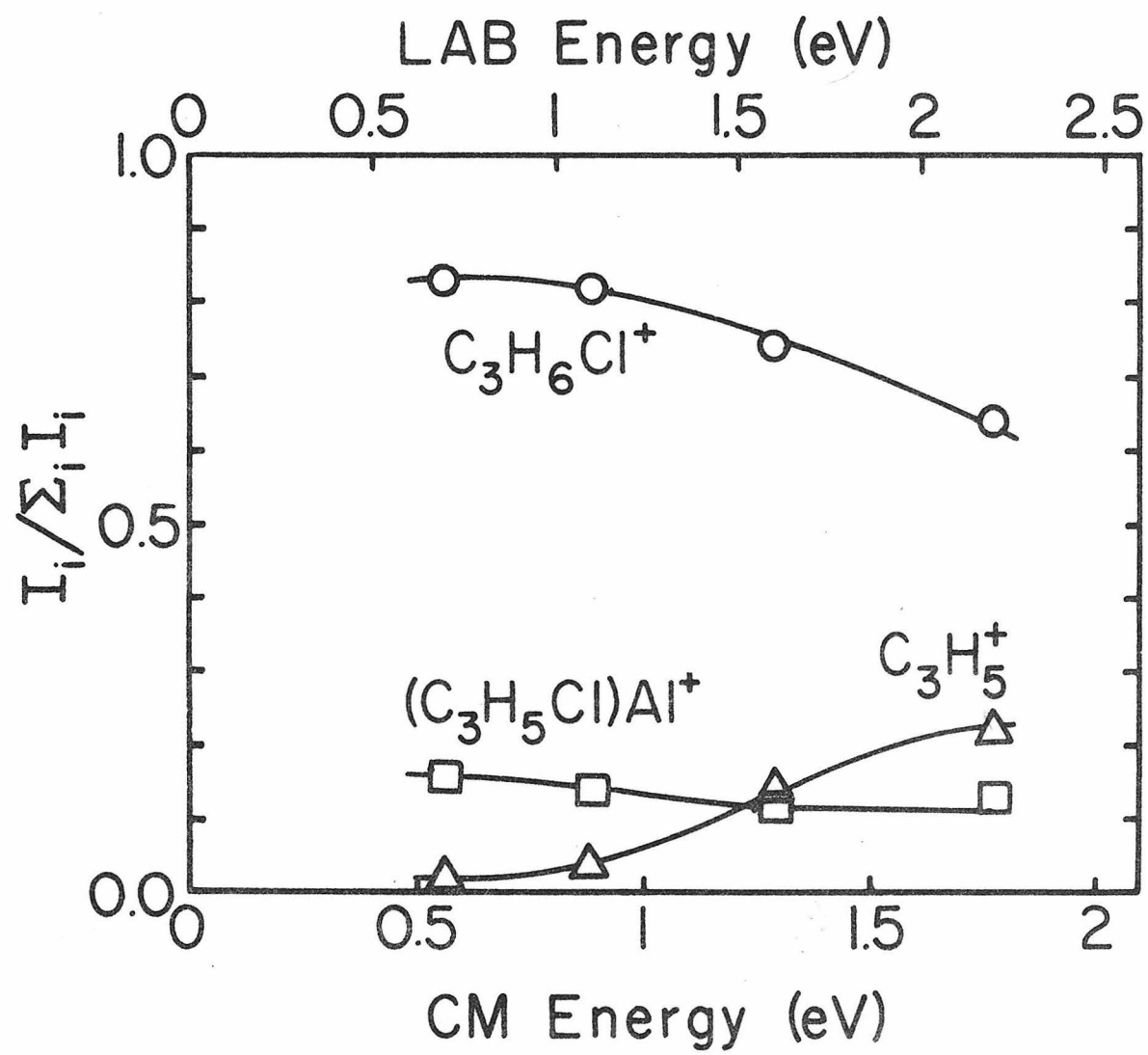
## FIGURE 7

Variation with energy of the relative product ion abundances in the reaction of  $\text{Al}^+$  and  $\text{CH}_2\text{ClCH}_2\text{ClCH}_3$  at 3.1 mtorr.



## FIGURE 8

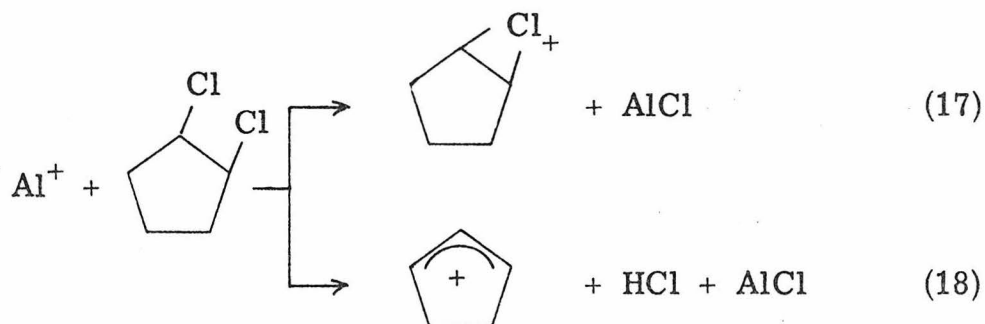
Variation with energy of the relative product ion abundances in the reactions of  $\text{Al}^+$  and  $\text{CH}_2\text{ClCH}_2\text{CH}_2\text{Cl}$  at 4.0 mtorr.



abundance was  $< 2\%$  of the total product ion signal at all energies in both cases.

### cis- and trans-1, 2-Dichlorocyclopentane

In an attempt to determine the effect of stereochemistry on the reactions of  $\text{Al}^+$  with dichloroalkanes, cis- and trans-1, 2-dichlorocyclopentane was studied. Chloride transfer (reaction 17), followed by HCl elimination (reaction 18) were the only processes



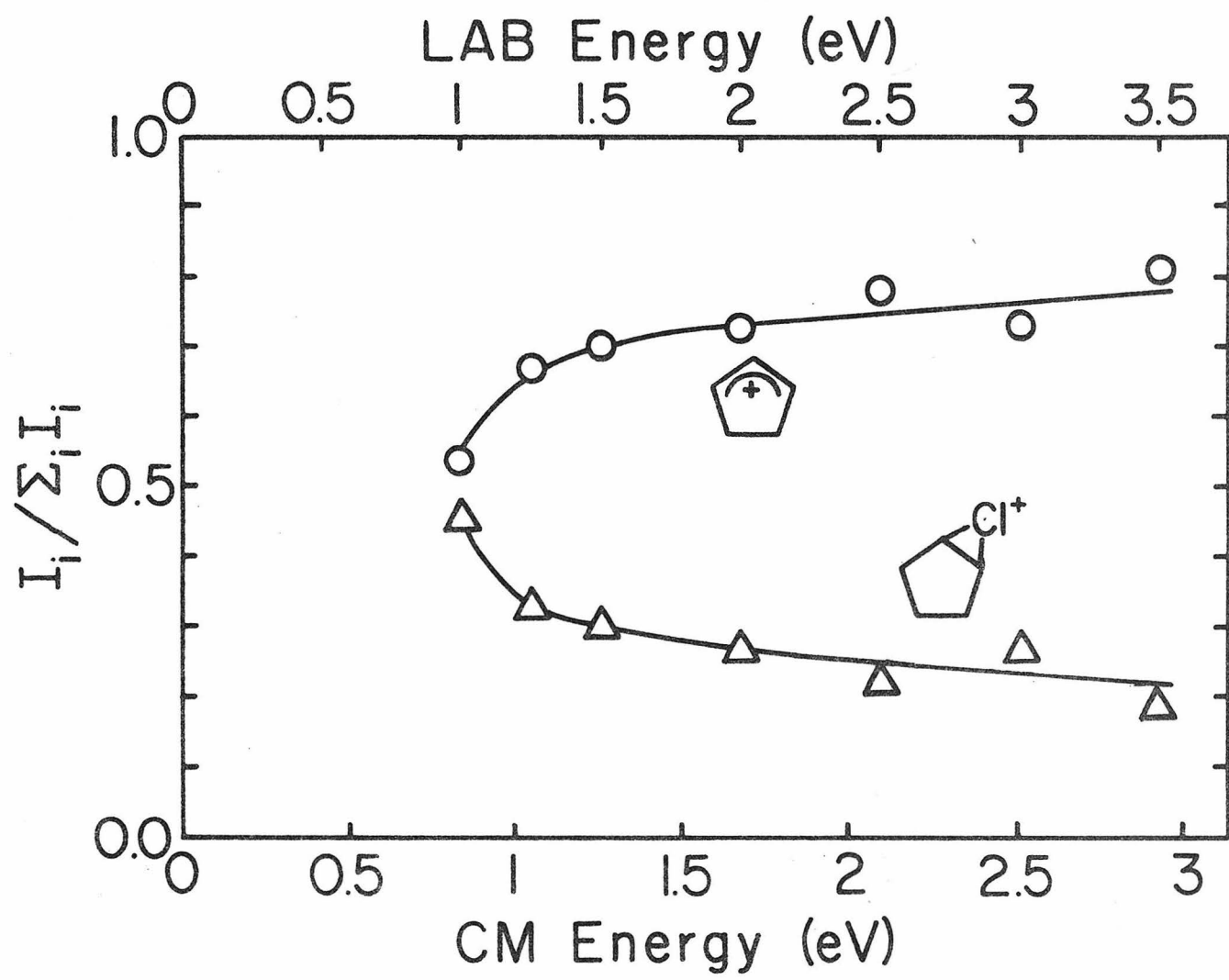
observed. For both isomers an increase in collision energy causes greater decomposition of the chloronium ion (Figs. 9 and 10).

### Cluster Ion Formation

Cluster ions of  $\text{Al}^+$  with  $\text{C}_2\text{H}_5\text{Cl}$ ,  $\text{C}_3\text{H}_7\text{Cl}$ ,  $\text{C}_2\text{H}_4\text{Cl}_2$  and  $\text{C}_3\text{H}_6\text{Cl}_2$  were observed at collision energies less than 2 eV in abundances comparable to those of other products. They are formed by termolecular clustering processes and possibly by  $\text{Al}^+$  transfer from the products of dehydrohalogenation reactions. Because these ions are not produced in primary bimolecular reactions, they have been omitted from the product abundances presented above.

## FIGURE 9

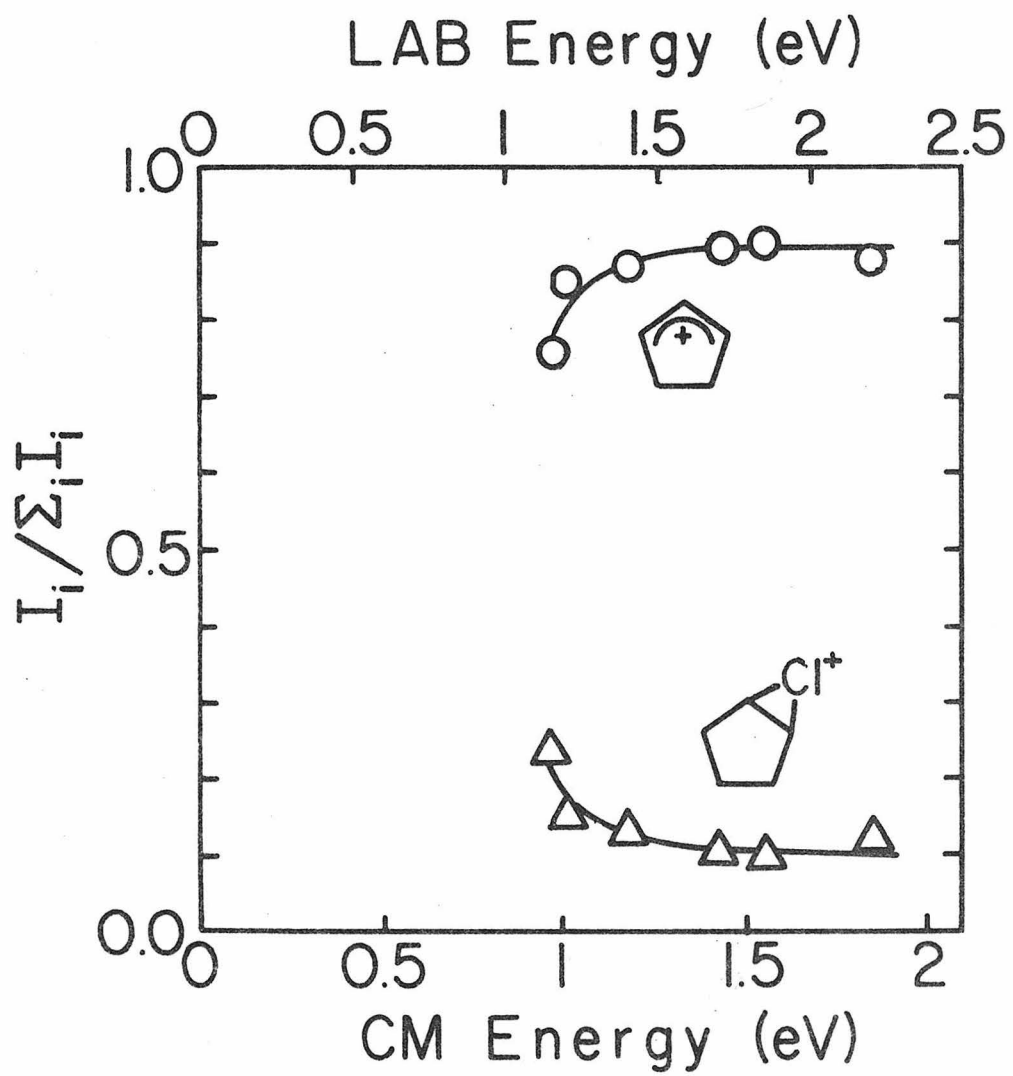
Variation with energy of the relative product  
ion abundances in the reaction of  $\text{Al}^+$  and  
trans-1, 2-dichlorocyclopentane at 2.3 mtorr.





## FIGURE 10

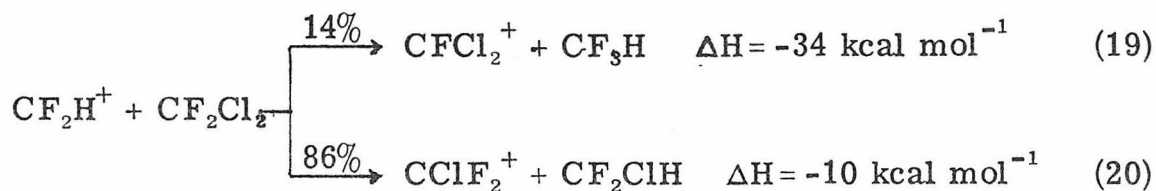
Variation with energy of the relative product ion abundances in the reaction of  $\text{Al}^+$  and cis-1, 2-dichlorocyclopentane at 1.6 mtorr.



## DISCUSSION

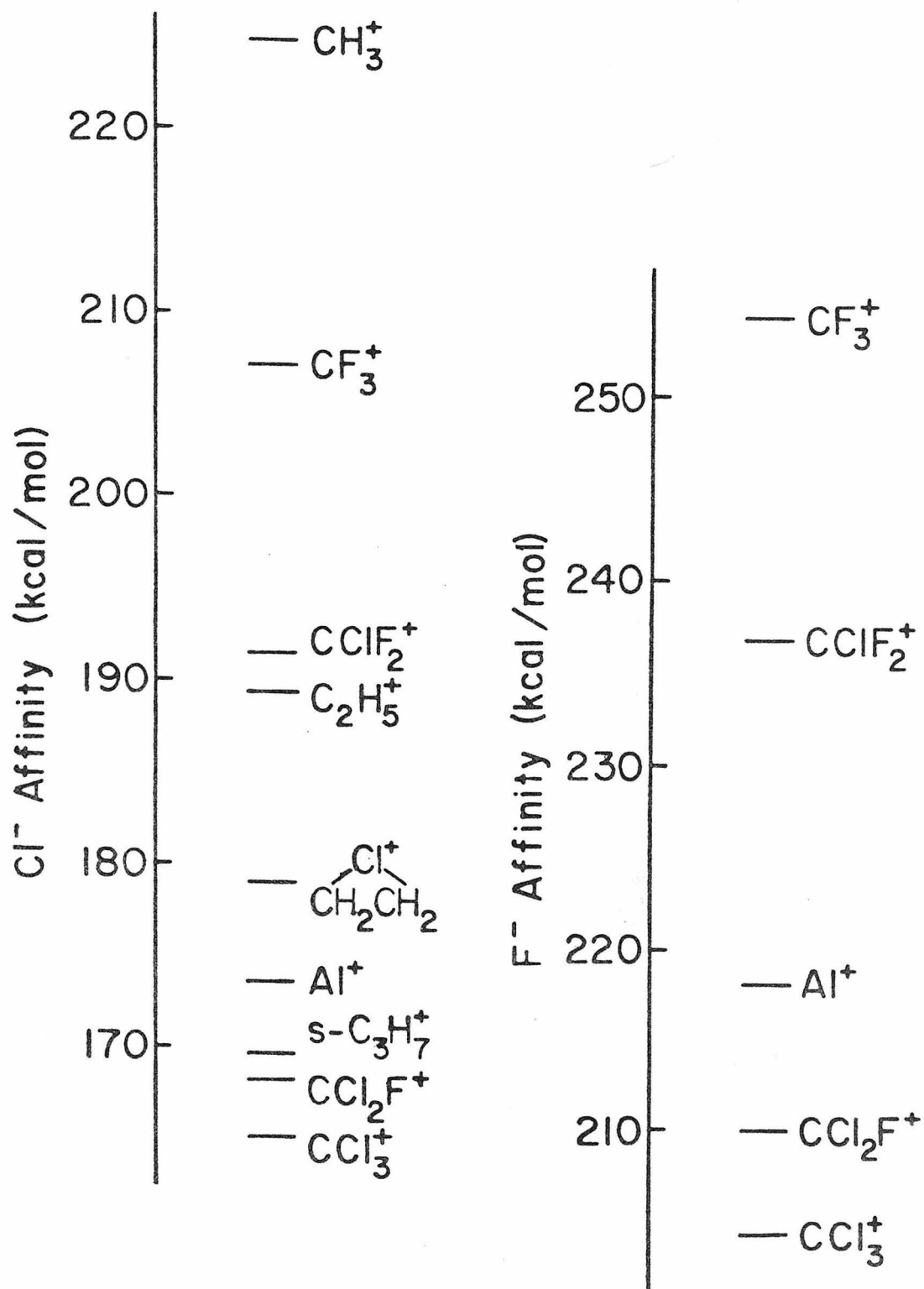
$\text{Al}^+$  undergoes three types of reactions with alkyl halides: (1) halide transfer, (2) dehydrohalogenation, and (3) oxidation. Halide transfer is the dominant reaction whenever it is exothermic. The enthalpy of a halide transfer reaction is given by the difference in the halide affinities of  $\text{Al}^+$ ,  $\text{D}(\text{Al}^+-\text{X}^-)$  and the product ion,  $\text{D}(\text{R}^+-\text{X}^-)$ . Chloride and fluoride affinities of positive ions relevant to this study are shown in Fig. 11. Halide transfer to form ions with higher halide affinities than that of  $\text{Al}^+$  is endothermic, while the formation of ions with lower halide affinities is exothermic.

The reactivities of the tetrahalomethanes parallel the enthalpies for the halide transfer reactions. Fluoride transfer from  $\text{CF}_4$  and  $\text{CF}_3\text{Cl}$  are 36 and 19 kcal mol<sup>-1</sup> endothermic, respectively, and no reaction in these systems was detected. The most favorable halide transfers from  $\text{CCl}_2\text{F}_2$ ,  $\text{CCl}_4$ , and  $\text{CCl}_3\text{F}$ , where reaction was observed, have enthalpies of -8, -9, and -14 kcal mol<sup>-1</sup>, respectively. In the systems where two halide transfer reactions are possible, the thermodynamically favored process,  $\text{F}^-$  transfer, is predominant. The selectivity decreases with increasing collision energy. In contrast, alkyl and halomethyl cations react with halomethanes principally by  $\text{Cl}^-$  transfer rather than  $\text{F}^-$  transfer whenever the former reaction is exothermic (e.g., reactions 19 and 20) [23].



## FIGURE 11

Chloride and fluoride affinities of positive ions  
of interest in this study.

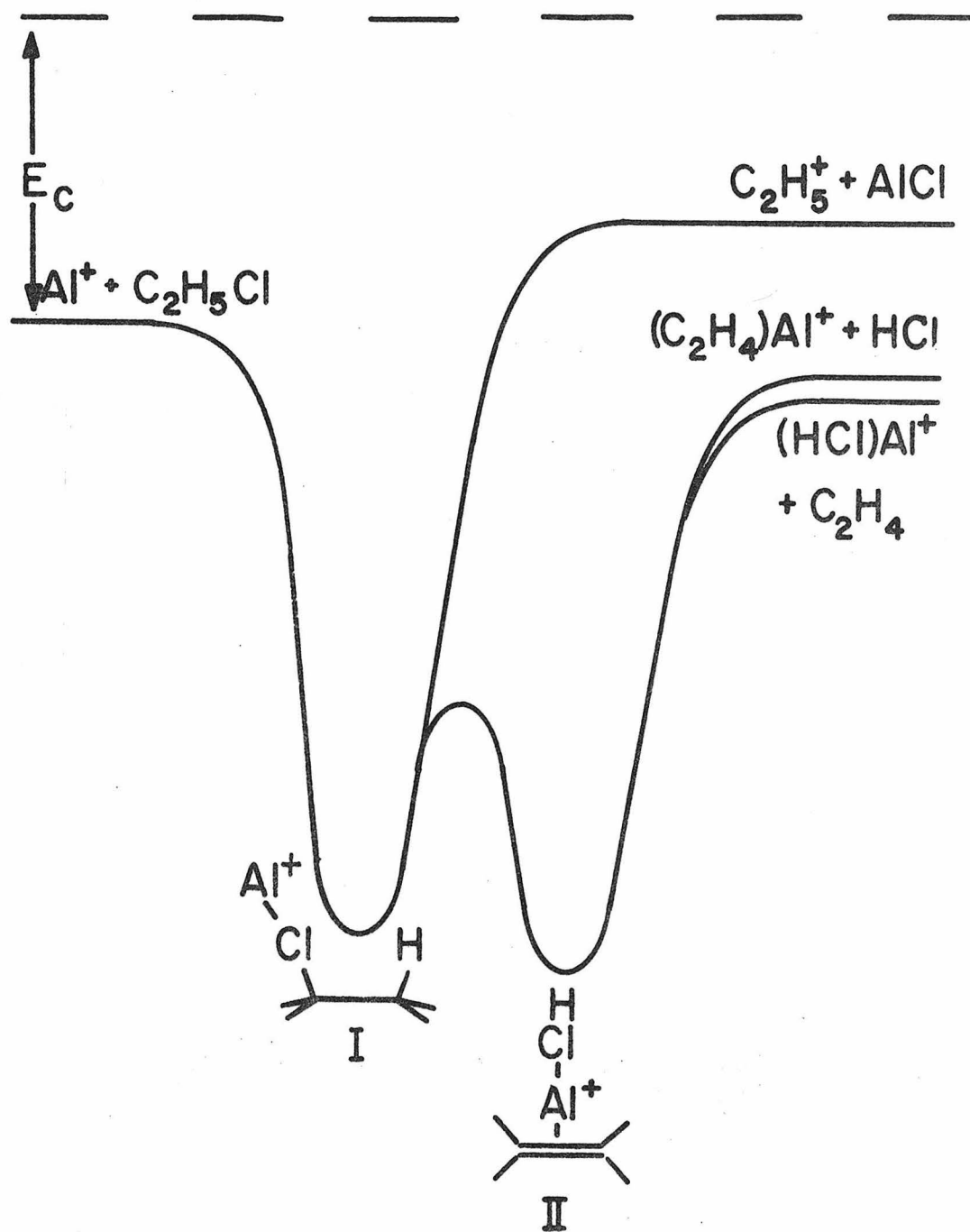


The cross sections for chloride transfer from the mono-chloroalkanes behave in a manner consistent with the reaction thermochemistry. Chloride transfer from methyl chloride is endothermic by  $51 \text{ kcal mol}^{-1}$  and within the limits of our sensitivity no reaction occurs. Chloride transfer from ethyl chloride is  $16 \text{ kcal mol}^{-1}$  endothermic and occurs in competition with dehydrohalogenation. The only significant reaction of isopropyl chloride is chloride transfer, which is  $4 \text{ kcal mol}^{-1}$  exothermic.

In a study of reactions of alkali ions with halogen compounds, the mechanism presented in Scheme I was inferred from variations in reactivity among halogen compounds [1]. An additional variable, the collision energy, is explored in the present study. The variation with energy of the product distribution in the reaction of  $\text{Al}^+$  with ethyl chloride (Fig. 3) can be accommodated by the mechanism in Scheme I. A potential surface for this reaction is presented in Fig. 12. At 0.5 eV the average collision energy is below the threshold for chloride transfer and dehydrohalogenation predominates.  $\text{Al}(\text{C}_2\text{H}_4)^+$  is the most abundant product at this energy, which implies that  $D(\text{C}_2\text{H}_4-\text{Al}^+) > D(\text{HCl}-\text{Al}^+)$ . With increasing collision energy, the lifetime of the collision complex decreases and processes which involve little rearrangement become more probable than complex processes. Thus, chloride transfer, which requires a simple bond cleavage, increases in relative importance with increasing collision energy above the threshold. Formation of  $\text{Al}(\text{ClH})^+$  does not require rearrangement to intermediate II, but can occur by H transfer in species I, while insertion of  $\text{Al}^+$  between the halogen and the carbon skeleton must

## FIGURE 12

A qualitative potential surface for the reaction  
of  $\text{Al}^+$  with  $\text{C}_2\text{H}_5\text{Cl}$ ,  $E_c$  = collision energy.

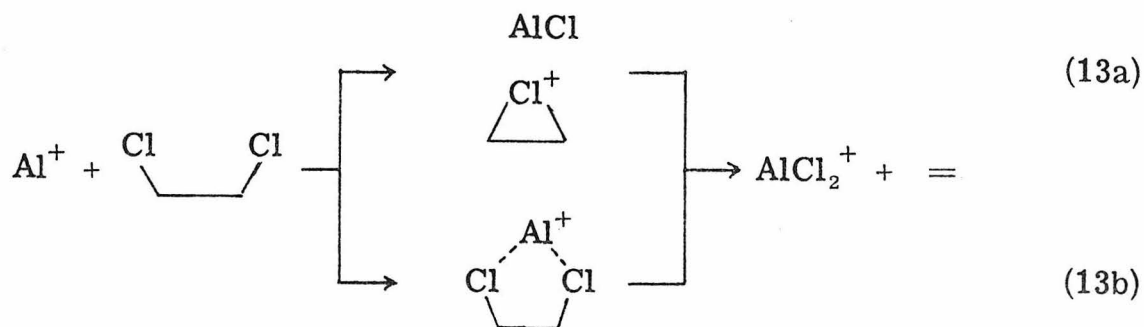




occur prior to the formation of  $\text{Al}(\text{C}_2\text{H}_4)^+$ . Consequently, the relative abundance of  $(\text{HCl})\text{Al}^+$  increases while that of  $(\text{C}_2\text{H}_4)\text{Al}^+$  decreases with increasing collision energy.

The reaction of  $\text{Al}^+$  with  $\text{CH}_2\text{ClCH}_2\text{Cl}$  to form  $\text{AlCl}_2^+$  and  $\text{C}_2\text{H}_4$  (reaction 8) is formally an oxidation of Al from the +1 to the +3 state. Products in which Al exhibits a +2 state, e.g.,  $\text{AlCl}^+$  and  $\text{AlCl}_2$ , are radicals and their formation is thermodynamically unfavorable.

At least two mechanisms for the oxidation reaction can be envisioned. In the first (reaction 13a), chloride abstraction occurs, followed by removal of the other chlorine. In the second, (reaction 13b), removal of the chlorines is concerted.



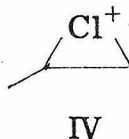
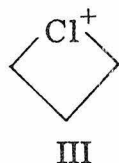
were operating, a decrease in the average lifetime of the complexes would reduce the number of complexes which reach the second step. The ratio of chloride transfer to oxidation would increase with increasing collision energy. However, this ratio remains relatively constant over 4 eV. Thus, the concerted mechanism seems more probable.

Despite the large exothermicity of the oxidation reaction (13) ( $\Delta H = -80 \text{ kcal mol}^{-1}$ ), its cross section is small compared to that for

halide transfer. The oxidation requires energy to  $sp$  hybridize  $Al^+$ . This requirement may be the source of a potential barrier in the reaction coordinate. This small cross section may also reflect a low probability for the formation of the five-centered transition state of a concerted mechanism.

A fraction of the chloronium ions, which result from chloride transfer from the dichloropropanes and dichlorocyclopentanes, is formed with sufficient internal energy to eliminate  $HCl$  (reactions 10 and 13). This fraction increases with collision energy and is considerably greater for the cyclopentyl chloronium ions than for the propenyl chloronium ions. The reasons for this latter fact are difficult to assess in the absence of thermodynamic data. The enthalpy for elimination from the cyclopentenyl chloronium ion may be significantly less than that for elimination from the propenyl chloronium ion.

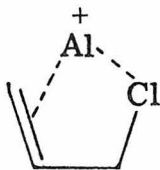
Chloride transfer from the dichloropropane isomers initially produces different product ions. Transfer from 1, 2-dichloropropane can yield either a primary or secondary carbonium ion, which may close to give the tetramethylene chloronium ion (III) or the propylene chloronium ion (IV), respectively. Abstractions from 1, 3-



dichloropropane must leave a primary carbonium ion. However, the similarity in the extent of  $HCl$  elimination at a given energy in Figs. 5 and 6 indicates that both isomers eventually yield a common ion with

similar internal energies prior to elimination. This requires an intermediate whose lifetime exceeds the time necessary for the rearrangement. The ion formed in this rearrangement is probably species IV. Ionization of any of the dichloropropane isomers in magic acid solution yields species IV, and not species III [24].

Among the dichloroalkanes only the dichloropropanes undergo dehydrohalogenation. This implies that the dehydrohalogenation product,  $(C_3H_5Cl)Al^+$ , is particularly stable. If this product is allyl chloride bound to  $Al^+$ , the bidentate character of allyl chloride could provide this additional stability.



## REFERENCES

1. R. D. Wieting, R. H. Staley and J. L. Beauchamp, J. Amer. Chem. Soc., 97 (1975) 924.
2. R. H. Staley and J. L. Beauchamp, J. Amer. Chem. Soc., 97 (1975) 5920.
3. R. V. Hodges and J. L. Beauchamp, Anal. Chem., 48 (1976) 825.
4. J. Allison and D. P. Ridge, J. Organomet. Chem., 99 (1975) C11.
5. S. A. Safron, G. D. Miller, F. A. Rideout and R. C. Horvat, J. Chem. Phys., 64 (1976) 5051.
6. G. D. Miller and S. A. Safron, J. Chem. Phys., 64 (1976) 5065.
7. P. Armentrout, R. Hodges and J. L. Beauchamp, J. Amer. Chem. Soc., 99 (1977) 3162.
8. P. B. Armentrout, R. V. Hodges and J. L. Beauchamp, J. Chem. Phys., 66 (1977) 4683.
9. J. A. Rutherford and D. A. Vroom, J. Chem. Phys., 65 (1976) 4445.
10. Michael S. Foster and J. L. Beauchamp, J. Amer. Chem. Soc., 93 (1971) 4924.
11. John Allison and D. P. Ridge, J. Amer. Chem. Soc., 99 (1977) 35.
12. J. P. Blewett and E. J. Jones, Phys. Rev., 50 (1936) 464.
13. I. Džidić and P. Kebarle, J. Phys. Chem., 74 (1970) 1466.
14. L. G. McKnight and J. M. Sawina, Bull. Am. Phys. Soc., 19 (1974) 154.
15. W. R. Davidson and P. Kebarle, J. Amer. Chem. Soc., 98 (1976) 6125.

16. W. R. Davidson and P. Kebarle, J. Amer. Chem. Soc., 98 (1976) 6133.
17. P. B. Armentrout, R. V. Hodges and J. L. Beauchamp, unpublished results.
18. A. D. Williamson and J. L. Beauchamp, J. Amer. Chem. Soc., 97 (1975) 5714.
19. Charlotte E. Moore, Atomic Energy Levels, Vol. I, National Bureau of Standards, Washington, D.C., 1949, p. 124.
20. H. W. Werner, Int. J. Mass Spectrom. Ion Phys., 14 (1974) 189.
21. B. S. Freiser and J. L. Beauchamp, J. Amer. Chem. Soc., 96 (1974) 6260.
22. J. S. Filippio, Jr., A. F. Sowinski and L. J. Romano, J. Amer. Chem. Soc., 97 (1975) 1599.
23. S. G. Lias and P. Ausloos, Int. J. Mass Spectrom. Ion Phys., 23 (1977) 273.
24. G. A. Olah, Halonium Ions, Wiley, New York, 1975, p. 102.